

Aus dem Institut für Neurogenetik  
Universität zu Lübeck  
Direktorin: Prof. Dr. Christine Klein

**Novel *NAXE* variants**  
**in neurometabolic disorders**  
**and deep sequencing of mitochondrial DNA**

Inauguraldissertation  
zur  
Erlangung der Doktorwürde  
der Universität zu Lübeck  
- Aus der Sektion Medizin –

vorgelegt von  
**Sophie Imhoff**  
aus Wipperfürth  
Lübeck 2021



**1. Berichterstatterin: Priv.-Doz. Dr. Joanne Trinh**

**2. Berichterstatter: Priv.-Doz. Dr. med. Yorck Hellenbroich**

**Tag der mündlichen Prüfung: 30.08.2021**

**zum Druck genehmigt. Lübeck, den 30.08.2021**

**-Promotionskommission der Sektion Medizin-**



## I. Contents

I.	Contents .....	I
II.	List of abbreviations .....	V
1	Introduction .....	1
1.1	Mitochondria genetics and function .....	1
1.2	Mitochondrial diseases.....	3
1.2.1	Prevalence of mitochondrial diseases.....	3
1.2.2	Clinical spectrum .....	4
1.2.3	Diagnostics .....	5
1.3	Whole exome sequencing as a diagnostic tool.....	6
1.4	Whole exome sequencing in mitochondrial diseases .....	7
1.5	Treatment of patients with mitochondrial disorders.....	8
1.6	The relevance of somatic mitochondrial DNA variants .....	9
1.7	Mitochondrial DNA genome integrity across tissues.....	10
1.8	Induced pluripotent stem cells as a research model in neurological diseases .. .....	10
1.9	Hypothesis .....	11
1.10	Objectives .....	11
2	Study individual demographics, Material and Methods.....	13
2.1	Whole exome sequencing and subsequent analyses .....	13
2.1.1	Study individual demographics .....	13
2.1.2	Material.....	14
2.1.3	Methods.....	15
2.2	Deep mitochondrial sequencing .....	28
2.2.1	Study individual demographics .....	28
2.2.2	Material.....	28

## Contents

2.2.3	Methods.....	29
3	Results.....	31
3.1	Patient history, whole exome sequencing result and subsequent analyses ..	31
3.1.1	Medical history of Family 1 .....	31
3.1.2	Whole exome sequencing result .....	33
3.1.3	<i>NAXE</i> and implications in mitochondria-related disorders .....	35
3.1.4	Sanger sequencing validation .....	36
3.1.5	RNA expression analysis and protein expression analysis .....	38
3.1.6	Mitochondrial network analysis .....	40
3.1.7	Treatment outcome.....	40
3.1.8	Replication and review of other <i>NAXE</i> variant carriers.....	41
3.1.9	Classification of <i>NAXE</i> variants and phenotype description .....	42
3.1.10	Location and conservation analysis of <i>NAXE</i> variants .....	51
3.2	Mitochondrial deep sequencing results .....	52
3.2.1	Mitochondrial sequencing dataset.....	52
3.2.2	Mitochondrial DNA genome integrity during the differentiation process and across tissues .....	53
3.2.3	Variant count in different tissues .....	56
3.2.4	Influence of age on the variant quantity .....	57
3.3	Deep mitochondrial sequencing in brain tissue .....	58
3.3.1	Mitochondrial sequencing dataset.....	58
3.3.2	Mitochondrial deep sequencing result.....	58
4	Discussion and Outlook .....	61
4.1	Whole exome sequencing and subsequent analyses .....	61
4.1.1	Diagnosis via whole exome sequencing .....	61
4.1.2	Variant analysis .....	62

4.1.3	Replication cohort.....	63
4.1.4	Clinical disease phenotype .....	64
4.1.5	Therapeutic approach.....	71
4.2	Integrity across cell types and role of somatic variants.....	72
4.2.1	Induced pluripotent stem cell model for neuronal studies.....	73
4.2.2	Overview of neuronal models and their benefit in neurological research	74
4.3	Appraisal of deep mitochondrial sequencing in brain samples .....	75
4.4	Conclusion .....	76
5	Summary .....	78
6	Zusammenfassung .....	79
7	References .....	82
8	Appendix.....	93
8.1	Chemicals .....	93
8.2	Kits.....	94
8.3	Antibodies .....	94
8.4	Solutions .....	94
8.5	Equipment.....	95
8.6	Timeline of the clinical course for patients II.1, II.3 and II.4 of Family 1 .....	95
8.7	Case descriptions for Family 2-4 .....	101
8.7.1	Family 2 (homozygous c.733A>C: p.Lys245Gln) .....	101
8.7.2	Family 3 (homozygous c.652G>A: p.Asp218Asn).....	101
8.7.3	Family 4 (homozygous c.640A>G: p.Ile214Val) .....	102
8.8	Primer design.....	102
8.9	Association of mitochondrial DNA variant quantity and age.....	103
8.10	Votum der Ethikkommission.....	103
9	Acknowledgments.....	104

## Contents

10	Curriculum vitae .....	105
10.1	Scientific publications.....	106
10.2	Oral presentations.....	107
10.3	Grants.....	107

## II. List of abbreviations

ACMG	American College of Medical Genetics and Genomics	LHON	Leber's hereditary optic neuropathy
ATP	adenosine triphosphate	MDS	Movement Disorders Society
bp	base pairs	MEM	Maximum Entropy Method
BWA	Burrows-Wheeler Aligner	MLPA	multiplex ligation-dependent probe amplification
CADD	Combined Annotation Dependent Depletion	MRI	magnetic resonance imaging
cDNA	complementary deoxyribonucleic acid	mRNA	messenger RNA
COX	cytochrome c oxidase	MRS	magnetic resonance spectroscopy
CSF	cerebrospinal fluid	mtDNA	mitochondrial DNA
Ct	threshold cycle	NADH/NAD <sup>+</sup>	nicotinamide adenine dinucleotide
DNA	deoxyribonucleic acid	NADPH/NADP <sup>+</sup>	nicotinamide adenine dinucleotide phosphate
ddNTP	dideoxyribonucleotides	NAXD	NAD(P)HX-Dehydratase
dNTP	desoxyribonucleotides	NAXE	NAD(P)HX Epimerase
ETT	endotracheal tube	nDNA	nuclear deoxyribonucleic acid
ExAC	Exome Aggregation Consortium	OMIM	Online Mendelian Inheritance in Man
GERP	Genomic Evolutionary Rate Profiling	OXPHOS	oxidative phosphorylation
GnomAD	Genome Aggregation Database	PBS	phosphate-buffered saline
HPO	human phenotype ontology	PCR	polymerase chain reaction
IPSC	induced pluripotent stem cell	PEG	percutaneous endoscopic gastrostomy

## List of abbreviations

PSC	pluripotent stem cell
qRT-PCR	quantitative real-time-PCR
RNA	ribonucleic acid
SD	standard deviation
THC	tetrahydrocannabinol
UniProt	Universal Protein Resource
WES	whole exome sequencing
WGS	whole genome sequencing

## 1 Introduction

This thesis focuses on a novel gene implicated in mitochondrial-like disorders and on the deep characterization of the mitochondrial genome. The introductory chapter provides an overview of the mitochondria, different mitochondria-related disorders, genetic diagnosis and treatment outcome. This is followed by the relevance of the mitochondrial DNA (mtDNA) genome integrity across cell types and tissues (e.g. induced pluripotent stem cells). Lastly, the hypothesis and the three goals of the project are presented.

### 1.1 Mitochondria genetics and function

The main function of the mitochondria is energy metabolism and this is necessary for normal cellular processes. The vast majority (90%) of a typical cell's adenosine triphosphate (ATP) is produced through the oxidative phosphorylation pathway (OXPHOS) <sup>1</sup>. ATP is an energy resource of indispensable importance for energy-dependent reactions <sup>2</sup>. Biological processes in which mitochondria participate are steroid hormone synthesis <sup>3</sup>, apoptosis <sup>4</sup>, calcium homeostasis <sup>5</sup> and free radical production <sup>6</sup>. Low levels of reactive oxygen species are required for normal cellular function, but their accumulation can generate cellular toxicity effects <sup>7</sup>.

In the OXPHOS pathway, five protein complexes and two electron shuttle systems (coenzyme Q<sub>10</sub> and cytochrome c) have a crucial role <sup>8</sup>. The respiratory chain is built of approximately 85 subunits. Out of these only 13 are encoded by mtDNA. Complex II is the only complex exclusively encoded by nuclear DNA (nDNA) genes <sup>9,10</sup>. More than 1,400 nuclear genes are involved in mitochondrial function <sup>11</sup>.

## Introduction

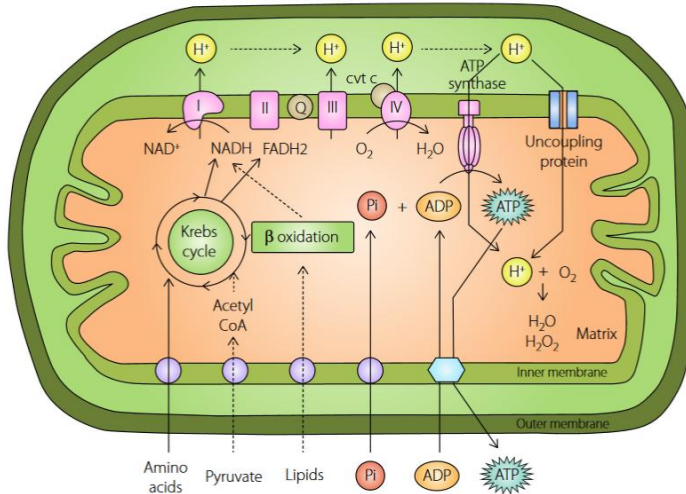


**Figure 1. Mitochondrial anatomy and respiratory chain reaction.** The figure schemes energy production in mitochondria with involved complexes I-IV and ATP-synthase, shuttle systems and most important processes. Figure adapted from Lee <sup>12</sup>. Q=coenzyme Q; cyt c=cytochrome c; Pi=ionic phosphate; ATP=adenosine triphosphate; ADP=adenosine diphosphate; NADH/NAD+=nicotinamide adenine dinucleotide; FADH<sub>2</sub>=flavine adenine dinucleotide.

Mitochondria have their own genetic information, mtDNA, which is maternally inherited. This is explained by their origin as eukaryotic endosymbionts <sup>13</sup>. Repair mechanisms in mitochondria seem to be less effective than the ones for nDNA <sup>14</sup>, so the amount of mtDNA variants is about ten times higher than in nDNA <sup>15</sup>. Mutated and wild-type mtDNA can coexist in the same cell. This condition is defined as heteroplasmy, whereas changes that are identical in all copies of the mitochondrial genome are homoplasmic. In a random process, one mtDNA variant can drift up, down or remain stable in different cell lines <sup>14</sup>. To have an impact on the cellular function the variant has to reach the genetic threshold, though this is variable in the literature. Values range from 15-90% heteroplasmy <sup>16,17</sup>. It is unclear whether low-level heteroplasmic variants may also play a role <sup>18</sup>. Through a fusion and fission process, which is vital for cellular function <sup>19</sup>, mitochondria can exchange components and reduce the rate of heteroplasmy in impaired mitochondria <sup>15</sup>. Large deletions causing mtDNA abnormality are most frequent in post-mitotic tissues, which are the most sensitive to mtDNA changes <sup>20</sup>, whereas in mitotic cells point mutations are the common mutation mechanism <sup>21,22</sup>.

## Introduction

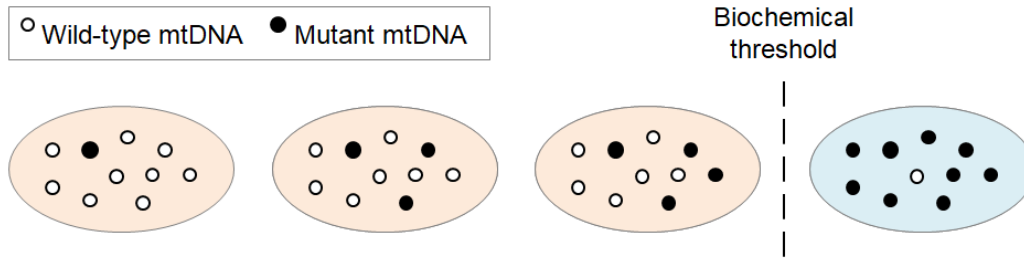


**Figure 2. mtDNA heteroplasmy and genetic threshold.** Each mitochondrion can harbor a different portion of mutant and wild-type mtDNA. The genetic threshold is defined as the amount of mutant mtDNA that is needed to have an impact on mitochondrial function. mtDNA=mitochondrial DNA. Figure adapted from Stewart and Chinnery <sup>14</sup>.

## 1.2 Mitochondrial diseases

Mitochondrial disorders affect the structure or function of the mitochondria. Genetic mitochondrial diseases can be caused by mtDNA variants as well as by nDNA variants. An estimated 75% - 90% of mitochondrial diseases that occur in children are caused by nDNA variants <sup>23</sup> of genes encoding proteins transported to the mitochondria <sup>9,24</sup>.

Although the brain accounts for about 2% of the total body mass, it requires 20% of oxygen and 50% of glucose <sup>25</sup>. The necessity of large energy turnover makes the brain more sensitive to mitochondrial defects compared to other tissues. Thus, a lack of ATP can lead to a broad spectrum of neurological disorders <sup>25</sup>. Not only primary mitochondrial defects can lead to disease, but also secondary mitochondrial dysfunction has been observed to occur in diverse situations like neurodegeneration and aging <sup>26-28</sup>.

### 1.2.1 Prevalence of mitochondrial diseases

Mitochondrial disorders are part of the most common inherited disorders of metabolism and are therefore a relevant burden to society. The prevalence has been studied in the United Kingdom in adults in 2015. The prevalence of disease-causing nDNA variants is approximately 2.9 per 100,000 and of mtDNA variants 1 per 5,000 - about 1 in 4,300 all together <sup>29</sup>. Likewise, the prevalence of respiratory chain disorders in Australia is conservatively estimated to be 1 in 5,000 births <sup>30</sup>.

## Introduction

Interestingly, the prevalence in the general population of the ten most common pathogenic mtDNA variants is approximately 1 in 200. Thus, potentially damaging mtDNA variants are very common, but they seem to stay below the threshold for deleteriousness<sup>31</sup>.

### 1.2.2 Clinical spectrum

Mitochondrial diseases represent a broad spectrum of clinical phenotypes. One reason might be genetics, because of the interplay between nDNA and mtDNA, which are both encoding mitochondrial proteins. Furthermore, many organ systems of the human body are dependent on mitochondrial function, which causes extremely various phenotypes<sup>10</sup>. The diagnosis mitochondrial disorder should be taken into consideration in patients of any age showing a progressive clinical course involving seemingly unrelated organs and tissues<sup>32</sup>.

Some symptoms are common in many patients affected by mitochondrial disorders and are highlighted in this section. Neurological symptoms are the most common, whereas prenatal manifestations are uncommon in mitochondrial diseases<sup>10</sup>. In terms of common motor features, cerebellar ataxia is one of the most frequent neurological symptoms in mitochondrial disorders. It includes disturbance of movement and gait, hyperkinesia and tremor. Other movement disorders like myoclonus, dystonia or parkinsonism are also part of the clinical spectrum<sup>33</sup>. Epilepsy has been shown to occur in 35%-60% of patients with confirmed mitochondrial disorders. In some subgroups, epilepsy is the main characteristic. Epileptic episodes in these patients are often difficult to manage and are associated with a poor prognosis. In 80% of cases, first seizures were preceded by other symptoms<sup>34</sup>. Other manifestations regarding the nervous system are nystagmus, spasticity, migraine-like headache, leukodystrophy, cortical atrophy and stroke-like episodes<sup>35</sup>. Psychiatric symptoms like generalized anxiety or depression are frequent, but often under-diagnosed. Dementia mainly presents with features like impairment of attention, flexibility and visual construction, but without deterioration of the general intelligence. Neurodevelopmental impairment can occur at any age<sup>36</sup> and peripheral nerve involvement is frequently reported, too<sup>35</sup>.

## Introduction

The main signs of mitochondrial myopathy are muscle weakness, muscle atrophy and exercise intolerance. Difficulties to swallow due to myopathy can occur in the disease course, which endangers patients to aspirate into the lung. Later even muscles responsible for ventilation can be affected <sup>37</sup>. Often this weakness appears in the eyes and eyelids first, which leads to symptoms like progressive external ophthalmoplegia, ptosis and limitation of the eye movement <sup>37</sup>. Other eye-specific manifestations are optic atrophy, diplopia, cataract and pigmentary retinal degeneration <sup>32</sup>.

Cardiac problems such as concentric hypertrophic cardiomyopathy or arrhythmias were observed. Hepatic failure or kidney impairment were also described, typically in a proximal tubulopathy called De Toni Debré Fanconi syndrome <sup>10</sup>. Conspicuous phenomena concerning the skin are mottled pigmentation of photo-exposed areas, trichothiodystrophy as well as dry, thick and brittle hair <sup>32</sup>. Reported intestinal symptoms are recurrent vomiting, chronic diarrhea and failure to thrive. Furthermore, hearing loss due to neurosensory dysfunction was observed. Diverse endocrine manifestations can occur as well as bone marrow alterations for example sideroblastic anemia, neutropenia or thrombopenia <sup>32</sup>. Investigations of the causes of death on a cohort of thirty adult patients with mitochondrial disorders showed that cardiopulmonary failure was the most common reason. Furthermore, pulmonary infections and acute neurological incidences were noticed. In more than half of the studied cohort, the cause of death remained unknown <sup>38</sup>.

### **1.2.3 Diagnostics**

Few neurological disorders are as phenotypically heterogeneous and diagnostically challenging as mitochondrial diseases <sup>10</sup>. Generally speaking, this condition often leads to trying circumstances for patients and their families. Figure 3 gives an overview of the most frequently used diagnostic procedures.

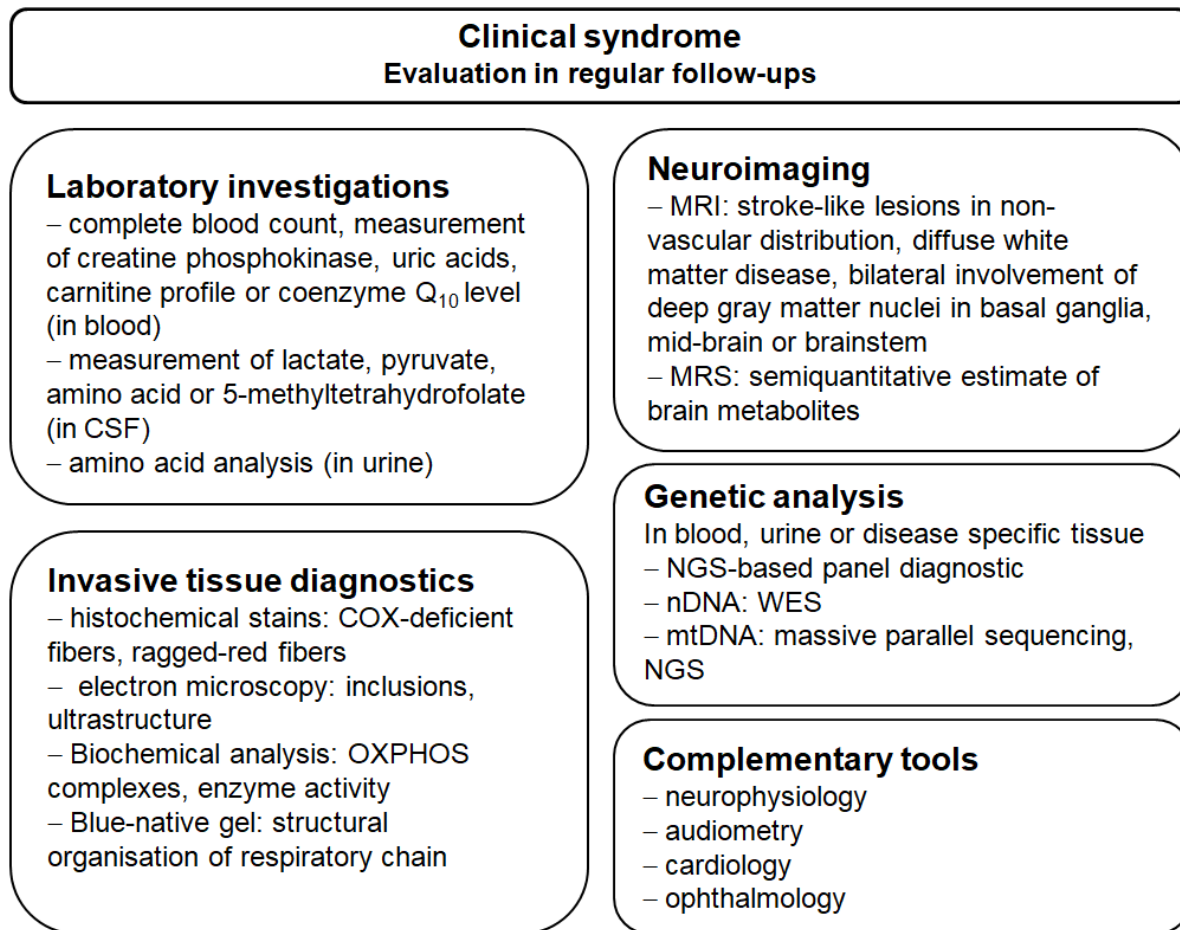


**Figure 3. Overview of the most frequently applied diagnostic investigations in mitochondrial disorders.** The clinical syndrome is the central base of all diagnostics. Complementary investigations can include creatine phosphokinase and uric acids, which are relevant in suspected acute rhabdomyolysis. Carnitine profile permits the diagnostic of defects in fatty acid oxidation. Amino acid analysis in urine can detect renal tubulopathy. MRS is more powerful than MRI in the diagnostic of neurometabolic disorders. CSF=cerebrospinal fluid; MRI=magnetic resonance imaging; MRS=magnetic resonance spectroscopy; NGS=next-generation-sequencing; nDNA=nuclear DNA; WES=whole exome sequencing; mtDNA=mitochondrial DNA; e.g.=exempli gratia; COX=cytochrome c oxidase; OXPHOS=oxidative phosphorylation. Information obtained from multiple publications<sup>8,11,23</sup>.

### 1.3 Whole exome sequencing as a diagnostic tool

It is hard to diagnose patients with a suspected genetic cause and unspecific symptoms. Therefore families are exposed to so-called ‘diagnostic odysseys’. Many of the used methods are invasive, costly and go along with numerous hospitalizations. A diagnostic tool, that can lead to diagnosis and has a low level of invasiveness with only a phlebotomy needed, is through genotype-phenotype correlations identified by exome sequencing. Furthermore, whole exome sequencing

## Introduction

(WES) can be used as a method to identify new genetic causes of disease<sup>39–41</sup>. In a large cohort of 278 participants, in 36.7% a molecular diagnosis was detected and in 52.0% of these cases, the medical management has been adapted to the genetic findings<sup>42</sup>. Additional publications support the effectiveness in the identification of disease causes in undiagnosed patients<sup>43,44</sup>.

WES has a diagnostic advantage, when conventional single-gene or gene-panel tests may not be appropriate because a relevant genetic test has not yet been developed or because of genetic heterogeneity, incomplete or atypical clinical presentation or lack of knowledge of the causal gene. As the cost of WES analysis goes down and previously it was shown that costs might be reduced by implementing WES earlier in the diagnostic process of patients with intellectual disability or epilepsy, it is important to consider the implementation<sup>44,45</sup>. Limitations of WES are that some variant types, such as copy number variations, low-level mosaicism, aneuploidy, structural chromosome rearrangements, variants in non-coding regions or trinucleotide repeat expansions, are not detected and cannot be excluded as disease-causing source<sup>46</sup>. Some of these limitations can be resolved with complementary analyses like multiplex ligation-dependent probe amplification (MLPA) or whole genome sequencing (WGS). WGS covers coding and non-coding regions. This method is currently costly, but could be an important tool in the future as it can detect disease-causing variants in regions not captured by WES and targeted panels such as regulatory regions. The non-coding sequences are less well conserved than the exons and the relevance of variants is hard to predict. Studying the adequate way to use WGS in medical diagnostics is still a challenge<sup>47</sup>. Today, the use of WES as a diagnostic tool increases in clinics.

### **1.4 Whole exome sequencing in mitochondrial diseases**

WES is a next-generation sequencing method to identify genetic defects in mitochondrial disorders<sup>48</sup>. Through WES or mtDNA sequencing, novel gene variants implicated in mitochondrial disease are being discovered<sup>10</sup>. The diagnostic yield in a cohort of 109 patients suspected to have a mitochondrial disorder was 38% wherein 19% were found via virtual gene-panels in the WES data and 19% outside of these panels<sup>48</sup>. In another cohort of 117 patients, mostly children, with a suggested

## Introduction

mitochondrial disease cause a diagnostic yield of 68% including variants in mtDNA and nDNA was detected <sup>49</sup>. As a diagnostic workflow for this disease group, researchers suggest a two-step approach starting with gene-panel analysis and if no diagnosis is obtained, the analysis of WES data should follow. This process is perceived as time and cost-effective with a high diagnostic yield <sup>48,50</sup>. Separation of a cohort into a low and high probability of mitochondrial disease using mitochondrial disease criteria <sup>51</sup> leads to the following. In patients with a high score, 90% could be diagnosed by WES, whereas patients with a low probability had a detection rate of about 36%. So a high likelihood of mitochondrial disease seems to be associated with a higher rate of genetic diagnosis <sup>52</sup>. If it remains unclear whether a candidate gene is deleterious or not, further investigation on the underlying pathogenic pathway is needed. A detailed description of the clinical symptoms and functional analysis in muscle cells or fibroblasts as well as research in animal models remain crucial to strengthen or to moderate its pathogenic relevance <sup>48</sup>.

### **1.5 Treatment of patients with mitochondrial disorders**

Therapy in mitochondrial disorders is mostly inadequate and palliative <sup>10</sup>. There is little data available from randomized clinical trials, so the treatment is often based on clinical experience and consensus-based recommendations <sup>53,54</sup>. Specific therapy for the different underlying disease causes is not well developed <sup>7,55</sup>. Multidisciplinary networks are needed to provide the best treatment for this patient group. Symptom control by application of medication (e.g. antiepileptics to treat epileptic seizures) is necessary to improve patients' condition and often is the greatest part of medical care. In mitochondrial epilepsy disorders of coenzyme Q<sub>10</sub> biosynthesis should be excluded as they are the only readily treatable form of seizures in mitochondrial disorders <sup>34</sup>.

Frequently prescribed oral medication is the so-called 'mitochondrial-cocktail' containing a mixture of vitamins and supplements, which should support the mitochondrial function by increasing the availability of substrates for the OXPHOS metabolism <sup>56</sup>. Components of this mixture can be L-carnitine, coenzyme Q<sub>10</sub>, riboflavin and thiamine. Coenzyme Q<sub>10</sub> is one of the best-studied components of therapy and most patients with a primary or secondary coenzyme Q<sub>10</sub>-deficiency

## Introduction

benefit from the supplementation. Therefore, it is an important differential diagnosis in patients with juvenile ataxia and infantile encephalomyopathy<sup>10</sup>. Vitamin C and E are applied because of their function as antioxidants. Recently, nicotinamide adenine dinucleotide (NADH/NAD<sup>+</sup>) precursors were proposed to ameliorate mitochondrial function and reduce neuronal loss in neurodegenerative disorders<sup>57</sup>. Increasing NADH/NAD<sup>+</sup> or vitamin B<sub>3</sub> levels might be an attractive therapeutic target for the treatment of mitochondria-related disorders<sup>58</sup>.

For disorders, due to mtDNA variants, there is progress in the development of gene therapy. For example, mitochondrial replacement in the context of in-vitro fertilization is studied<sup>59</sup>. Another approach is mitochondrial genome manipulation of heteroplasmic mtDNA variants for example by restriction endonucleases leading to the degradation of the targeted mutant mtDNA<sup>7,60</sup>. The CRISPR/Cas system as a gene-editing method is also discussed as a potential therapeutic option in mitochondrial diseases. In the first studies, it was applied to selectively degrade pathogenic mitochondrial genomes<sup>61,62</sup>.

### **1.6 The relevance of somatic mitochondrial DNA variants**

Accumulation of mtDNA variants in individual cells, e.g. fibroblast and blood cell types, is a common phenomenon<sup>22</sup>. Even stronger than for point mutations is the effect for large deletions in mtDNA that accumulate during lifetime<sup>1,63</sup>. Only a small portion of variants appear in early development. Most mtDNA variants in adults are of a somatic origin<sup>22</sup>, which makes it important to investigate as there are implications in age-related disorders and neurological diseases<sup>1</sup>. The functional consequences of these variants remain to be elucidated for neurodegenerative diseases, where age is a critical risk factor. Parkinson's disease is an example of an age-related disease wherein an altered mtDNA deletion and somatic variant load has been observed compared to control subjects<sup>64</sup>. The number of mtDNA variants was shown to be associated with increasing age<sup>22</sup>. It remains uncertain, if somatic variants play a role in disease pathogenesis or if they are a normal phenomenon of aging<sup>1</sup>. MtDNA point mutations at a heteroplasmy level between 30% and 50% can change the transcriptional regulation. Increasing levels of variant heteroplasmy result in a

discontinuous remodeling of the gene expression profiles of nDNA and mtDNA. This observation may contribute to the complexity of mitochondrial diseases and aging<sup>65</sup>.

### **1.7 Mitochondrial DNA genome integrity across tissues**

The mtDNA variant load varies between cells and different tissues. Wildtype mtDNA seems to have a selection advantage in rapidly dividing cells like leukocytes. The selection might be caused by the fitness of a cell to divide. As the analysis of blood DNA risks to underestimate the effect of mtDNA variants in the affected tissues<sup>66</sup>, hair follicle or muscle tissue is a better base for diagnostics of mitochondrial defects<sup>67</sup>.

### **1.8 Induced pluripotent stem cells as a research model in neurological diseases**

Genetic changes in mtDNA are associated with aging and age-related diseases like insulin resistance<sup>68</sup> and neurodegenerative diseases<sup>21</sup> for example Parkinson's disease, Alzheimer's disease and multiple sclerosis<sup>20</sup>. Induced pluripotent stem cell (iPSC)-derived neurons enable investigations without the problem of paucity of material, which is naturally limited in brain tissue of patients. The availability of neurons for studies is important. For example changes on the cellular level due to a homoplasmic pathogenic variant were observed in neuron progenitors and neurons, but were not observed in patient fibroblasts<sup>69</sup>. One main goal of the developed models is to observe which variants cause which effect on the neuronal level and how the dysfunctions can be influenced by drugs. This makes iPSC-based models interesting also for the investigation of variant effects in inherited mitochondrial disorders.

According to the variant concordance in iPSC generation, some mtDNA variants are present at low levels in blood and fibroblasts, while iPSCs have higher levels of variants. In contrast to this, it was observed that some heteroplasmic variants in fibroblasts were not transmitted to the iPSC lines, which is explained by a negative selection for pluripotency<sup>22</sup>. It is important to study the genetic integrity of mtDNA in different cell types and the relevance of iPSC-derived neurons as a model for neurological disorders. MtDNA variants in iPSCs are not well characterized and seem

to show variable results in the literature. The variant load of homoplasmic variants was shown to not change throughout the generation of iPSCs<sup>69,70</sup>. However, other studies showed that the heteroplasmic variant load can vary greatly among different iPSC lines from the same individual and remain constant upon differentiation<sup>71–73</sup>. Positive selection of mtDNA variants during the iPSC induction, the differentiation process and during extended culture cannot be excluded<sup>22</sup>.

iPSC models have been successfully used for drug discovery in multiple neurological diseases: Friedreich ataxia<sup>74</sup>, spinal muscular atrophy<sup>75</sup> and sporadic as well as familial Alzheimer's disease<sup>76,77</sup>. The ideal iPSC model would generate the cell type affected by the disease with accurate OXPHOS-dependent metabolism and carry the patient-specific nDNA-mtDNA match<sup>78</sup>.

### **1.9 Hypothesis**

- (1) We hypothesize that a genetic diagnosis can be obtained through WES of a parent-offspring trio with a suspected inherited mitochondrial disorder.
- (2) We hypothesize that the genome integrity of mtDNA variants (heteroplasmic and homoplasmic) is sustained across iPSC reprogramming and differentiation.
- (3) We hypothesize that besides the nuclear genome, other disease-causing somatic mtDNA variants can be found in patient brain tissue with a suspected inherited mitochondrial disorder.

### **1.10 Objectives**

- (1) The first aim is to identify the genetic cause by WES in a Family with three affected siblings with severe encephalopathy including seizures, neuropsychiatric symptoms, cognitive impairment, cerebellar ataxia, spasticity, myoclonus, respiratory insufficiency and episodes of intermittent comatose states. If we find a genetic cause in this Family, the objective is to identify other reports on patients with a similar phenotype and a genetic change in the same gene. One main objective of this study is to optimize the disease management of the living patient.
- (2) The second aim is to investigate the mtDNA genome integrity in different tissues of the same individual as well as during the reprogramming process of fibroblasts and the differentiation to neurons.

## Introduction

- (3) The last objective is to investigate mtDNA variants in different brain tissue samples (Frontal Cortex, Putamen, Cerebellum) of one patient with the neurometabolic disorder described in aim 1 (II.4, Family 1) compared to control brain samples (Frontal Cortex) and to identify variants that could explain the disease phenotype of the patient.

## 2 Study individual demographics, Material and Methods

The methods are divided into two sections:

2.1) methodical background for WES diagnostic and subsequent variant and functional analysis;

2.2) information on deep mtDNA sequencing analysis.

### 2.1 Whole exome sequencing and subsequent analyses

#### 2.1.1 Study individual demographics

Patients were examined by movement disorders specialists (Prof. Dr. Norbert Brüggemann (MD), Dr. Vera Tadic (MD), Prof. Dr. Christine Klein (MD), Prof. Dr. Alexander Münchau (MD)). The original exome Family consists of three offsprings with severe encephalopathy (one boy, two girls) and one healthy offspring. The father is of German descent and the mother is of Lebanese descent (Figure 5).

**Table 1** Demographics of the affected children of Family 1.

Patient	AAO [years]	AAD [years]	Disease duration [years]	Gender	Ethnicity
II.1	3	6	3	M	German
II.3	22	.	9 (in 2021)	F	German
II.4	20	22	2	F	German

Legend: AAO=age at onset, AAD=age at death, M=male, F=female.

A Replication cohort of 4,351 cases with neurodevelopmental disorders was used. Written informed consent was obtained from all patients or guardians prior to the inclusion in the study. The study was approved by the ethics committee at the University of Lübeck.

**Table 2** Cohort demographics of patients with developmental disorders.

	<b>No. of patients with DD (%)</b>
<b>Geographic region</b>	
<i>Middle East</i>	2904 (66.74)
<i>Europe</i>	693 (15.93)
<i>South/North America</i>	298 (6.85)
<i>South Asia</i>	291 (6.69)
<i>Africa</i>	109 (2.51)
<i>Oceania</i>	43 (0.99)
<i>Unknown</i>	13 (0.3)
<b>Total number of patients</b>	<b>4351</b>
Gender ratio	1.26:1
<b>Age of patients</b>	
<i>&lt;1 year</i>	594 (13.65)
<i>1-5 years</i>	1717 (39.46)
<i>5-15 years</i>	1377 (31.65)
<i>15-30 years</i>	272 (6.25)
<i>&gt;30 years</i>	105 (2.41)
<i>Unknown</i>	286 (6.57)
<b>Average age (SD)</b>	<b>7.75 (8.04)</b>
<b>Consanguineous parents</b>	<b>1861 (41.07)</b>
<b>Positive Family history</b>	<b>1206 (27.71)</b>

Legend: No.=number; SD=standard deviation; DD=developmental disorders; including developmental delay, intellectual disability, delayed speech and language development, seizures, motor delay, microcephaly and macrocephaly.

As a control subject for experiments with fibroblast cell lines, we included a healthy individual of German ancestry. At the time of sample donation, the man was 62 years old. His in-house de-identified number is L-4646.

### 2.1.2 Material

All material used for this study is listed together with the manufacturers' names in the Appendix.

Study individual demographics, Material and Methods

### **2.1.2.1 Patient material**

Individuals in this study provided blood samples for deoxyribonucleic acid (DNA) extraction. WES was subsequently performed. Skin biopsy and subsequent fibroblast culture were performed on the healthy parents (I.1, I.2 of Family 1), the patient (II.3, Family 1) and a control subject (L-4646). The skin biopsy of the unaffected control subject was collected in Kassel and provided to the Institute of Neurogenetics.

### **2.1.3 Methods**

#### **2.1.3.1 DNA extraction**

DNA extraction was performed by the Institute of Neurogenetics using a standardized protocol.

#### **2.1.3.2 Whole exome sequencing**

WES was performed using Illumina's Nextera Rapid Capture Exome Kit, which covers 214,405 exons, up to 37 megabases. Subsequently, massive parallel sequencing was performed on a NextSeq500 or HiSeq 4000 Sequencer (Illumina, San Diego, CA, USA). Coverage with a 100X mean depth was obtained for all samples.

#### **2.1.3.3 Bioinformatic analysis**

Raw sequencing reads were transformed into Fastq format via the bcl2fastq software 2.17.1.14 (Illumina). Read alignment to the human reference genome (GRCh37, hg19 build) was assessed by Burrows-Wheeler Aligner (BWA) software <sup>79</sup> and the Maximum Entropy Method (MEM) algorithm. This process was performed by an in-house developed pipeline. Alignments were converted to binary bam file. Three different variant callers (GATK HaplotypeCaller, FreeBayes and SAMtools) were used for variant calling. Variants were annotated by Annovar and in-house ad-hoc bioinformatic tools. Integrative Genomics Viewer v.2.3 and Alamut v.2.4.5 (Interactive Biosoftware, Rouen, France) were used to visually verify the alignments <sup>80</sup>. All data were compared to an in-house database consisting of 17,797 individuals and 8,570 families. WES and bioinformatic analysis were performed.

### 2.1.3.4 Exome filtering and variant analysis

Annotation of the exome data was performed with ANNOVAR, which stands for ANNOtate VARIation <sup>81</sup>. Consideration of multiple online databases was applied including Online Mendelian Inheritance in Man (OMIM) and in-silico predictions (Table 3).

**Table 3** Annotation tools and online services used to assess the pathogenic relevance of the called variants.

Annotations	Online services
ExAC	Ensembl
GnomAD	UCSC Genome Browser
CADD score	NCBI
Quality score	GERP
pLI score	UniProt Consortium
Z score	OMIM

Legend: ExAC=Exome Aggregation Consortium <sup>82</sup>; GnomAD=Genome Aggregation Database <sup>83</sup>; CADD=Combined Annotation Dependent Depletion <sup>84</sup>; UCSC=University of California, Santa Cruz <sup>85</sup>; NCBI=National Center for Biotechnology Information <sup>86</sup>; GERP=Genomic Evolutionary Rate Profiling <sup>87</sup>; UniProt=Universal Protein Resource <sup>88</sup>; OMIM=Online Mendelian Inheritance in Man <sup>89</sup>.

The Exome Aggregation Consortium (ExAC) provides information from exome sequencing results of 60,706 unrelated individuals, which gives us insight into population variant frequencies and makes it possible to estimate, if a variant might be benign or pathogenic. Individuals affected by severe pediatric diseases were excluded from the cohort <sup>82</sup>. The Genome Aggregation Database (GnomAD) is a continuation of sequencing efforts after ExAC. It aggregates and harmonizes the existing exome sequencing data from ExAC and additional genome sequencing results. The database provides data of 125,748 exomes and 15,708 genomes, so from 141,456 individuals in total. Like ExAC, GnomAD excludes individuals with severe pediatric diseases <sup>83</sup>. Another used annotation is the Combined Annotation Dependent Depletion (CADD) score, which classifies variants by their predicted deleteriousness. This method combines information from multiple functional annotations into a single score <sup>84</sup>. The pLI score reflects the tolerance of a given gene to the loss of function based on the number of protein-truncating variants, that is referenced for this gene in control databases weighted by the size of the gene and

the sequencing coverage<sup>90</sup>. The z-score is a method predicting the likely deleteriousness of variants. This measure expects normal distribution for synonymous variants, but right-shifted (higher constraint) for missense and protein-truncating variants, indicating that more genes are intolerant to these classes of variation<sup>91</sup>.

The filtering process was performed in conjunction with Priv.-Doz. Dr. Joanne Trinh. The pedigree (Figure 5) implicated a recessive mode of inheritance. In the search for rare and damaging variants in the exome data, the following filtering criteria were applied: GnomAD minor allele frequency < 0.01, quality score > 200 and a CADD score > 15 for homozygous or compound-heterozygous variants, present in both affected siblings.

For the analysis of the location of the different variants in *NAXE*, of the gene transcripts as well as of the evolutionary conservation different online databases were applied: Ensembl, UCSC Genome Browser and NCBI<sup>85,86,92</sup>. The Genomic Evolutionary Rate Profiling (GERP) score identifies constrained elements in multiple alignments by quantifying substitution deficits. These deficits represent substitutions that would have occurred if the element were neutral DNA, but did not occur because the element has been under functional constraint<sup>87</sup>. Information on the protein structure and function was provided by the website Universal Protein Resource (UniProt)<sup>88</sup>. The online catalog OMIM harbors referenced information on inherited diseases and over 15,000 human genes. It is focused on the phenotype-genotype relationship<sup>89</sup>.

### **2.1.3.5 Replication cohort: exome analysis**

The Replication dataset was first filtered by Human Phenotype Ontology (HPO) terms<sup>93</sup>. We used the following criteria for HPO-terms: 'global developmental delay' (HP:0001263), 'seizures' (HP:0001250), 'microcephaly' (HP:0000252), 'delayed speech and language development' (HP:0000750) and 'intellectual disability' (HP:0001249). Then, we filtered for individuals with variants in the *NAXE* gene.

### 2.1.3.6 Polymerase chain reaction

The polymerase chain reaction (PCR) allows the exponential amplification of a specific region of DNA<sup>94</sup>. Primers, which consist of specific oligonucleotides, were designed to bind complementarily to the targeted sequence. Via an enzymatic reaction, the DNA polymerase extends the amplicon. The cycles of the reaction were controlled by temperature changes leading to three steps: 1. denaturation of the double-stranded DNA, 2. primer annealing and 3. amplification of the DNA sequence by DNA polymerases.

**Table 4** Standard PCR reaction mixture.

Substance	Volume [µl]
dH <sub>2</sub> O	15.00
dNTPs (1mM)	3.00
Forward Primer (10µM)	0.60
Reverse Primer (10µM)	0.60
Buffer (10x)	1.50
Taq Polymerase (5 U/ µl)	0.07
DNA (~ 15 ng/µl)	5.00

Legend: dH<sub>2</sub>O=sterile distilled water; dNTP=deoxyribonucleotides.

**Table 5** Cycling conditions for standard PCR.

	Temperature [°C]	Time	Nr. of cycles
Initial denaturation	95	5 min	1
Denaturation	95	30 sec	35
Annealing	55-60	30 sec	
Elongation	72	30 sec	
Final elongation	72	10 min	1

Legend: Nr.=Number; min=minutes; sec=seconds.

### 2.1.3.7 Agarose gel electrophoresis

The experiment was performed on a 1% agarose gel at 120 V and 400 mA for 20 minutes in Tris-Borate-EDTA buffer. The bands were visualized by Midori Green in a BIO-RAD Imager. For each gel, a 100 base pair (bp) ladder was used as a length reference.

### 2.1.3.8 Sanger sequencing

The candidate variants obtained by WES were separately validated by Sanger sequencing<sup>95</sup>. The PCR product of the selected gene region was treated with exonuclease and alkaline phosphatase. Afterward, the sequencing PCR was assessed using deoxyribonucleotides (dNTPs) as well as dideoxynucleotides (ddNTPs), which lead to the termination of the DNA fragments. The DNA was precipitated with Sodium acetate buffer solution (3M). In suspension with formamide, the DNA fragments were sequenced on a 3130XL Genetic Analyzer. The result was visualized using the software program Chromas (Technelysium Pty Ltd, Australia).

**Table 6** Sequencing PCR mixture.

Substance	Volume [ $\mu$ l]
Purified PCR product	1
5x Buffer	1.5
Primer (10 $\mu$ M)	0.5
Termination mix (3.1)	0.5
dH <sub>2</sub> O	6.5

Legend: dH<sub>2</sub>O=sterile distilled water.

**Table 7** Cycling conditions for sequencing PCR.

	Temperature [°C]	Time	Number of cycles
<b>Initial denaturation</b>	96	1 min	1
<b>Denaturation</b>	96	10 sec	25
<b>Annealing</b>	60	10 sec	
<b>Elongation</b>	60	1:10 min	
	4	∞	

Legend: min=minutes; sec=seconds.

**Table 8** Sodium acetate precipitation mixture.

Substance	Volume [µl]
<b>PCR product</b>	10
<b>dH<sub>2</sub>O</b>	10
<b>Sodium acetate (3M)</b>	2
<b>Ethanol (95%)</b>	50

Legend: dH<sub>2</sub>O=sterile distilled water.

### 2.1.3.9 Genetic analysis

All primers for the genetic analysis were designed according to the reference genome Build 37 (hg19). For the primer design, multiple online services were utilized<sup>85,96,97</sup>. For primers at complementary DNA (cDNA) specific exonic junctions, sequences of the *NAXE* transcript NM\_144772 provided by Ensembl were used<sup>92</sup>.

### 2.1.3.10 Fibroblast culture and Mycoplasma test

Fibroblasts were cultured at 37°C in an atmosphere containing 5% CO<sub>2</sub>. The Dulbecco's Modified Eagle Medium contains 10% fetal bovine serum and 1% penicillin/streptomycin antibiotics.

#### 2.1.3.10.1 Passaging cells

To passage cells, the media was aspirated and 1X phosphate-buffered saline (PBS) was used as a wash. Afterward, cells were then incubated with 2 mL of accutase for 5 minutes. Cells were transferred into a falcon tube with media and centrifuged for 5

minutes at 1000 rpm. The pellet was resuspended in media and fibroblasts were distributed into the double amount of culture flasks than before the process.

### 2.1.3.10.2 Freezing down fibroblasts

To freeze down the fibroblasts for storage, a pellet was obtained by applying the steps described previously. The pellet was resuspended in 1mL of media containing 10% Dimethyl sulfoxide and transferred into a cryogenic vial. In a Nalgene Cyro 1°C Freezing Container with isopropyl alcohol, the critical cooling rate of -1°C per minute in a -80°C freezer was guaranteed. After the cooling process cells were stored in a liquid nitrogen container.

### 2.1.3.10.3 Mycoplasma polymerase chain reaction

All cell lines were free of contamination which influences cell physiology and metabolism<sup>98</sup>. Tests included the visual control of the growth process under the microscope and tests for mycoplasma contamination before the start of experiments.

Therefore, the cell medium was incubated with proteinase K under the following conditions:

**Table 9** Proteinase K digestion mixture.

Substance	Volume [µl]
10x Buffer without MgCl <sub>2</sub>	1
Proteinase K (10mg/ml)	1
dH <sub>2</sub> O	8

Legend: dH<sub>2</sub>O=sterile distilled water.

**Table 10** Cycling conditions for Proteinase K digestion.

Temperature [°C]	Time
55	50 min
95	10 min
4	∞

Legend: min=minutes.

Subsequently, a PCR with primers specific for mycoplasma was performed using controls in each run to prevent false-positive or false-negative results<sup>99</sup>.

**Table 11** Mycoplasma-PCR mixture.

Substance	Volume [ $\mu$ l]
10x Buffer with MgCl <sub>2</sub>	1
dNTPs	2
Forward Myco-primer	0.4
Reverse Myco-primer	0.4
Taq Polymerase	0.07
dH <sub>2</sub> O	3.13
Sample/ dH <sub>2</sub> O/ positive tested sample	3

Legend: dH<sub>2</sub>O=sterile distilled water; dNTP=desoxyribonucleotide.

**Table 12** Cycling conditions for Mycoplasma-PCR.

	Temperature [°C]	Time	Number of cycles
Initial denaturation	95	5 min	1
Denaturation	94	30 sec	40
Annealing	58	30 sec	
Elongation	72	1 min	
Final elongation	72	10 min	1
	4	$\infty$	

Legend: min=minutes; sec=seconds.

### 2.1.3.11 RNA extraction and quantitative real-time polymerase chain reaction

The RNA extraction Kit (QIAGEN) was applied including the DNaseI treatment to extract total ribonucleic acid (RNA) out of fibroblasts.

To generate cDNA out of RNA samples, they were reverse-transcribed and amplified by a 'Thermo scientific Maxima First Strand cDNA Synthesis Kit' (ThermoFisher) for quantitative real-time (qRT).

## Study individual demographics, Material and Methods

Two commonly used 'housekeeping' genes: hypoxanthine phosphoribosyl-transferase (*HPRT*) and Tyrosine 3-Monooxygenase/Tryptophan 5-Monooxygenase Activation Protein Zeta (*YWHAZ*) were used as control genes. For the qRT-PCR SYBR-Green was applied, which is fluorescent when it intercalates in double-stranded DNA<sup>100</sup>. This property makes the amplification detectable during the PCR and it is necessary to detect the threshold cycle (Ct) during the reaction. The Ct is the point when the level of fluorescence gives a signal over the background and is in the linear portion of the amplified curve.

**Table 13** qRT-PCR reaction mixture.

<b>Substance</b>	<b>Volume [<math>\mu</math>l]</b>
<b>SYBR Green I</b>	5
<b>Forward Primer</b>	0.3
<b>Reverse Primer</b>	0.3
<b>dH<sub>2</sub>O</b>	2.4
<b>cDNA/ standard</b>	2

Legend: dH<sub>2</sub>O=sterile distilled water.

**Table 14** Cycling conditions for qRT-PCR.

	<b>Temperature [°C]</b>	<b>Time</b>	<b>Number of cycles</b>
<b>Preincubation</b>	95	10 min	1
<b>Denaturation</b>	95	15 sec	40
<b>Annealing</b>	55-60	30 sec	
<b>Elongation</b>	72	30 sec	

Legend: min=minutes; sec=seconds.

The *NAXE* expression level was normalized by dividing the results through the geometric mean of the control gene expression. The analysis was performed two times using technical replicates in order to minimize variability.

### **2.1.3.12 Protein expression analysis**

Total protein was extracted from fibroblast cultures derived from Family 1 (I.1, I.2, II.3) and a control subject. To extract proteins from the cultured fibroblast cells, cell pellets were dissolved in extraction buffer (50 mM Tris–HCl pH 7.6, 150 mM NaCl, 1% DOC, 1% NP-40, and 0.1% SDS) and extracted proteins separated on gels, which were blotted onto nitrocellulose membranes. Blotting of NAXE was done with a polyclonal rabbit antibody (anti-NAXE HPA048164 Sigma-Aldrich, 1:500) and with a mouse monoclonal antibody for  $\beta$ -actin (Sigma-Aldrich, 1:1,000,000).  $\beta$ -Actin was used as a loading control. Protein expression analysis was performed by Dr. Marija Dulovic (MD, PhD).

### **2.1.3.13 Immunofluorescence staining and form factor analysis**

Immunofluorescence staining for the mitochondrial network includes multiple steps. Fibroblasts were fixed in 4% formaldehyde for 15 minutes, permeabilized, and blocked with 0.1% Triton X-100 in 4% normal goat serum in PBS for one hour. Immunofluorescence staining was performed with primary antibody against GRP75 at 4°C overnight. The secondary fluorescence antibody was stained for one hour at room temperature. Coverslips were washed with PBS after each incubation. Before microscopy, coverslips were mounted with DAPI- mounting medium and rested overnight at 4 °C. A confocal microscope generated z-stack images with the AxioVision software (Zeiss). The mitochondrial area and outline were measured and the form factor was calculated (defined as  $[Pm^2] / [4pAm]$ ), where Pm is the length of the mitochondrial outline and Am is the area of the mitochondrion<sup>101,102</sup>. This was performed by the software ImageJ (NIH software) and repeated for at least fifteen cells per cell line.

### **2.1.3.14 ACMG classification**

The American College of Medical Genetics and Genomics (ACMG) classification for the interpretation of sequence variants recommends specific standard terminology to describe variants that cause Mendelian disorders ('pathogenic', 'likely pathogenic', 'uncertain significance', 'likely benign', and 'benign'). Furthermore, the guideline provides criteria to subdivide the variants into five categories including population data, computational data, functional data and segregation data<sup>103</sup>.

### **2.1.3.15 Literature review**

A literature review of publications in English language on variants in *NAXE* was performed. The Medline database PubMed<sup>86</sup> was searched in November 2020 using the search terms 'NAXE' (27 articles) and 'APOA1BP' (13 articles), which is the ancient name of *NAXE*. Four out of these articles were reports on cases with encephalopathy that was accredited to *NAXE* variants. Additionally, we searched reports on patients with *NAXD* variants using the search term 'NAXD' (6 articles). Out of these, there were two reports on patients with *NAXD* variants suffering from a novel neurodegenerative disorder.

## Study individual demographics, Material and Methods

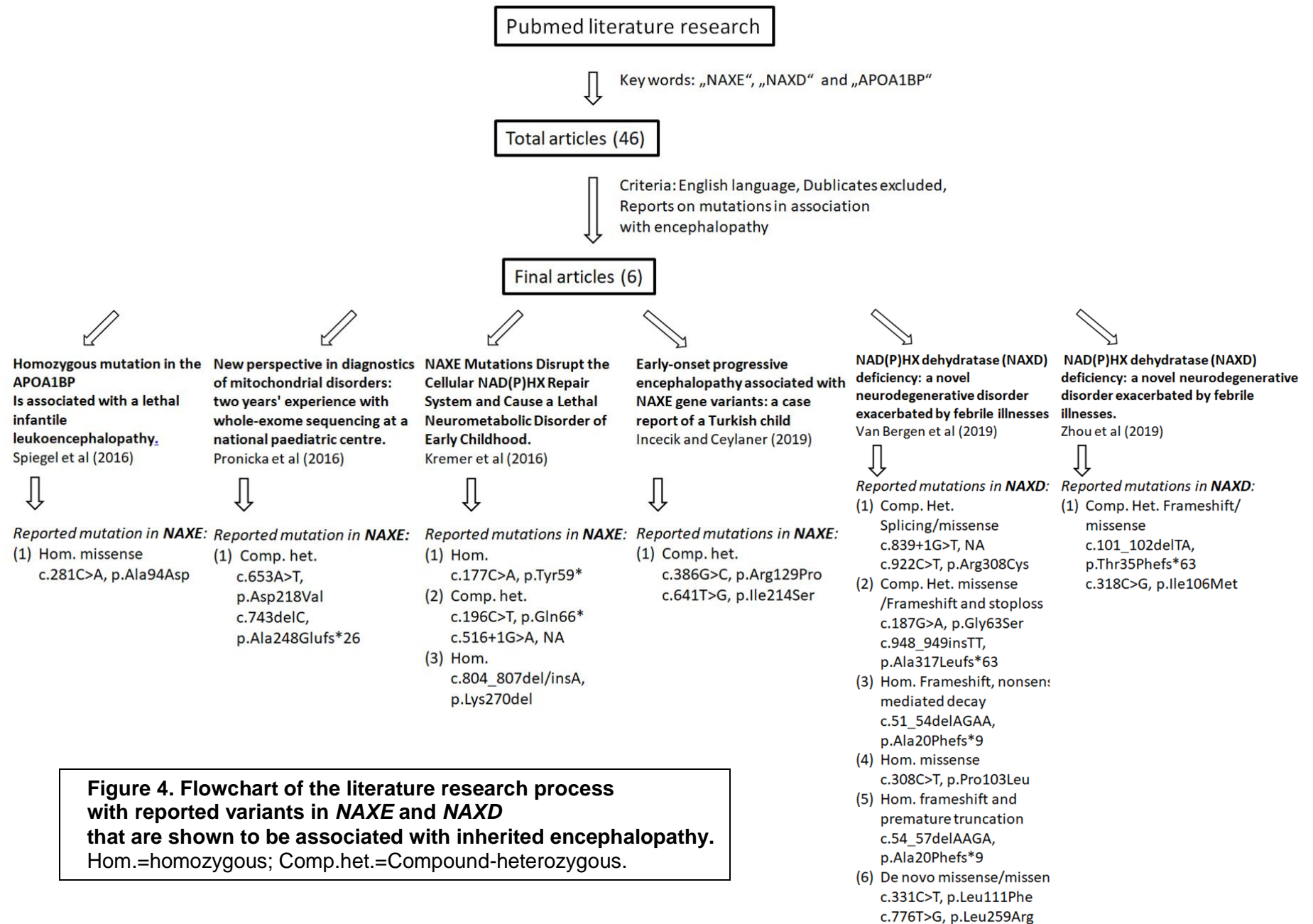


**Figure 4. Flowchart of the literature research process with reported variants in *NAXE* and *NAXD* that are shown to be associated with inherited encephalopathy.** Hom.=homozygous; Comp.het.=Compound-heterozygous.

### **2.1.3.16 Statistical analysis**

All statistical analyses were performed in GraphPad Prism version 6.04 for Windows (La Jolla, California USA). Differences were analyzed statistically using unpaired t-tests with a Bonferroni-Dunn post-hoc correction. P-values were considered significant  $<0.05$ . The reported p-values were not corrected for multiple testing.

## 2.2 Deep mitochondrial sequencing

### 2.2.1 Study individual demographics

Samples of seven unrelated control subjects were used in this project. All individuals were examined by neurologists, who are movement disorders specialists (Dr. Alexander Balck (MD), Prof. Dr. Christine Klein (MD)). The average age at sample donation in this group is 64 years (range 40 – 82 years).

**Table 15** Control demographics including information on gender and age.

ID	Gender	Age at biopsy
L-10886	F	76
L-11148	M	73
L-11156	M	59
L-11167	M	60
L-3857	F	82
L-2131	M	59
L-2135	M	40

Legend: ID=in-house de-identified number; F=female; M=male.

Samples of patient II.4 of Family 1 (Table 1) and two control brain samples were included.

**Table 16** Control demographics brain samples including information on gender and age at death.

ID	Gender	Age at death
SK00047	F	82
SK00148	M	81

Legend: ID=in-house de-identified number; F=female; M=male.

Written informed consent was obtained for all patients or guardians.

### 2.2.2 Material

The control subjects donated skin biopsies and five of them additionally blood samples. These were further processed so that we had access to the cell lines listed in Table 17.

From patient II.4 of Family 1 brain tissue of three different sections was available: frontal cortex, putamen and cerebellum. Frontal Cortex samples were available for control brain samples SK00047 and SK00148.

**Table 17** List of 33 samples included in this project. Passage and clone numbers for cell lines are indicated.

ID	Blood	Fibros	iPS no.1	iPS no.2	NP	Neuron	Cerebellum	Putamen	Frontal Cortex
L-10886	✓	✓	✓ c1 p7	✓ c11 p7	-	-	-	-	-
L-3857	✓	✓	✓ c3 p11	✓ c8 p9	-	-	-	-	-
L-11148	✓	✓	✓ c4 p7	✓ c1 p7	-	-	-	-	-
L-11156	✓	✓	✓ c3 p7	✓ c10 p8	-	-	-	-	-
L-11167	✓	✓	✓ c2 p5	✓ c11 p4	-	-	-	-	-
L-2131	-	✓	✓	-	✓	✓	-	-	-
L-2135	-	✓	✓	-	✓	✓	-	-	-
II.4	-	-	-	-	-	-	✓	✓	✓
SK00047	-	-	-	-	-	-	-	-	✓
SK00148	-	-	-	-	-	-	-	-	✓

✓ =available; - =not available, ID=in-house de-identified number; p=passage number; pNA=passage number not available; c=clone number; Fibros=fibroblasts; iPS=induced pluripotent stemcells; NP=neuron progenitor. Fibroblasts of control L-10886 are from passage number two and of L-11156 from passage number three.

## 2.2.3 Methods

### 2.2.3.1 Mitochondrial DNA deep sequencing

Sequencing of mtDNA and the bioinformatic analysis was performed. In total, 33 samples were sequenced by Illumina NextSeq. A mean coverage of >10,000X was obtained, which enables the detection of low-level variants, comprising as little as 1% of the original sample<sup>104</sup>. Variants were called by three variant callers: mutect, verdict and frebnaive. Gene annotations were performed with centomd\_patho, ClinVar and in-house database information including 19,604 individuals and 10,453 families. Gene annotations for samples of patient II.4, SK00047 and SK00148 were provided by centopatfreq (allele frequency), ClinVar, OMIM and in-house database information.

### **2.2.3.2 Cell culture**

Cells were provided by the iPSC platform at the Institute of Neurogenetics (Lead PI: Dr. Philip Seibler (PhD)). The iPSC colonies were reprogrammed from patient-derived fibroblasts. The differentiation process was initiated once a confluence of 100% was reached. The iPSCs were differentiated to neuronal progenitors (aged for 50-70 days) and dopaminergic neurons (cultured up to day 20). Expression of neuronal markers TUJ1 and TH was confirmed by immunostaining. Detailed information on the cell culture was provided previously<sup>105</sup>.

### **2.2.3.3 Gene annotations**

ClinVar is a public database with free access that is maintained by NCBI. This database provides information on variants and interpretations of their relevance to disease. Multiple external experts like research labs can share their data with ClinVar<sup>106</sup>. Information provided by OMIM was considered<sup>89</sup>.

### **2.2.3.4 Statistical analysis**

All statistical analyses were performed in GraphPad Prism version 6.04 for Windows (La Jolla, California USA). Differences were analyzed statistically using unpaired t-tests and Pearson correlation coefficient with a Bonferroni-Dunn post-hoc correction. P-values were considered significant <0.05. The reported p-values were not corrected for multiple testing.

### **3 Results**

The results are divided into three sections:

3.1) identification of novel NAXE variants in a Family with a neurometabolic disease;

3.2) deep mtDNA sequencing and characterization of different tissues;

3.3) deep mtDNA sequencing of three brain sections from the Family presenting with a neurometabolic disease compared to control subjects.

#### **3.1 Patient history, whole exome sequencing result and subsequent analyses**

##### **3.1.1 Medical history of Family 1**

Family 1 consists of three affected children born to healthy non-consanguineous parents and one unaffected child (Figure 5). The eldest brother of the original Family had disease onset at the age of 3 years (II.1) and died at the age of 6 due to aspiration pneumonia and asphyxia. His two affected sisters had disease onset in early adulthood (II.3, II.4) and showed phenotypes with varying degrees of clinical expressivity including a fluctuating course, seizures, movement disorders and respiratory insufficiency. Patient II.4 died due to pulmonary embolism at the age of 22 years. Patient II.3 is regularly followed-up in the neurological outpatient clinic of the UKSH in Lübeck.

##### **3.1.1.1 Patient history II.1**

Diagnosis: unclear encephalopathy.

According to his parents, he had an unremarkable early mental and physical development. At three years of age, he developed symptoms reminiscent of cerebellar ataxia and intermittent states of reduced vigilance. The patient's clinical course is outlined in Table 29. More detailed symptoms are listed in Table 20. The disease course was reported to fluctuate with episodes of improvement and relapses. His parents reported that brain imaging showed enlarged ventricular spaces. Detailed medical records from more than 15 years ago and DNA samples were not available.

## Results

### **3.1.1.2 Patient history II.3**

Diagnosis: suspected mitochondriopathy with progressive myoclonus epilepsy, severe polyneuropathy and spastic tetraparesis.

Patient II.3 initially reported intermittent headache and unspecific visual and speech problems at 22 years of age which was considered to be a somatoform disorder in combination with depression. The disease rapidly progressed with cognitive impairment, confusion, strabismus, gaze-evoked nystagmus, severe tetraspasticity, relapses of unexplained fever of up to 40°C and seizures including status epilepticus despite anticonvulsant treatment with clobazam, lamotrigine, levetiracetam and topiramate. She was treated at an intensive care unit for months and underwent tracheostomy and percutaneous endoscopic gastrostomy (PEG) tube implantation. In 2015, piracetam was introduced which resulted in the improvement of myoclonic jerks. Fresh muscle tissue did not show signs of mitochondrial dysfunction. Lactate levels in the cerebrospinal fluid were normal and brain, as well as spinal magnetic resonance imaging (MRI), did not show any abnormalities. Retinal fundoscopy was unremarkable. A severe sensorimotor, axonal polyneuropathy was clinically diagnosed in 2020 and electrophysiologically confirmed. Therapy with pregabalin was introduced due to neuropathic leg pain resulting in a clear improvement.

### **3.1.1.3 Patient history II.4**

Diagnosis: suspected mitochondriopathy with organic psychosis and cerebellar ataxia; suspected myoclonus epilepsy.

Patient II.4 is the fourth child of the Family, who developed the disease at the age of 20 years. Initially, she had two episodes of transient and fully remittent cerebellar ataxia and behavioral abnormalities lasting for some weeks. The second episode was triggered by tetrahydrocannabinol (THC). Four months later, she presented with a relapse including headache, vertigo, cerebellar ataxia, mild chorea and fine myoclonus. The symptoms fully remitted after several weeks. Triggered by alcohol consumption 15 months later, she developed organic psychosis with visual and acoustic hallucinations, delusion, anxiety, bizarre behavior, intermittent catatonic stupor and intermittent comatose states. Brain MRI and 31P-MRS (magnetic

## Results

resonance spectroscopy) imaging were normal. A skin biopsy did not show Lafora bodies. She deceased at the age of 22 years as a consequence of pulmonary embolism and subsequent hypoxia. Post mortem examination confirmed severe hypoxic brain damage.

### 3.1.2 Whole exome sequencing result

A total variant count of 118,561 was detected in four blood samples from four individuals of Family 1 (I.1, I.2, II.3 and II.4). By filtering the data for homozygous/biallelic variants two candidates were identified: *NAXE* and *ZNF17*. *ZNF17* is not implicated in neurometabolic disorders and there is no other disease implication of this gene found in the literature. Furthermore, the pLI score is 0.02 and the z-score is -1.91 for *ZNF17* (Table 18). In comparison, *NAXE* has a pLI of 0.00 and a z-score of 0.61. In *NAXE*, the identified compound-heterozygous missense and splicing variants (c.757G>A: p.G253S, c.665-1G>A; NM\_144772.2) were considered disease-causing. The mother is a heterozygous carrier of the splice variant (c.665-1G>A), and the father is a carrier of the missense variant (c.757G>A: p.G253S) in *NAXE*. Sanger sequencing confirmed the compound-heterozygous variants in both affected daughters and thus segregation with the disease (Figure 5).

## Results

**Table 18** Summary of compound-heterozygous variants found in two affected sisters.

Chr	Pos	Ref	Alt	Members (zygosity)	Gene	Transcript	cDNA Change	Protein Change	Functional impact	ExAC	GnomAD	CADD score	pLI score	z-score
3	75786256	T	A	Index-affected(Het) :Father-unaffected(Het):Sister-affected(Het)	ZNF717	NM_00112822 3.1	c.2518A>T	p.Lys840*	stopgain	NA	NA	37	0.02	-1.91
3	75786355	T	A	Index-affected(Het) :Mother-unaffected(Het):Sister-affected(Het)	ZNF717	NM_00112822 3.1	c.2419A>T	p.Thr807Ser	Non-synonymous	NA	NA	16.22		
3	75786516	G	T	Index-affected(Het) :Mother-unaffected(Het):Sister-affected(Het)	ZNF717	NM_00112822 3.1	c.2258C>A	p.Thr753Asn	Non-synonymous	0.036	0.189	15.14		
1	15656367 3	G	A	Index-affected(Het) :Father-unaffected(Het):Sister-affected(Het)	NAXE	NM_144772.2	c.665-1G>A	NA	Splice	NA	NA	17.64	0.00	0.61
1	15656376 6	G	A	Index-affected(Het) :Father-unaffected(Het):Sister-affected(Het)	NAXE	NM_144772.2	c.757G>A	p.Gly253Ser	Missense	2.5 x10 <sup>-5</sup>	1.22 x10 <sup>-5</sup>	34		

Legend: Chromosomal position is based on human genome hg19 (assembly GRCh37), Chr=chromosome, Pos=position, Ref=reference allele, Alt=alternate allele, Members=Family members, Het=heterozygous, ExAC/GnomAD=minor allele frequency reported.

## Results

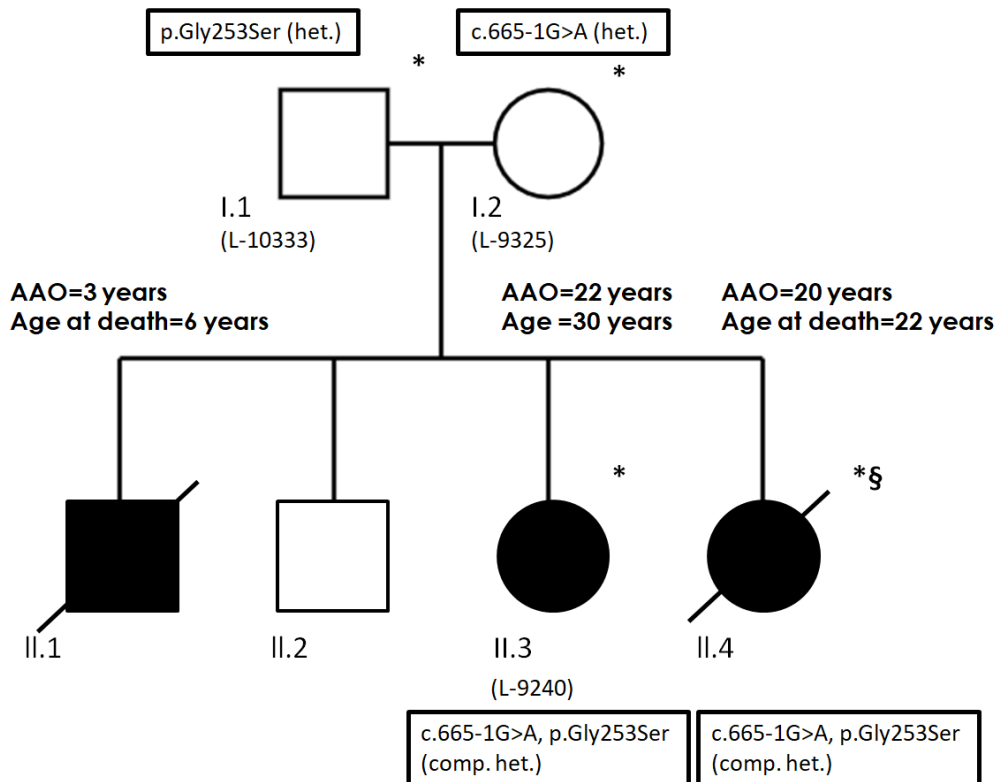


**Figure 5. Pedigree of Family 1.** Box=male; circle=female. Black symbols represent affected Family members. White symbols indicate healthy individuals. Deceased Family members are crossed out. \* blood samples available; § urine, hair and brain tissue available; AAO=age at onset; het.=heterozygous; comp.het.=compound-heterozygous.

### 3.1.3 *NAXE* and implications in mitochondria-related disorders

The gene *NAXE* consists of 6 exons. *NAXE* encodes the NAD(P)X-Epimerase (*NAXE*), an enzyme that is involved in the maintenance of cell metabolism and homeostasis. Two fundamental metabolic redox equivalents, NADH/NAD<sup>+</sup> and nicotinamide adenine dinucleotide phosphate (NADPH/NADP<sup>+</sup>) are electron donors for the mitochondria respiratory chain and necessary cofactors for many metabolic pathways<sup>107</sup>. Fibroblasts with loss-of-function variants in *NAXE* were shown to have an elevated level of cyclic-NAD(P)HX and heat stress aggravates the accumulation of the toxic metabolite<sup>108</sup>. *NAXE* is essential in cellular metabolite repair consequentially preventing mitochondrial dysfunction. Biallelic *NAXE* variants may lead to a deficiency of this repair system and cause mitochondrial diseases. Recently, an association of

## Results

NAXE with vitamin B<sub>6</sub> enzymes was observed by analysis of fusion, clustering and expression patterns in plants and yeast. If there is a secondary function of NAXE involving vitamin B<sub>6</sub>, patients with NAXE deficiency could benefit from a supplementation<sup>109</sup>.

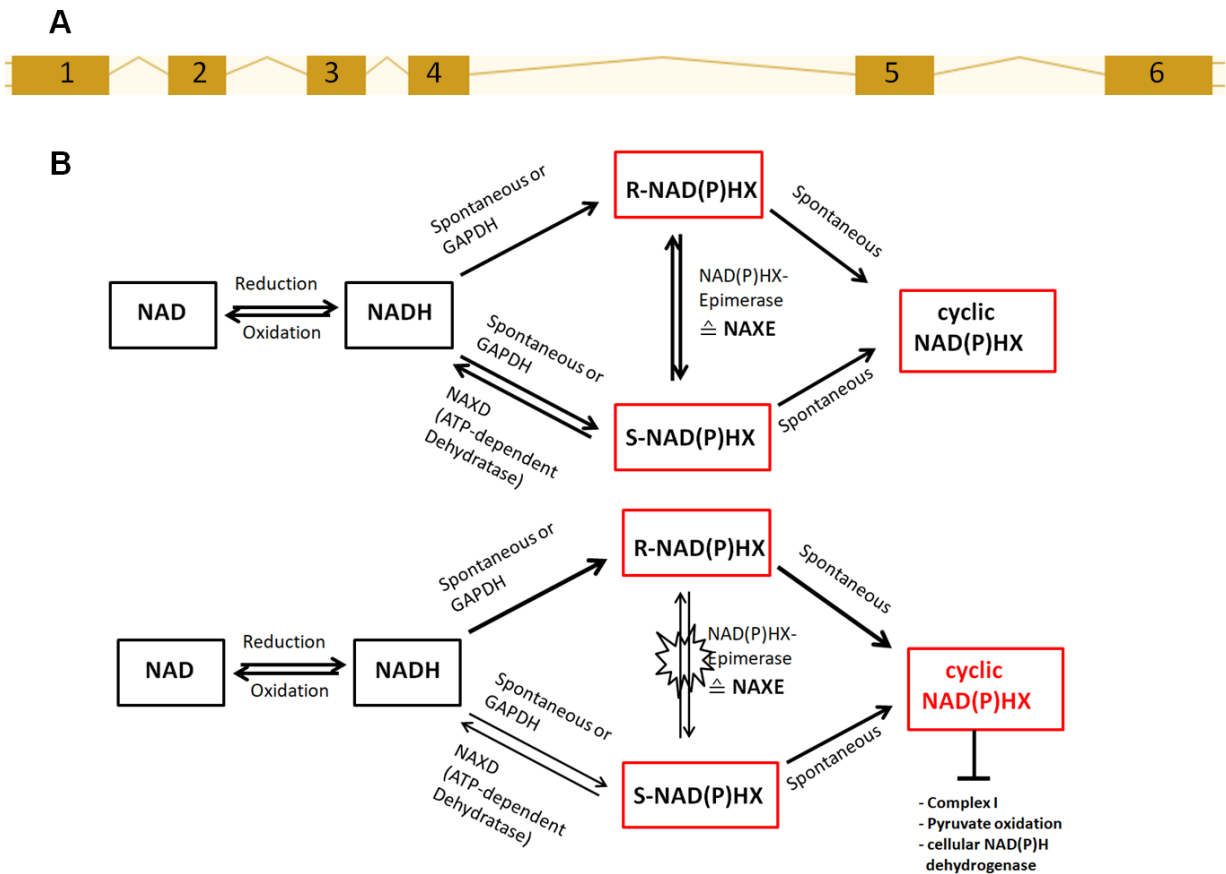


**Figure 6. NAXE gene structure and function of the protein NAD(P)HX-Epimerase (NAXE).** **A** NAXE gene structure. The boxes represent exons 1-6 and the connecting lines represent the introns. **B** Role of the protein NAXE in the NADH/NAD<sup>+</sup> metabolism. Hydration of NAD(P)H causes the generation of toxic metabolites, NADHX and NADPHX, which have been shown to inhibit several important mitochondrial enzymes (Complex I, pyruvate dehydrogenase (PDH), NADH dehydrogenase). NAXE makes reconversion of NAD(P)HX to NAD(P)H possible, so it prevents the accumulation of toxic metabolites. NAXE=NAD(P)HX-Epimerase; GAPDH=Glyceraldehyde-3-phosphate dehydrogenase; NAXD=NAD(P)HX-dehydratase; ATP=adenosine triphosphate. This figure has been adapted from Kremer et al<sup>108</sup>.

### 3.1.4 Sanger sequencing validation

The missense variant was validated by Sanger sequencing (Figure 7A). The variant c.665-1G>A at the acceptor splice site of exon 6 was observed to produce an

## Results

alternative PCR product retaining intron 5 (326 base pairs) between exon 5 and 6 and, as a consequence, introducing a premature stop codon. The normal transcript has a length of 250bp and the alternative transcript includes parts of the intron with 576bp (Figure 7B+C).

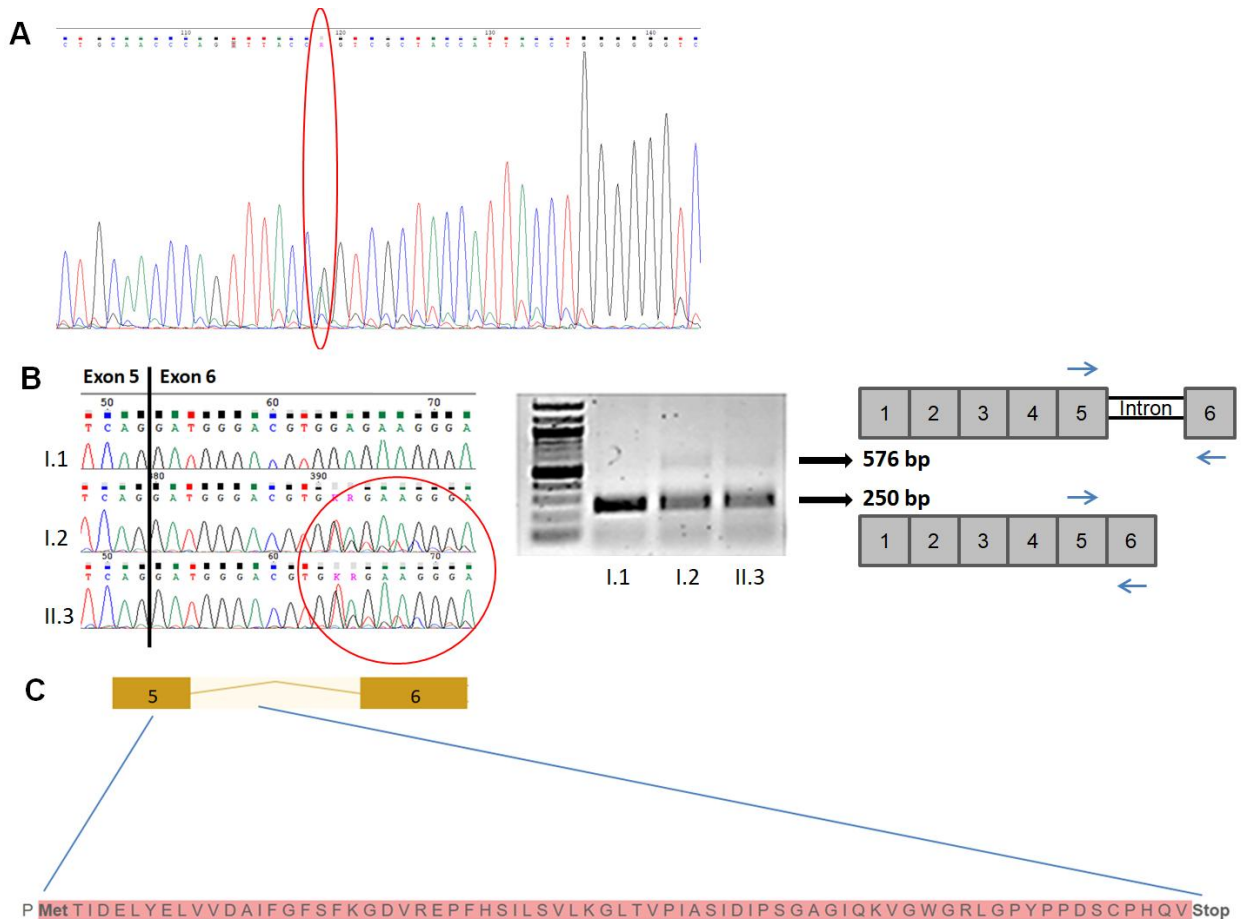


**Figure 7. Sanger sequencing validation and splice site analysis. A)** Sanger sequencing result for missense variant in patient II.3, Family 1 (c.757G>A, p.G253S). Primer sequences are provided in the Appendix. **B)** Sanger sequencing (left panel) of *NAXE* cDNA in Family 1 with primers in exon 5 and 6 resulted in double peaks after the exon5-exon6 junction in carriers of the splice site variant (I.2, II.3) indicating intronic retention overlapping with exon 6. Agarose gel electrophoresis of respective PCR products (right panel) demonstrated two bands in carriers of the splice variant. While the smaller product at 250bp, which was present in all investigated Family members, corresponds to the exon5-exon6 junction-containing transcript, the upper product at 576bp represents a transcript with retained intron 5 in carriers of the splice site variant. Gray boxes=exons 1-6; white bar=intron; blue arrays=position of primers; bp=base pairs. Primer sequences are provided in the Appendix. **C)** Suggested alternative transcript including parts of the intron and a complete loss of exon six, caused by an introduced premature stop codon. The boxes represent exons 5 and 6 and the connecting line represents the intron.

## Results

### 3.1.5 RNA expression analysis and protein expression analysis

The effect of the splice variant (c.665-1G>A) on a molecular level was assessed with the following analysis. To measure the quantity of the RNA expression of different transcripts, three primer pairs were designed. They define the total, the canonical and the alternative transcript, which is the consequence of the splice variant (Figure 8).

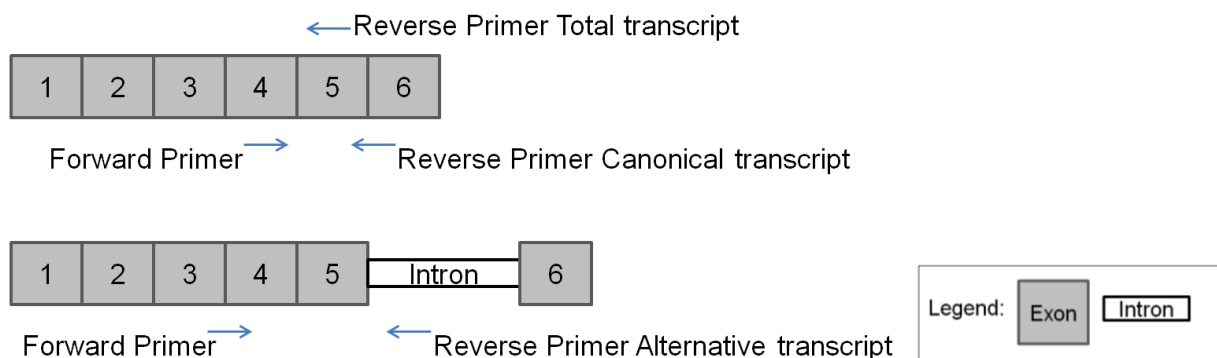


**Figure 8. Location of primers used to assess NAXE transcript expression.** Location of primers used to assess *NAXE* transcript expression levels in splice variant carriers, the missense variant carrier and a control. The forward primer for the canonical transcript is on exon 4 and the reverse primer is at the exon 5-6 junction. We used the same forward primer for the total transcript, but the reverse primer is on exon 5. As for the alternative transcript, the forward primer is at the exon 3-4 junction and reverse on intron 5. Primer sequences are provided in the Appendix.

In fibroblasts, we observed a significant reduction of canonical *NAXE* gene expression in all *NAXE* variant carriers (I.1, I.2, II.3) compared to the control subject ( $p < 0.001$ ) (Figure 9). Of note, a reduction of 40% was also present in the father (I.1) who carries a missense variant only, but was less pronounced compared to the carriers of the splice site variant with a reduction of approximately 70% (I.2, II.3). In turn, the alternative transcript with the retained intron 5 was elevated in the splice site variant carriers ( $p < 0.001$ ) but also expressed at a low level in the control and the father (I.1). Due to preferential binding of the primers designed for the total transcript to the canonical one, the total quantity of the transcripts could not be detected properly (Figure 9).

## Results

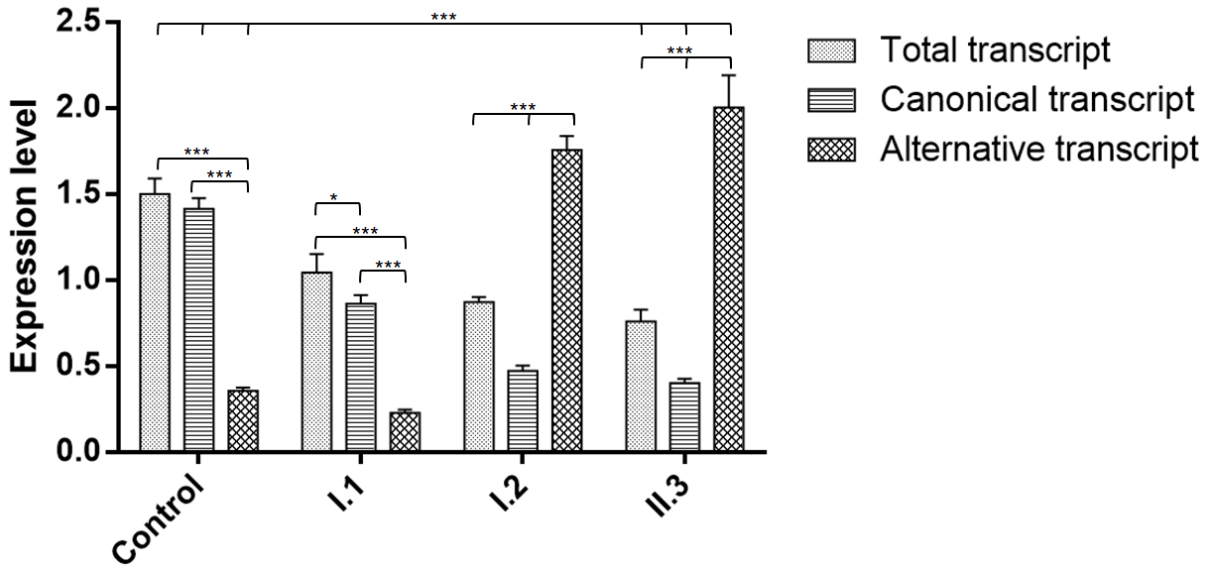


**Figure 9. *NAXE* gene expression analysis.** *NAXE* gene expression analysis in splice variant carriers (I.2 and II.3), the missense variant carrier (I.1) and a control regarding the total, canonical and alternative transcript (s. Figure 8). \*\*\*  $p < 0.0001$ ; \*  $p < 0.05$ .

Corresponding to the *NAXE* messenger RNA (mRNA) expression levels, there were no detectable *NAXE* protein levels in the patient (II.3) (Figure 10). The splice variant carrier (I.2) showed only weak *NAXE* levels compared to the missense variant carrier (I.1) and the control subject.

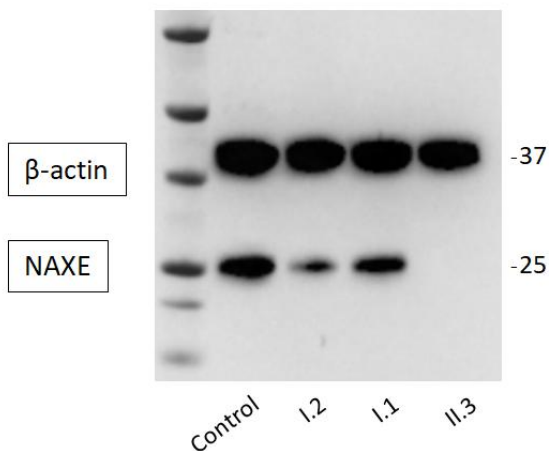


**Figure 10. Western blot analysis.** The Western blot shows *NAXE* protein levels in a control, the healthy parents (I.1 and I.2) and fibroblasts of the patient (II.3).  $\beta$ -Actin was used as a loading control.

## Results

### 3.1.6 Mitochondrial network analysis

The immunostaining with GRP75 visualizes the anatomy of the mitochondrial network in patient fibroblasts (II.3) compared to a control cell line. The results showed a non-significant reduction of mitochondrial branching in patient-derived fibroblasts.

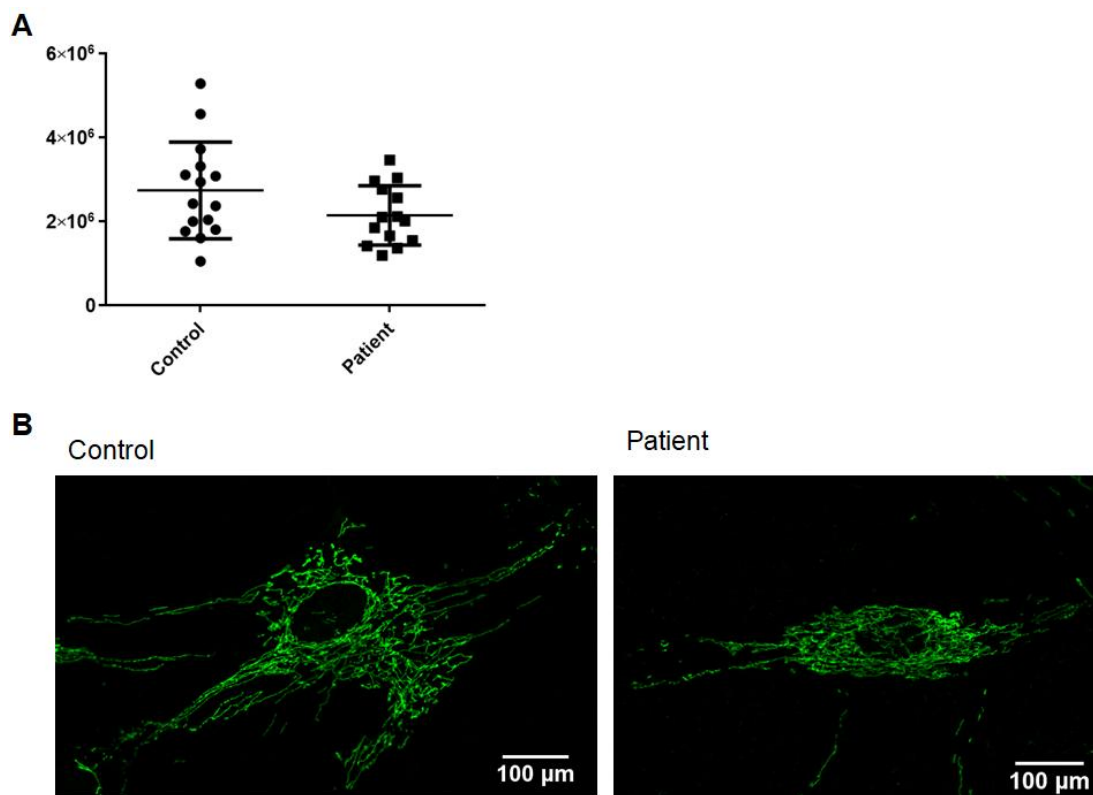


**Figure 11. Mitochondrial network analysis and examples of immunocytochemical staining and quantification.** Mitochondrial morphology of fibroblasts was investigated under basal conditions by confocal microscopy in fixed cells immunostained with anti-GRP75. **A)** The form factor as a measure for mitochondrial branching was calculated for one unaffected control fibroblast line and one patient (II.3). Each dot represents a measurement in a single cell (n=15). The median, the interquartile range, the minimum and the maximum value of the investigated individuals are shown (p=0.11). **B)** Mitochondrial network visualized by immunocytochemistry staining (antibody against GRP75) of a control subject and patient II.3 of Family 1.

### 3.1.7 Treatment outcome

Before the start of the specific therapy, the status of the patient began to improve and her tracheostomy could be removed. After the *NAXE* variants were identified as disease cause in patient II.3, treatment with coenzyme Q<sub>10</sub> and vitamin B<sub>3</sub> was introduced in spring 2017. Under daily therapy with coenzyme Q<sub>10</sub> and vitamin B<sub>3</sub>, the vitamin B<sub>3</sub> level in the blood was in the physiological range. Attentiveness, cognitive

## Results

function, mobility, speech, eating abilities and fine motor skills improved. From 2016 to 2018 the degree of spasticity decreased from 4 in the beginning to 1 at the Modified Ashworth Scale <sup>110</sup>. At the most recent follow-up in summer 2020 the patient was still wheelchair-bound and dependent on help for activities of daily living. She showed a stable disease course with a slight improvement in her mobility. It was reported that she suffered from pain sometimes. The patient was orientated to person and location. Her speech showed slight dysarthria and hypophonia. Strabismus, gaze-evoked nystagmus, tetraparesis with atrophy of muscle and hypesthesia and -algia of the lower extremities were part of her phenotype.

Therapy with 20mg vitamin B<sub>6</sub> per day was introduced in fall 2018 referring to the recently published paper on a potential moonlighting function of NAXE <sup>109</sup>. The blood level of vitamin B<sub>6</sub> was elevated twice under the supplementation so that at the most recent follow-up in summer 2020 the therapy was stopped and regular controls of the blood level of vitamin B<sub>6</sub> were recommended.

### **3.1.8 Replication and review of other *NAXE* variant carriers**

The next step was to verify if additional patients with variants in the same gene can be identified in the Replication cohort. Three other patients with homozygous missense variants (c.733A>C: p.Lys245Gln; c.652G>A: p.Asp218Asn and c.640A>G: p.Ile214Val) and unclear encephalopathy were found. They share features like developmental impairment, muscular hypotonia, respiratory insufficiency and brain MRI abnormalities. Family history for a similar disease phenotype was reported in all three cases. The case descriptions of Family 2-4 are reported in the Appendix.

## Results

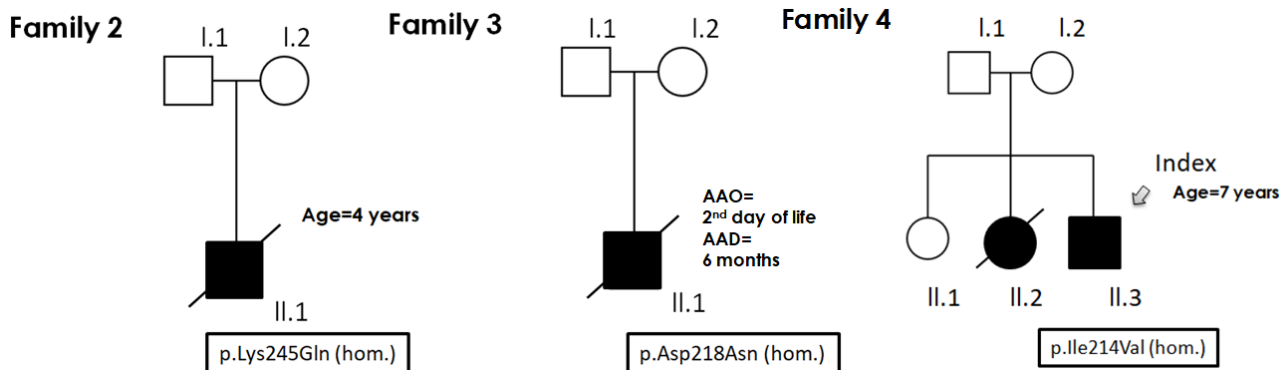


**Figure 12. Pedigrees of Family 2, 3 and 4.** The families are part of the Replication cohort. Box=male; circle=female. Black symbols represent affected Family members. White symbols indicate healthy individuals. Deceased Family members are crossed out. The array identifies the index patient. AAO=age at onset; AAD=age at death.

### 3.1.9 Classification of *NAXE* variants and phenotype description

Reports of other patients with *NAXE* variants and encephalopathy are present in the literature. The first report was on a fever-triggered neurological deterioration in five children born to consanguineous parents caused by a homozygous *NAXE* variant (p.Ala94Asp)<sup>111</sup>. The following two studies with a similar neurological phenotype and additional extensive Lyell-like bullous skin lesions reported compound-heterozygous and homozygous variants in *NAXE* comprising mostly truncating variants (p.Tyr59\*, p.Gln66\*, p.Lys270del, p.Asp218Val, p.Ala248Glufs\*26)<sup>52,108</sup>. Together with our findings, there are 18 patients and 14 different variants reported. Detailed information on the reported variants, including the ACMG classification, is provided in the following Table 19. Five variants were classified as pathogenic, two as likely pathogenic and for seven variants the relevance remained uncertain. The average minor allele frequency provided by GnomAD is  $2.032 \times 10^{-5}$  (range  $4.07 \times 10^{-6}$  -  $7.58 \times 10^{-5}$ ) and the average CADD score 30.4 (range 14.76 - 40). The average GERP score in the positions of all known variants is 4.73 (range 3.13 - 5.55).

## Results

**Table 19** Summary of the identified *NAXE* variants in all 14 reported cases.

ID	Chr	Position	cDNA	Protein	Type	Zygo sity	ExAC	Gnom AD	CADD score	GERP score	Fulfilled Criteria	ACMG Classif ication	Report ed clinical onset	Protein changes	Ref
Fam 1	1	1565636 73	c.665- 1G>A	NA	Splice	Cp. het	NA	NA	17.64	5.04	PVS1, PM2, PP1, PP3, PP4	Path	22/20 years	Undetect able protein levels	Our study
Fam 1	1	1565637 66	c.757G> A	p.Gly253 Ser	Missense	Cp. het	2.5 $\times 10^{-5}$	1.22 $\times 10^{-5}$	34	5.07	PM2, PP3, PP4	VUS	22/20 years	Undetect able protein levels	Our study
Fam 2	1	1565637 42	c.733A> C	p.Lys245 Gln	Missense	Hom	6.6 $\times 10^{-5}$	7.58 $\times 10^{-5}$	26.9	4.89	PM2, PP3, PP4	VUS	NA	NA	Our study
Fam 3	1	1565633 35	c.652G> A	p.Asp218 Asn	Missense	Hom	8.3 $\times 10^{-6}$	1.22 $\times 10^{-5}$	34	5.55	PM1, PM2, PM5, PP3, PP4	Likely Path	2nd day of life	NA	Our study
Fam 4	1	1565633 23	c.640A> G	p.Ile214 Val	Missense	Hom	NA	NA	14.76	4.42	PM2, PP3, PP4	VUS	NA	NA	Our study
Fam 5	1	1565617 73	c.177C> A	p.Tyr59*	Stop	Hom	NA	NA	36	3.13	PVS1, PM2, PP1, PP3, PP4	Path	20 months	Undetect able protein levels	Krem er et al <sup>2</sup>
Fam 6	1	1565619 06	c.196C> T	p.Gln66*	Stop	Cp. het	NA	2.17 $\times 10^{-5}$	40	4.57	PVS1, PM2, PP1, PP3, PP4	Path	15 months	Undetect able protein levels	Krem er et al <sup>2</sup>
Fam 6	1	1565624 63	c.516+1 G>A	NA	Splice	Cp. het	NA	4.07 $\times 10^{-6}$	25.5	4.27	PVS1, PM2, PP1, PP3, PP4	Path	15 months	NA	Krem er et al <sup>2</sup>
Fam 7	1	1565638 13	c.804_80 7del/insA	p.Lys270 del	Missense	Hom	NA	4.07 $\times 10^{-6}$	35	5.29	PM2, PP3, PP4	VUS	16 months	Highly decrease d protein levels	Krem er et al <sup>2</sup>

## Results

Fam 8	1	156563336	c.653A>T	p.Asp218Val	Missense	Cp. het	NA	1.22 x10 <sup>-5</sup>	32	5.55	PM1, PM2, PM5, PP3, PP4	Likely Path	16 months	NA	Krem er et al <sup>2</sup>
Fam 8	1	156563752	c.743delC	p.Ala248Glu	Frameshift	Cp. het	NA	NA	35	4.86	PVS1, PM2, PP1, PP3, PP4	Path	16 months	NA	Krem er et al <sup>2</sup>
Fam 9	1	156561991	c.281C>A	p.Ala94Asp	Missense	Hom	NA	NA	34	3.63	PM2, PP3, PP4	VUS	6-12 months	NA	Spieg el et al <sup>1</sup>
Fam 10	1	156562251	c.386G>C	p.Arg129Pro	Missense	Cp. Het.	NA	NA	32	4.41	PM2, PP3, PP4	VUS	18 months	NA	Inceci k and Ceyla ner
Fam 10	1	156563324	c.641T>G	p.Ile214Ser	Missense	Cp. het.	NA	NA	28.7	5.55	PM2, PP3, PP4	VUS	18 months	NA	Inceci k and Ceyla ner

Legend: Chromosomal position is based on human genome hg19 (assembly GRCh37), transcript NM\_144772.2, protein NP\_658985.2  
 Fam=Family, Cp. Het=compound-heterozygous, Hom=homozygous, Path=pathogenic, VUS=variants of uncertain significance, ExAC/GnomAD=minor allele frequency reported, Ref=reference of publication, NA=not available.

## Results

Table 20 gives an overview of the similarities and differences in the clinical phenotype of the 18 documented patients with *NAXE* variants and their affected siblings. Most of the patients, excluding Family 1 with a later age at onset, developed first symptoms within the first two years of life. The majority died within 1- 36 months of disease manifestation (average: 51.8 months; standard deviation (SD):  $\pm 76.53$  months). Patient II.3 was excluded as she is still alive and for Family 9 no exact data is available. The mitochondrial analysis in fresh muscle biopsy was assessed for seven patients. In four patients it was negative and in three, there were myopathic changes, complex I deficiency, generally decreased ATP or decreased oxidation of pyruvate-containing substrates. The literature research led not only to relevant information on variants in *NAXE*, but also on patients with *NAXD* variants showing a similar phenotype.

Results

**Table 20** Summary of the clinical phenotype of all 18 documented cases with *NAXE* variants and their affected siblings.

Family	ID	Sex	Origin	NAXE variants	AAO	AAD	Trigger	Mitochondrial analysis in fresh muscle biopsy	clinical and laboratory features
Family 1	II.1	M	Germany	NA	3 years	6 years	unclear	NA	fluctuating disease course, coma, vertigo, cognitive deficits, dysarthria, dysphagia, movement disorder, visual impairment, respiratory insufficiency
	II.3	F	Germany	c.665-1G>A, c.757G>A: p.G253S	22 years	8 years of disease duration, living patient	unclear	negative	initially headache, fluctuating disease course, seizures, coma, severe polyneuropathy, developmental impairment, speech problems, decreased oral intake, aseptic fever, movement disorder, ataxia, hypomimia, spastic tetraparesis, visual impairment, nystagmus, strabismus, neuropsychiatric symptoms, respiratory insufficiency
	II.4	F	Germany	c.665-1G>A, c.757G>A: p.G253S	20years	22 years	unclear	NA	initially headache, fluctuating disease course, coma, cognitive deficits, dysarthria, movement disorder, ataxia, hypomimia, nystagmus, diplopia, neuropsychiatric symptoms, respiratory insufficiency

## Results

Family 2	II.1	M	Saudi Arabia	c.733A>C: p.Lys245Gln	NA	NA	unclear	NA	developmental impairment, muscular hypotonia, respiratory insufficiency, sepsis, FH for mitochondrial encephalopathy
Family 3	II.2	M	Jordan	c.652G>A: p.Asp218Asn	2nd day of life	6 months	unclear	NA	coma, developmental impairment, decreased oral intake, muscular hypotonia, strabismus, respiratory insufficiency, hypoventilation, bradycardia, mitral regurgitation, thrombocytosis, decreased serum creatinine, brain atrophy, abnormality of the white matter, abnormal brainstem MRI signal intensity, intracranial hemorrhage
Family 4	II.3	M	India	c.640A>G: p.Ile214Val	NA	NA	unclear	NA	developmental impairment, pigmentary retinopathy, elevated serum creatine phosphokinase, elevated lactate in CSF, leukodystrophy, lissencephaly, cortical dysplasia, pachygyria, ventriculomegaly
Family 5	II.1	M	Gambia	c.177C>A: p.[Tyr59*]	20 months	21 months	fever/ infection	mild mitochondrial complex I deficiency; generally decreased ATP	fluctuating disease course, seizures, coma, movement disorder, ataxia, tetraparesis, torticollis, nystagmus, respiratory insufficiency, skin manifestations, elevated lactate in CSF and blood, brain edema, myelopathy

## Results

	II.2	F	Gambia	NA	19 months	24 months	fever/ infection	NA	fluctuating disease course, seizures, movement disorder, ataxia, tetraparesis, respiratory insufficiency, skin manifestations, elevated lactate in CSF, brain atrophy, myelopathy
Family 6	II.1	F	Croatia	c.196C>T: p.Gln66*, 516+1G>A	15 months	24 months	fever/ infection	myopathic changes; respiratory chain enzyme + PDH activity normal	fluctuating disease course, coma, developmental impairment, movement disorder, ataxia, tremor, muscular hypotonia, nystagmus, strabismus, respiratory insufficiency, skin manifestations, elevated lactate in CSF, brain edema, brain atrophy, myelopathy
Family 7	II.1	M	Germany	c.804_807delinsA: p.Lys270del	16 months	18 months	fever/ infection	decreased oxidation of pyruvate-containing substrates; acetylcarnitine-substrates normally oxidized; normal complex I-V +PDH activity	rapidly progressive, coma, developmental impairment, movement disorder, ataxia, nystagmus, bilateral ptosis, respiratory insufficiency, elevated lactate in CSF, brain edema
Family 8	II.1	M	Poland	c.653A>T: p.Asp218Val, c.743delC: p.Ala248Glufs*26	16 months	29 months	unclear	NA	fluctuating disease course, coma, dysarthria, movement disorder, ataxia, muscular hypotonia, nystagmus, respiratory insufficiency, skin manifestations, elevated lactate in CSF, brain edema

## Results

	II.2	M	Poland	c.653A>T: p.Asp218Val, c.743delC: p.Ala248Glufs*26	8 months	24 months	unclear	NA	fluctuating disease course, seizures, coma, muscular hypotonia, respiratory insufficiency, elevated lactate in CSF, brain atrophy, acute hydrocephalus
Family 9	II.1	F	Israel	NA	6-12 months	1-3 years	fever/ infection		
	II.2	F	Israel	c.281C>A: p.Ala94Asp	6-12 months	1-3 years	fever/ infection		
	II.4	F	Israel	NA	6-12 months	1-3 years	fever/ infection	3 patients: normal mitochondrial anatomy (light-, electron microscopy, immuno-histochemistry); activity of 5 enzymatic complexes and PDH normal	fluctuating disease course (2), coma (5), developmental impairment (5), movement disorder (5), muscular hypotonia (5), respiratory insufficiency (5), abnormality of the white matter (2)
	II.6	M	Israel	c.281C>A: p.Ala94Asp	6-12 months	1-3 years	fever/ infection		
	II.7	M	Israel	c.281C>A: p.Ala94Asp	6-12 months	>5.5 years	fever/ infection		

## Results

Family 10	II.1	M	Turkey	c.386G>C: p.Arg129Pro c.641T>G: p.Ile214Ser	18 months	3 years	fever/ infection	NA	Progressive course, seizures, coma, developmental impairment, cognitive impairment, speech problems, movement disorder, ataxia, muscular hypotonia, tetraparesis, torticollis, strabismus, respiratory insufficiency, skin manifestations, CSF normal, abnormality of the white matter, symmetrical hyperintensity of the basal ganglia (MRI)
--------------	------	---	--------	--	-----------	---------	---------------------	----	---

Legend: (number)=count of affected Family members showing the symptom; ID=in-house de-identified number; AAO=age at onset; AAD= age at death; M=male; F=female; NA=not available; FH=Family history; MRI=magnetic resonance imaging; CSF=cerebrospinal fluid; ATP=adenosine triphosphate; PDH=pyruvate dehydrogenase.



## Results

**Figure 13. Variant positions and evolutionary conservation of missense variants. A)** Location of all known variants in the *NAXE* gene. The gene is depicted with its six exons (boxes) and interrupting introns (lines). The location of identified variants is indicated by arrows. Variants in blue- and gray-shaded boxes (depending on the source) represent previously reported variants and white boxes represent variants found in our study. **B)** High conservation of amino acids altered by missense variants (highlighted by boxes and red letters) across species is shown. Pan troglodytes=chimpanzee; Sus scrofa=wild boars; Mus Musculus=house mouse; Lepidothrix coronata=blue-crowned manakin; Crocodylus porosus=saltwater crocodile; Seriola dumerili=greater amberjack.

## 3.2 Mitochondrial deep sequencing results

### 3.2.1 Mitochondrial sequencing dataset

A total variant count of 1,761 was detected in 28 samples of different cell types from seven individuals. 704 (39.98%) variants were homoplasmic (>70%) and 100 (5.68%) were at a heteroplasmy level between 15% and 70%. 957 (54.34%) variants were of low-level heteroplasmy (<15%). The mean sequencing depth was >10,000X across all 28 samples and the average total number of mtDNA variants detected per sample was 62.89 (SD:  $\pm 26.95$ ).

## Results

### 3.2.2 Mitochondrial DNA genome integrity during the differentiation process and across tissues

During the differentiation process from iPSCs to neurons, the concordance of homoplasmic variants (>70%) remained identical. For heteroplasmic variants (15-70%) the integrity remained high, but for variants at low-level heteroplasmy (<15%) the concordance was less than 20% (Table 21).

**Table 21** Integrity of mtDNA genome in iPSCs, neuron progenitors and neurons during the differentiation process derived from one individual.

Subject ID		>70%	15%-70%	<15%
		number of identical variants in IPSC/NP/Neuron integrity in (%)	number of identical variants in IPSC/NP/Neuron integrity in (%)	number of identical variants in IPSC/NP/Neuron integrity in (%)
L-2131	<i>IPSC/ NP/ Neuron</i>	37/ 37/ 37 (100.00%)	1/ 1/ 1 (75.00%)	11/ 14 /16 (17.75%)
L-2135	<i>IPSC/ NP/ Neuron</i>	37/ 37/ 37 (100.00%)	2/ 2/ 2 (100.00%)	5/ 11/ 10 (20.16%)
<b>Total</b>		<b>222/222</b>	<b>9/10</b>	<b>67/360</b>
<b>Total Concordance Percentage</b>		<b>100.00%</b>	<b>90.00%</b>	<b>18.61%</b>

Legend: The variants were separated into homoplasmic variants (>70%) and heteroplasmic variants, which were subdivided into 15-70% and <15% of heteroplasmy taking into account the minimum threshold associated with pathogenic effects of 15%. IPSC=induced pluripotent stem cell, NP=neuron progenitor; ID=in-house de-identified number.

## Results

Different iPSC clones of the same individual had high genome integrity for homoplasmic variants (>70%), but for heteroplasmic variants (<70%) the genome integrity was much lower (Table 22).

**Table 22** Integrity of mtDNA genome in different iPSC clones of the same individual.  
**mtDNA genome integrity in iPSC clones of the same individual**

<b>Subject ID</b>	<b>&gt;70%</b>	<b>15%-70%</b>	<b>&lt;15%</b>
	number of identical variants in iPSC clone 1+clone 2/ total variant count	number of identical variants in iPSC clone 1+clone 2/ total variant count	number of identical variants in iPSC clone 1+clone 2/ total variant count
	integrity in (%)	integrity in (%)	integrity in (%)
L-10886	29/32 (90.63%)	2/14 (14.29%)	6/43 (13.95%)
L-11148	66/67 (98.51%)	6/10 (60.00%)	8/41 (19.51%)
L-11156	34/34 (100.00%)	16/16 (100.00%)	8/28 (28.57%)
L-11167	40/41 (97.56%)	2/5 (40.00%)	2/21 (9.52%)
L-3857	36/39 (92.31%)	4/6 (66.66%)	4/40 (10.00%)
<b>Total</b>			
(identical variants/ total variants)	<b>205/213</b>	<b>30/51</b>	<b>28/173</b>
<b>Average</b>			
<b>Concordance</b>			
<b>Percentage</b>	<b>96.24%</b>	<b>58.82%</b>	<b>16.18%</b>

Legend: iPSC clones were chosen from multiple badges of the same individual for further differentiation. The variants were separated into homoplasmic variants (>70%) and heteroplasmic variants, which were subdivided into 15-70% and <15% of heteroplasmy taking into account the minimum threshold associated with pathogenic effects of 15%. mtDNA=mitochondrial DNA; iPSC=induced pluripotent stem cell; ID=in-house de-identified number.

## Results

Similar were the results for the concordance in blood and fibroblasts of the same individual. The extent of the genome integrity was very high in homoplasmic variants (>70%) and decreased with lower levels of heteroplasmy (Table 23).

**Table 23** Integrity of mtDNA variants in blood and fibroblasts of the same individual.  
**mtDNA genome integrity in blood and fibroblasts of the same individual**

Subject ID	>70%	15%-70%	<15%
	number of identical variants in blood+fibroblasts/ total variant count  integrity in (%)	number of identical variants in blood+fibroblasts/ total variant count  integrity in (%)	number of identical variants in blood+fibroblasts/ total variant count  integrity in (%)
L-10886	34/34 (100.00%)	4/4 (100.00%)	14/104 (13.46%)
L-11148	64/66 (96.97%)	4/10 (40.00%)	4/77 (5.19%)
L-11156	34/34 (100.00%)	4/8 (50.00%)	2/51 (3.92%)
L-11167	42/43 (97.67%)	4/5 (80.00%)	4/45 (8.88%)
L-3857	38/38 (100.00%)	4/4 (100.00%)	4/79 (5.06%)
<b>Total</b>			
(identical variants/ total variants)	<b>212/215</b>	<b>20/31</b>	<b>28/356</b>
<b>Average</b>			
<b>Concordance</b>			
<b>Percentage</b>	<b>98.60%</b>	<b>64.52%</b>	<b>7.87%</b>

Legend: The variants were separated into homoplasmic variants (>70%) and heteroplasmic variants, which were subdivided into 15-70% and <15% of heteroplasmy taking into account the minimum threshold associated with pathogenic effects of 15%. mtDNA=mitochondrial DNA; ID=in-house de-identified number.

Figure 14 gives an overview of the genome integrity across the different cell lines including all three comparisons (Table 21-23). During the differentiation process, the concordance was high over 15% heteroplasmy. The other two results show, that the variants in different tissues (blood and fibroblasts) and even in different iPSC clones

## Results

with a heteroplasmy under 70% were relatively unstable. In all investigations, homoplasmic variants (>70%) were nearly identical.

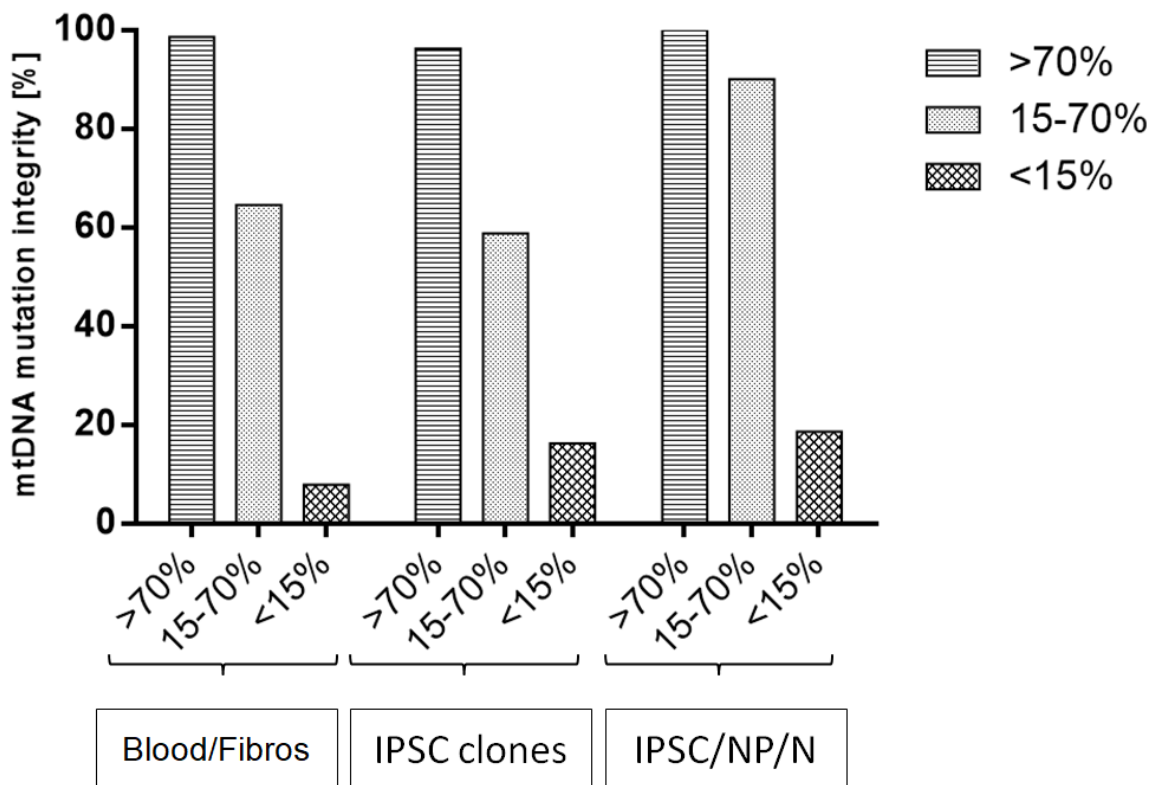


**Figure 14. The integrity of mtDNA variants across different tissues and during the differentiation process.** x-axis: percentages are referring to the level of heteroplasmy of the mtDNA variants. IPSC=induced pluripotent stem cell, NP=neuron progenitor, N=neuron.

### 3.2.3 Variant count in different tissues

The variant count of homoplasmic variants (>70%) was relatively similar in blood, fibroblasts and IPSCs. For heteroplasmic variants (<70%) the variant load varied between tissues mostly at a non-significant level. Regarding the reprogramming, there were significantly fewer heteroplasmic variants detected in IPSCs than in the fibroblast cell line for the five control cell lines in Figure 15A. In Figure 15B the difference was non-significant. During the differentiation process, there seems to be a trend of heteroplasmic variants to be fewer in neuron progenitors than in other cell lines (Figure 15).

## Results

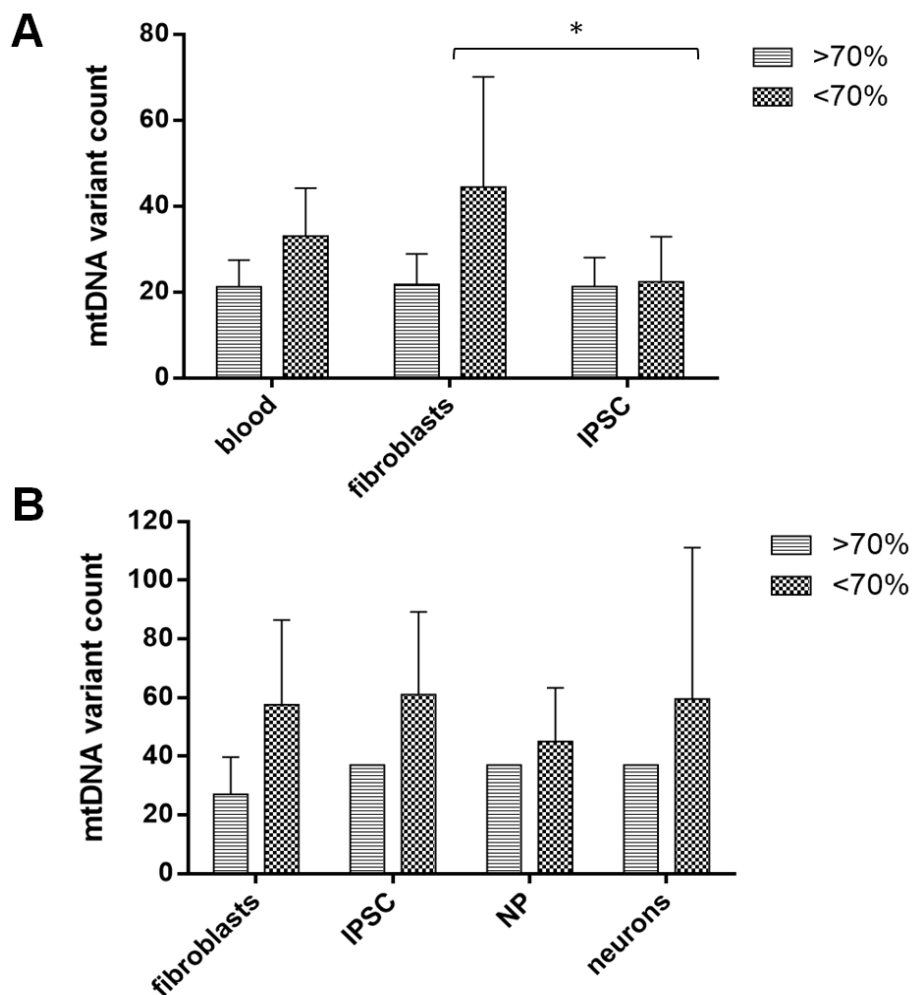


**Figure 15. Count of mtDNA variants in different tissues of healthy individuals. A)** mtDNA variants of a heteroplasmy >70% and <70% in blood, fibroblasts and IPSCs of five controls. \*= $p$ -value of 0.03; otherwise non-significant. **B)** mtDNA variants of a heteroplasmy >70% and <70% in fibroblasts, IPSCs, NPs and neurons of two controls.  $p$ -values >0.3; non-significant. IPSC=induced pluripotent stem cell; NP=neuron progenitor.

### 3.2.4 Influence of age on the variant quantity

Furthermore, the association of the mtDNA variant load and age was tested. The results showed no influence of the age on homoplasmic variants (>70%), but a non-significant trend that with a higher age the number of variants with a heteroplasmy <70% increases (Figure 16, Appendix).

### 3.3 Deep mitochondrial sequencing in brain tissue

#### 3.3.1 Mitochondrial sequencing dataset

A total variant count of 145 was detected in five brain tissue samples from patient II.4 and two control brains (SK00047, SK00148). 77 (53.10%) variants were homoplasmic (>70%), 68 (46.90%) heteroplasmic (<70%) and out of these 56 (82.35%) were of low-level heteroplasmy (<15%). The mean sequencing depth was >10,000X across all five samples and the average total number of mtDNA variants detected per sample was 29 (SD:  $\pm 9.87$ ).

**Table 24** Variant count of mtDNA variants in brain samples of patient II.4 and two controls (SK00047, SK00148).

	Heterozygous variant count (<70%)	Homozygous variant count (>70%)	Total variant count
FC II.4	4	14	18
PUT II.4	12	14	26
CB II.4	15	14	29
FC SK00047	28	17	45
FC SK00148	9	18	27

Legend: FC=frontal cortex; PUT=putamen; CB=cerebellum.

#### 3.3.2 Mitochondrial deep sequencing result

Excluding duplicates between brain regions, there are in total 37 variants found in the tissue of patient II.4 and 45 and 27 variants in the control samples. In total the five samples include ten variants with a ClinVar annotation classifying the variants as 'benign', 'likely pathogenic' or 'pathogenic'. The variants were filtered for 'pathogenic' and 'likely pathogenic' variants, wherein 7 variants were identified.

## Results

**Table 25** Pathogenicity of detected mtDNA variants classified as ‘pathogenic’ or ‘likely pathogenic’ in brain samples of patient II.4 and two controls (SK00047, SK00148).

Sample	Status	ClinVar	Variant	Variant type	ClinVar (MD)	Hp [%]	freq	qual
CB and PUT II.4	Patient	24697 [pathogenic]	NC_012920.1_ MT- CO2:c.2T>C, p.Met1?	Start-lost	Mitochondrial Encephalo- myopathy	0.7	5.38 $\times 10^{-9}$	26.8
CB, FC and PUT II.4	Patient	*150284 [likely_pathogenic]	NC_012920.1_ MT- CYB:c.580A>G , p.Thr194Ala	missense	NA	100	0.987	465. 3
FC SK00047	Control	76424 [pathogenic]	NC_012920.1_ MT- ND6:c.395C>T, p.Ser132Leu	missense	LHON	0.3	1.35 $\times 10^{-4}$	4.74
FC SK00047	Control	150279 [likely_pathogenic]	NC_012920.1_ MT- CYB:c.20C>T, p.Thr7Ile	missense	NA	0.3	0.75	5.73
FC SK00047	Control	*150284 [likely_pathogenic]	NC_012920.1_ MT- CYB:c.580A>G , p.Thr194Ala	missense	NA	100	0.987	465. 3
FC SK00148	Control	76417 [pathogenic]	NC_012920.1_ MT- ND4:c.494T>C, p.Ile165Thr	missense	LHON; PD	99. 9	7.09 $\times 10^{-3}$	457
FC SK00148	Control	*150284 [likely_pathogenic]	NC_012920.1_ MT- CYB:c.580A>G , p.Thr194Ala	missense	NA	100	0.987	465. 3

Legend: MD=Mito-Disease, FC=frontal cortex, PUT=putamen, CB=cerebellum, Hp=heteroplasmy, qual=quality score, freq=frequency, LHON= Leber’s hereditary optic neuropathy, PD=Parkinson’s disease, NA=not available, \*=variant is present in multiple samples.

## Results

A start loss variant in *MT-CO2* (c.2T>C, p.Met1?) was detected. It was present in the cerebellum and the putamen sample of patient II.4, but not in the frontal cortex samples. The ClinVar annotation identifies the variant as pathogenic for mitochondrial encephalopathy. OMIM (516040) reports a general association between the gene *MT-CO2* and movement disorders like ataxia and myopathy. The homoplasmic (100%) missense variant in *MT-CYB* (c.580A>G, p.Thr194Ala) was present in all five brain samples. The ClinVar annotation classifies it as likely pathogenic for familial cancer of the breast. Another heterozygous missense variant in *MT-CYB* (c.20C>T, p.Thr7Ile) that was observed in a control is classified as likely pathogenic. OMIM (516020) presents patient reports wherein *MT-CYB* is generally associated with movement disorders and myopathy. In one control sample, a missense variant was found in *MT-ND6* (c.395C>T, p.Ser132Leu). ClinVar classifies the variant as pathogenic. ClinVar as well as OMIM (516006) describe an association with the mitochondrial disease LHON (Leber's hereditary optic neuropathy). In the gene *MT-ND4*, a missense variant was identified (c.494T>C, p.Ile165Thr) in the second control sample. ClinVar classifies this variant as pathogenic in association with LHON and Parkinson's disease. OMIM (516003) also mentions an association of a variant in *MT-ND4* with LHON.

## 4 Discussion and Outlook

The Discussion sections correspond to the three Results sections:

4.1) evaluation of the WES result and subsequent analyses;

4.2) deep mtDNA sequencing and characterization of different tissues and iPSC models;

4.3) deep mtDNA sequencing in brain sections from patient II.4 (Family 1) compared to control subjects.

Lastly, the hypothesis and objectives that were presented in the introduction will be evaluated in the Conclusion.

### 4.1 Whole exome sequencing and subsequent analyses

#### 4.1.1 Diagnosis via whole exome sequencing

WES on a parent-offspring trio detected compound-heterozygous disease-causing variants in *NAXE* (c.757G>A: p.G253S, c.665-1G>A). The advantages and the effectiveness of WES are promising. It could expedite accurate genetic diagnosis in inherited mitochondria-related diseases with a negative gene panel diagnostic. As new variants causing mitochondrial diseases are identified and this list is still growing, WES is preferable to panel-based approaches<sup>49</sup>. It would be beneficial if WES were firmly integrated into the clinical guidelines for these rare diseases. The multidisciplinary work together with clinicians is indispensable for the diagnosis of neurogenetic disorders. If new variants were identified, there is still a need for additional laboratory diagnostics and functional tests to validate the relevance of a variant.

Even if it is not possible to revert the disease phenotype of patients with this diagnosis, it is a big step for the patients and their families to understand the source of their disorder. In general, establishing a genetic diagnosis allows better counseling regarding etiology, prognosis, recurrence risk and disease management.

### 4.1.2 Variant analysis

It is important to critically evaluate the results of WES. Sometimes it can be a challenge to determine if a variant is relevant to a disease. Critical assessment is necessary to evaluate how the variants explain the phenotype, especially in missense variants. If a variant is classified as damaging, it remains uncertain if it is one factor or the main cause. It is possible, that other disease modifiers or genetic causes play a role. Previously reported cases can shed light on whether there is an association between variants in the same gene and a specific disease phenotype. Our literature review confirmed this association for *NAXE* variants. The high evolutionary conservation and the fact that the gene annotations predict the variants as rare and potentially pathogenic help to identify *NAXE* as a good candidate. The ACMG classification is one method to classify a certain variant according to its level of pathogenicity. Our classification of all known 14 variants indicated five of the variants as pathogenic, two as likely pathogenic and for seven variants the relevance remained uncertain. Some criteria are flexible and open to interpretation so that new information can change the variant classification. The flexibility is necessary to modify the categorization if new relevant information is published. The interpretation is arbitrary since different people might come to different classifications based on the same information. The limits of the ACMG classification have to be considered in the interpretation.

Further experiments can help to strengthen the relevance of the specific variants in Family 1. The investigation of the splice site variant showed that it causes the production of an alternative transcript, which leads to the loss of the transcript encoded by exon 6. RNA expression showed that the canonical transcript was lower in expression for *NAXE* variant carriers compared to the control. In splice variant carriers the alternative transcript was overexpressed. This result shows, that the variants affect the gene expression and likely also on the canonical *NAXE* enzyme availability. A loss-of-function disease mechanism is suggested. A possible limitation is that the loss-of-function effect of *NAXE* variants was investigated in fibroblasts, but not brain tissue. Because *NAXE* is highly expressed in the brain, the consequences of missense and splice variants on *NAXE* expression could even be more deleterious

## Discussion and Outlook

there. This effect was not only detected in the patient, but also in the healthy parents, who carry heterozygous variants. One theory to explain this phenomenon is that the wildtype allele in parents can compensate for the defect, whereas in biallelic variant carriers the compensation is impossible, especially in the presence of a disease trigger. Genetic modifiers, such as high body temperature, alcohol or THC seem to play a role in the pathogenesis of NAXE deficiency. A negative effect of alcohol and THC on mitochondrial function is reported in the literature<sup>112,113</sup>. To date, NAXE protein levels were only investigated in samples of three patients (p.Tyr59\*, p.Gln66\* and 516+1G>A, and p.Lys270del) wherein NAXE was not detectable<sup>108</sup>. We observed the same effect as NAXE protein levels were undetectable in our patient, too (Figure 10). The heterozygous splice variant carrier (I.2, Family 1) had a decreased NAXE protein level, but did not show any symptoms. This leads to the assumption, that the human body can manage a decreased amount of protein up to some degree. An effect of the *NAXE* variants on the mitochondrial network was not present, even though there was a trend of reduced branching in the patient-derived fibroblasts. The reason could be that fibroblasts are not the affected cell type in this patient. For the following studies, it would be interesting to apply RNA expression analysis and mitochondrial form factor analysis in neurons.

A limitation of our study is the lack of cyclic-NADHX measurements that would have been valuable to confirm the involvement of our identified variants and their impact on this pathway but were beyond the scope of this project. Looking into available data from the literature, *NAXE* variants (p.Tyr59\*, p.Gln66\* and 516+1G>A, and p.Lys270del) were previously shown to lower NAXE protein levels and perturb cyclic-NADHX levels<sup>108</sup>. Thus, it would be interesting to investigate, if there is a similar effect for our variants. Another idea is to reprogram patient-derived fibroblasts into iPSCs and differentiate them into neurons for additional experiments in the tissue that is primarily affected in *NAXE* deficiency. To investigate the effect of missense variants without patient material, the variants could be introduced in fibroblast cell lines.

### 4.1.3 Replication cohort

The identification of additional patients with *NAXE* variants in the Replication cohort led to three more cases harboring homozygous missense variants (c.733A>C:

## Discussion and Outlook

p.Lys245Gln; c.652G>A: p.Asp218Asn and c.640A>G: p.Ile214Val). Other databases might detect even more patients with NAXE deficiency. This could mean that the disease is not as rare as reported so far. The phenotype is very complex and a diagnosis hard to assess. Maybe we talk about a lot more patients, who benefit from research advances and who could lead to important information on the disease.

The base of further studies is a good network of databases, which share information on rare diseases and make research in this domain fruitful. One point, which is a limitation in this study, is the scarce clinical information on the three *NAXE* variant carriers of the Replication cohort. Of course, to work with the data the information has to be standardized, for example by HPO-terms, but if the analysis detects a case of interest, it would be great to have access to as much raw data as possible. To ameliorate networks is an important challenge for research politics and in some fields, there is progress, e.g. the recently founded MDS gene database maintained by the International Parkinson and Movement Disorders Society (MDS), which is the first online database for movement disorders <sup>114</sup>.

### 4.1.4 Clinical disease phenotype

There are many overlapping symptoms across the 18 patients. For some patients the report on clinical symptoms is scarce, thus the overlap is likely underestimated. The main parallels are listed in Table 26.

**Table 26** Overlap of described symptoms in 18 reported cases.

Symptom	Count of patients showing the symptom (out of 18)
Respiratory insufficiency	17
Movement disorders	15 (including 8 with ataxia)
Comatose states	15
Developmental impairment	12
Fluctuating disease course	10
Muscular hypotonia	11
Abnormal MRI of CNS	11
Correlation: fever and clinical relapses	10
Increased lactate in CSF	7

## Discussion and Outlook

Ocular symptoms	7
Nystagmus	5
Seizures	5
Skin manifestation	5
Speech impairment/ dysarthria	5
Tetraparesis	4
Reduced oral intake/ dysphagia	3
Neuropsychiatric symptoms	2
Cardiac symptoms	1

Legend: MRI=magnetic resonance imaging; CNS=central nervous system; CSF=cerebrospinal fluid. Abnormal MRI of CNS includes brain atrophy, brain edema, abnormality of the white matter, ventriculomegaly and myelopathy. Ocular symptoms include visual impairment, diplopia, strabismus and ptosis. Neuropsychiatric symptoms include dementia, depersonalization, unsteady mood, visual hallucinations, organic psychosis, anxiety, bizarre behavior, catatonia and stuporous states.

We evaluated if the phenotype seen in these patients fits into the mitochondrial disorder spectrum. The complex clinical phenomenology described in the introduction overlaps strikingly with the symptoms observed in *NAXE*-deficient patients. First of all, the fluctuating disease course with episodes of improvement and deterioration seems to be a typical feature. Myopathy has been described as a very central manifestation<sup>37</sup>. In eleven of the cases muscular hypotonia has been observed, but also ocular problems like diplopia, strabismus and ptosis can be symptoms of muscular weakness, which often presents in small muscles first. Also, the hypomimia described in patients II.3 and II.4 of Family 1 and the speech problems might be due to a dysfunction of facial muscles. In periods of severe deterioration the described respiratory insufficiency might also be part of a myopathy. The absence of prenatal manifestations is common in mitochondrial diseases. Ataxia, seizures and psychiatric symptoms are the main characteristics. Other symptoms like cardiac problems were only described in one patient (Family 3). All in all the cases are clinically highly reminiscent of mitochondrial disease.

In contrast to the previously reported patients with biallelic *NAXE* variants, patients of Family 1 show a milder phenotype with disease onset in early adulthood and longer disease duration. This might be due to different variant types and positions as well as the variable expressivity of the disease. The origin of the patients might also play a role in different disease courses, as the medical care systems and standards are at

## Discussion and Outlook

different states. Two variants lie in the amino acid position of the predicted binding site of the encoded protein. One patient with a homozygous missense variant (c.652G>A: p.Asp218Asn) and two patients harboring a compound-heterozygous missense and stop variant (c.653A>T: p.Asp218Val; c.743delC: p.Ala248Glufs\*26). They showed a very early age at onset between the second day of life and 16 months. All three patients deceased between 6 and 29 months. Interestingly, patient II.1 of Family 3 is the only one presenting cardiac symptoms. We cannot observe a striking difference in severity compared to the other patients. A hypothesis could be that only variants in sensitive regions on the gene are disease-causing. Additional disease causes and modifiers cannot be excluded. For example, patient II.3 of Family 4 showed not only neurometabolic features, but also symptoms like pachygyria that are more reminiscent of early neurodevelopmental impairment. Whether or not this patient has an additional genetic cause, as it is observed in about 5% of genetic patients<sup>115,116</sup>, or if his phenotype is solely caused by the *NAXE* variants is uncertain. To elucidate the full clinical spectrum of *NAXE* variants, report and evaluation of more variant carriers is necessary.

Recently, homozygous and compound-heterozygous *NAXD* variant carriers with a very similar disease phenotype were reported<sup>117,118</sup>. NAD(P)HX-Dehydratase (*NAXD*) is an enzyme that is also part of the NADH/NAD<sup>+</sup> metabolism as shown in Figure 6B. The following Table 27 provides information on their variants and clinical features. In three patients the mitochondrial analysis in fresh muscle biopsy identified a decreased activity of respiratory chain complexes and in a fourth patient cytochrome c oxidase (COX) positive ragged red fibers were detected. The results highlight that mitochondria are affected by this disease.

**Table 27** Summary of the clinical phenotype of all seven reported cases with *NAXD* variants.

Family	ID	Sex	Origin	<i>NAXD</i> variants	AAO	AAD	Trigger	Mitochondrial analysis in fresh muscle biopsy	Clinical and laboratory features
Family 11	C1	M	NA	c.839+1G>T, p.(?) c.922C>T, p.Arg308Cys	3 years 7 months	4 years 6 months	fever/ infection	Mitochondrial respiratory chain enzymology (liver) normal, sequencing <i>POLG</i> gene and mitochondrial deletion and duplication studies normal	seizures, neurodegeneration, delayed speech development, progressive loss of speech, movement disorders (chorea, dystonia), gait unsteadiness, spastic tetraparesis, bilateral ophthalmoplegia, bilateral hearing loss, aggression (behavior change), 'burn like' skin lesions (axillae, groins), pancytopenia, oligoclonal bands in CSF, abnormal MRI
Family 12	C2	F	NA	c.187G>A, p.Gly63Ser c.948_949insTT, p.Ala317Leufs*64	14 months	3 years 10 months	fever/ infection	Respiratory chain studies (muscle): decreased activity of complex II and III	6-7 episodes of deterioration, neurodegeneration, developmental regression, progressive generalized dystonia, axial hypotonia, ophthalmoplegia, irritability, diarrhea, oral mucositis, skin rash, pancytopenia, CSF normal, abnormal MRI

## Discussion and Outlook

Family 13	C3	F	NA	c.51_54delAGAA, p.Ala20Phefs*9	1 year	1 year	fever/ infection	NA	vomiting, uprolling of eyeballs, lethargy, cyanosis, bradycardia, blood lactate elevated, MRI normal at 10 months, FH sibling very similar clinical course
Family 14	C4	M	United Kingdom	c.308C>T, p.Pro103Leu	3 months	NA	fever/ infection	Respiratory chain studies (muscle): decreased activity of complex I	infantile spasms (seizures), neurodegeneration, developmental regression, bilateral cataract, respiratory collapse, left ventricular hypertrophy, skin lesions (purple rash: axillae, neck, occiput, back, buttocks), pancytopenia, abnormal MRI
Family 15	C5	F	India	c.54_57delAAGA, p.Ala20Phefs*9	2 years 6 months	NA	fever/ infection	Muscle: COX positive ragged red fibers, full sequencing of mitochondrial genome no abnormalities	vomiting, unsteady gait (ataxia), jerky movements (limbs), lethargy, respiratory insufficiency, dilated cardiomyopathy, cardiopulmonary resuscitation, ECMO needed, cardiac failure, elevated lactate, CSF normal, MRI abnormal, FH sister with similar clinical course and death at 13 months

## Discussion and Outlook

Family 16	C6	F	Germany	c.331C>T, p.Leu111Phe c.776T>G, p.Leu259Arg	8 months	22 months	fever/ infection	Respiratory chain studies (muscle): decreased activity of complex I and IV	seizures, neurodegeneration, developmental delay, developmental regression, impaired coordination, unknown bowel disease, skin lesions (redness, blistering, peeling: anogenital region, hand), abnormal MRI, gastrointestinal imaging: erythematous, aphthous lesions
Family 17	C7	M	China	c.101_102delTA, p.Thr35Phefs*63 c.318C>G, p.Ile106Met	2 years 10 months	>5 years	fever/ infection	NA	Fluctuating disease course, disturbance of consciousness, vomiting, developmental regression, speech problems, dysphagia, movement disorder, dystonia, unsteady gait, involuntary movements, hypermyotonia, skin lesions, abnormal EEG, serum biotin reduced, CSF normal, brain edema of the cerebellum and basal ganglia (MRI), brain atrophy (MRI)

Legend: ID=in-house de-identified number; AAO=age at onset; AAD=age at death; M=male; F=female; NA=not available; FH=Family history; CSF=cerebrospinal fluid; MRI=magnetic resonance imaging; ECMO=extracorporeal membrane oxygenation; POLG gene=DNA Polymerase Gamma; COX=cytochrome c oxidase.

**Table 28** Additional NAXD-deficient patients showing symptoms observed in NAXE-deficient cases and their overlap in 25 reported cases (*NAXE* and *NAXD*). Referring to Table 26.

<b>Symptom</b>	<b>Additional patients <i>NAXD</i> (out of 7)</b>	<b>Count of patients <i>NAXE</i> and <i>NAXD</i> (out of 25)</b>
Respiratory insufficiency	2	19
Movement disorders	5 (including 1 with ataxia)	20 (including 9 with ataxia)
Comatose states	0 (excl. 1 with disturbance of consciousness)	15 (excl. 1 with disturbance of consciousness)
Developmental impairment	5	17
Fluctuating disease course	2	12
Muscular hypotonia	1	12
Abnormal MRI of CNS	6	17
Correlation: fever and clinical relapses	7	17
Increased lactate in CSF	0	7
Ocular symptoms	2	9
Nystagmus	0	5
Seizures	3	8
Skin manifestation	5	10
Speech impairment/ dysarthria	1	6
Tetraparesis	1	5
Reduced oral intake/ dysphagia	1	4
Neuropsychiatric symptoms	4	6
Cardiac symptoms	3	4

Legend: MRI=magnetic resonance imaging; CNS=central nervous system; CSF=cerebrospinal fluid. Abnormal MRI of CNS includes brain atrophy, brain edema, abnormality of the white matter, abnormal signal in basal ganglia, ventriculomegaly and myelopathy. Ocular symptoms include ophthalmoplegia, visual impairment, diplopia, strabismus and ptosis. Neuropsychiatric symptoms include dementia, depersonalization, unsteady mood, visual hallucinations, organic psychosis, anxiety, bizarre behavior, catatonia, stuporous states, lethargy, aggression and irritability.

Early death before five years of age was observed in 15 out of 25 cases. In seven cases the age at death was not available. This similar clinical picture of *NAXD* and *NAXE*-deficient patients supports the pathogenesis in the impaired NADH/NAD<sup>+</sup> metabolism. All collected information stresses *NAXE* as an important candidate to

be disease-causing in the reported cases. Testing for pathogenic *NAXE* variants should be considered in patients with a suspected mitochondrial disorder or inherited neurometabolic disease.

### 4.1.5 Therapeutic approach

Our study is an example of how a molecular diagnosis based on WES can shift from a phenotype-oriented symptomatic treatment to a molecular-based causal treatment. Other known disorders disrupting the NADH/NAD<sup>+</sup> metabolism have similarities to *NAXE* deficiency. For example, in neurons affected by GBA-Parkinson's disease, the NADH/NAD<sup>+</sup> metabolism and mitochondrial function are altered and can be rescued by NAD<sup>+</sup> precursor nicotinamide riboside<sup>57</sup>. Patients with Pellagra<sup>119</sup> suffer from a chronic lack of nicotinamide, which causes amongst other features skin lesions as observed in some of the reported cases with *NAXE*- and *NAXD*-deficiency. Hartnup disease<sup>120</sup> is an inherited disease that affects the renal and intestinal tryptophan transport. Tryptophan is an essential amino acid that is converted within the body to NAD<sup>+</sup>. Patients suffering from this and other diseases with symptoms similar to pellagra<sup>121</sup> do also develop a phenotype with skin lesions and neurological signs including ataxia. These patients could be successfully treated with vitamin B<sub>3</sub>, which promotes NAD<sup>+</sup> biosynthesis. Recently, a beneficial therapy for a patient with a compound-heterozygous *NAXD* variant was reported (Family 17, C7). A so-called 'mitochondrial cocktail' was applied including a high dose vitamin B<sub>3</sub> (10mg/kg/d) and coenzyme Q<sub>10</sub> (5mg/kg/d) substitution as well as vitamin B<sub>1</sub>, B<sub>2</sub>, C, E, idebenone and carnitine. Experience with vitamin B<sub>3</sub> medication in these diseases strengthens it to be a good therapeutic approach for patients with *NAXE* deficiency.

Vitamin B<sub>3</sub> supplementation has been shown to have an impact on cell homeostasis. NAD<sup>+</sup> is a substrate in NAD-mediated reactions of ADP-ribosyltransferases, which regulate important cellular processes including gene expression as well as apoptosis and cell cycle progression<sup>122,123</sup>. A knockout study of *NAXE* and *NAXD* in yeast and human cell lines showed that the NAD<sup>+</sup> pool is decreased in the knockout cell line. In human cell lines, a significant decrease was not measured<sup>124</sup>. NAD<sup>+</sup> pools can be restored by supplementation of vitamin B<sub>3</sub>, which gives us a chance to ameliorate patients' cell metabolism. To investigate the direct consequence of the treatment, a thorough investigation of

## Discussion and Outlook

vitamin B<sub>3</sub> supplementation on iPSC-derived neurons is warranted, but beyond scope of the present study, that describes the clinical outcome of vitamin B<sub>3</sub> treatment in a single patient (II.3, Family 1).

The new, applied therapy with vitamin B<sub>3</sub>, coenzyme Q<sub>10</sub> and the surveillance of the vitamin B<sub>6</sub> level in the blood for patient II.3 (Family 1) could be one factor for her improving clinical state. It is impossible to say, if this improvement is part of the normal disease course or if it is the benefit of the medication. However, for the applied treatment more evidence is warranted by follow-up over a longer period of the patient and more participants to fully assess the outcome of this medical administration. Even small treatment effects are important in diseases where no alternative therapy is available, although the application of new medication without experience should always be carefully controlled<sup>55</sup>.

A mean to evaluate the medical treatment could be to carry out a second skin biopsy and compare the OXPHOS metabolism to the fibroblasts, which were obtained before the start of the therapy. For example, ATP measurements or the activity of the respiratory chain complexes could be relevant. Nevertheless, with each additional patient, who is documented, the knowledge about the disease and possible management will grow and help to improve care for NAXE-deficient patients in the future.

### **4.2 Integrity across cell types and role of somatic variants**

Somatic variants are the main focus in the mtDNA section. In mitochondrial diseases, somatic variants may have an impact on disease onset and phenotype. We demonstrated in our analysis that not only the mtDNA genome integrity, but also the variant count varied between different cell types like blood and fibroblasts of the same individual. There is a trend indicating that heteroplasmic mtDNA variants were fewer in blood than in fibroblasts. This might be due to the fact, that blood cells were not in culture conditions as well as the shorter lifespan and higher turnover rate compared to fibroblasts<sup>66</sup>. In diagnostics and research, it is crucial for successful investigations to take the tissue that is affected by the disease. In neurological diseases, brain tissue is often not available for tests. As an alternative, hair follicle cells or muscle tissue are good candidates for the investigation of somatic variants.

## Discussion and Outlook

Aging and its association with mitochondrial dysfunction is a passionately discussed topic. Previous publications observed a higher mtDNA variant frequency in aged individuals<sup>22</sup>. In our cell lines, the differences between older and younger people were not significant, but the trend supported the observation for heteroplasmic variants (<70%). Mitochondrial impact on age-related diseases and aging itself remains an enigma. For example, advances in this area were made in Parkinson's disease research as one age-related disorder<sup>125,126</sup>.

### 4.2.1 Induced pluripotent stem cell model for neuronal studies

Additional studies through iPSC models could supplement our observations of the effect of *NAXE*-variants on the cellular, and especially the neuronal homeostasis. In our analyses, we assessed the changes of mtDNA genome integrity and count introduced by the reprogramming and differentiation process. We showed that heteroplasmic variants (<70%) were significantly less frequent in iPSCs compared to fibroblasts. A negative selection for pluripotency might be part of the reprogramming process and could explain the reduction of heteroplasmic variants in iPSCs. Homoplasmic mtDNA variants remained relatively stable as already observed in previous cell studies<sup>69,70</sup>. Extended culturing of iPSCs with high mtDNA heteroplasmy progressively purged mutant mtDNA<sup>72</sup>. It is recommendable to use an early iPSC passage to conserve the heteroplasmy level of variants.

Concerning mtDNA variants with a heteroplasmy >15%, the variants of the fibroblast that was picked for reprogramming were influenced, but did not change considerably during the differentiation process (Table 21). A limitation of the analysis during the differentiation process to neurons is the availability of only two different control cell lines. Different iPSC clones derived from one fibroblast cell line harbor different heteroplasmic variants and even homoplasmic variants were not identical. So it is recommended to validate findings with multiple iPSC clones to contribute more evidence to the results. Especially the concordance of heteroplasmic mtDNA variants (<70%) and variants at low-level heteroplasmy (<15%) seemed unstable. This makes it difficult to study somatic variants in iPSC-derived neurons. To optimize the success and the reliability of this model, it is important to analyze multiple fibroblast cell lines of the patient to obtain a better resolution. Experiments based on fibroblast cell lines of an early passage might have a higher chance to reflect the mtDNA changes of the original fibroblasts in

the skin biopsy. Thus, experiments based on early cell passages including multiple fibroblasts that are reprogrammed and multiple iPSC clones might be a good approach for these disease models.

### **4.2.2 Overview of neuronal models and their benefit in neurological research**

Multiple alternative methods including pluripotent stem cells (PSCs) have been developed. Cybrids are one of them allowing the investigation of the influence of mtDNA on cell function. Studies using this model elucidated the contribution of mtDNA to a variety of biochemical parameters and gave insight into the relationship between mtDNA and phenotype alterations. The main limitation of the cybrid-model is the disruption of patient-specific interaction between nDNA, which is taken from human PSCs, and mtDNA introduced from patients. Additionally, they rely mainly on glycolysis for energy production instead of OXPHOS metabolism, so effects upon mitochondrial insufficiency could be weaker<sup>78,127,128</sup>. Another alternative reduces the time needed to generate patient-specific neurons by reprogramming them directly out of patient fibroblasts by-passing the step of iPSCs. This could also preserve the aging-associated transcriptomic signature<sup>129</sup>. A limitation of this method is the lack of self-renewable cells leading to a paucity of material for high-throughput screening<sup>78</sup>. More physiological than these models might be the three-dimensional organoid, which harbors complex brain region-specific structures containing glial and neuronal cells derived from human PSCs<sup>130,131</sup>. However, they are still immature in comparison to the post-natal and adult brain. The last presented possibility is the use of iPSC-derived neuron progenitor cells, which were shown to have a similar gene expression pattern to human brain derived neuron progenitor cells<sup>69</sup>. This approach was successfully applied in Huntington's disease<sup>132,133</sup>. Proliferating neural progenitors are critically dependent on OXPHOS metabolism, which strengthens the promising preconditions of the model<sup>134</sup>.

PSC-derived neurons show signs of electrophysiological activity, but their gene expression pattern may still be immature compared to neurons of the human brain<sup>135</sup>. Of course, it is always a limitation that PSC-based models are in vitro cellular models, so culture conditions can influence the results and cannot completely imitate the reaction of the complex system of a whole organism<sup>136</sup>. Nevertheless,

the methods using PSCs as a source of neuronal cells can give a good impression of the genetic processes in mitochondria. It is not the aim to completely imitate the complexity of the neuronal network, because this is utopian. The goal is to develop good evaluated models, which facilitate the reality to get ideas of how the effects might be and verify these findings in the real neuronal system. They should complement each other in their possibilities to analyze different aspects. PSC models need to be studied in detail for their opportunities and limits, but they are a good base for research in mitochondrial and generally in neurological diseases. Validation of results observed in PSC models could be assessed in isolated patient's neurons<sup>64</sup> as well as in the brain itself.

### **4.3 Appraisal of deep mitochondrial sequencing in brain samples**

One limitation of the sequencing we applied is that it does not detect large deletions or duplications. Therefore we did not exclude the presence of large deletions in brain tissue, even if this is the most frequent variant type in post-mitotic tissues<sup>20</sup>.

The genes *MT-CO2* and *MT-CYB*, which were identified by deep mitochondrial sequencing are generally associated with movement disorders and myopathy. Even the ClinVar annotation for the start loss variant in *MT-CO2* (c.2T>C, p.Met1?) describes an association with mitochondrial encephalopathy, but the variant had a very low level of heteroplasmy with 0.7%. This is far away from the minimum threshold associated with pathogenic effects of 15%. The relevance of the mtDNA variants remains uncertain, but most likely not relevant to this disease. In general, the variant count in samples of the patient was not elevated compared to the controls. Taking into account the minimum threshold associated with pathogenic effects of 15% and a minor allele frequency of <0.01, there was only one variant showing these criteria: the homoplasmic (99.9%) missense variant in *MT-ND4* (c.494T>C, p.Ile165Thr) in a control brain sample. Variants in *MT-ND4* have been reported to associate with LHON and Parkinson's disease, but in this case, the control did not show a specific disease phenotype. There is much information missing for gene annotations and their analysis. For example, it is unclear, which demands should be applied regarding quality for low-level heteroplasmic variants. Furthermore, out of in total 109 different variants, there was information for the classification of pathogenicity for ten variants. For the other

## Discussion and Outlook

99, it remains unclear, which relevance they might have. In the absence of gene annotations, the analysis is limited. The reported investigation of mtDNA variants in NAXD-deficient patients (Family 10 and 14) did not detect any relevant variants, too. Analysis of large deletions or duplications was not part of this project, but would be a good supplementation for following studies. By improving methods for the analysis of mtDNA sequencing data, likely more novel mtDNA variants and their implication in diseases will be found. More knowledge on mtDNA variants and their pathogenic pathways could also help to develop better treatments than only symptomatic ones.

### 4.4 Conclusion

In reference to the hypothesis and objectives described in the introduction, the conclusions are presented:

- (1) Via WES we identified a compound-heterozygous missense and splicing variant in *NAXE* (p.G253S, c.665-1G>A) as a disease cause, which stresses the importance of WES as a diagnostic method in inherited diseases. The literature review led to three reports on twelve patients with a similar phenotype and biallelic variants in *NAXE*. Three additional patients with homozygous missense variants in *NAXE* (p.Lys245Gln, p.Asp218Asn, p.Ile214Val) were identified in the Replication cohort. Lastly, a genotype-specific therapy with substitution of vitamin B<sub>3</sub>, coenzyme Q<sub>10</sub> and vitamin B<sub>6</sub> was introduced to patient II.3 (Family 1). The effect of the medication remains unclear due to the fluctuating disease course and the lack of experience in other patients.
- (2) The mtDNA genome between different tissues, like blood and fibroblasts, was not identical. It is crucial for diagnostics and research to investigate the tissue which is affected by the disorder to obtain the best representation of mtDNA variations. The variants of the fibroblasts, which were picked for reprogramming, were influenced especially in heteroplasmic variants. In contrast, the variants did not change considerably during the differentiation process. As heteroplasmic variants varied across different iPSC clones and underwent most changes by reprogramming and differentiation compared to homoplasmic variants, it is important to reprogram multiple fibroblasts and analyze multiple iPSC clones to arrive at a more representative result. Cells should be chosen from early passages. Knowing the limits and opportunities of

## Discussion and Outlook

IPSC models, they are a promising way to study the effects of mtDNA variants on the cell and to identify new therapeutic approaches in mitochondrial and generally in neurological diseases. The number of mtDNA variants in aged compared to younger individuals was not significantly higher in our cell lines, but the trend supports the observation of previous studies for heteroplasmic variants (<70%).

- (3) In the deep mtDNA sequencing data of three brain samples (II.4, Family 1) we did not identify a variant candidate that explains the clinical picture. The variant count in samples of the patient was not elevated compared to controls. Analysis of mtDNA variants at all heteroplasmy levels is challenging.

## 5 Summary

Massive parallel sequencing is an effective diagnostic means in inherited mitochondrial and generally in neurological disorders. The whole exome sequencing data of a parent-offspring trio was analyzed. Compound-heterozygous missense and splicing (p.G253S, c.665-1G>A) variants in *NAXE*, that segregated with disease in this Family, were identified. Variant as well as RNA and protein expression analysis and investigation of mitochondrial morphology was performed, which strengthened the pathogenic relevance. Based on the metabolic pathway, vitamin B<sub>3</sub>, B<sub>6</sub> and coenzyme Q<sub>10</sub> treatment was introduced in one patient resulting in continuous improvement. The molecular diagnosis can lead to a more refined treatment based on genotype. Additional screening in 4,351 patients identified novel homozygous missense variants (p.Lys245Gln, p.Asp218Asn, p.Ile214Val) in three patients. Compared to other patients with biallelic *NAXE* variants, patients of Family 1 showed a milder phenotype with a later age at disease onset. Otherwise, a considerable overlap of the phenotype was observed. The clinical picture falls into the mitochondrial disorder spectrum.

The behavior of somatic variants in mtDNA was elaborated by analysis of deep mitochondrial sequencing data. The correlation of increasing age and higher mtDNA variant quantity could be supported for heteroplasmic variants (<70%). We observed that somatic variants vary between tissues of the same individual and therefore it is crucial in diagnostics to choose, if available, the affected tissue. It was shown that different iPSC clones may have differences in their variant profile, especially in heteroplasmic variants (<70%). Variants were influenced by reprogramming. The differentiation process from iPSCs to neurons had a more stable mtDNA variant profile with  $\geq 90\%$  concordance for variants >15% heteroplasmy. In combination with other iPSC models and with a detailed evaluation of limits and chances the model promises to advance research in inherited mitochondrial and generally neurological disorders.

Deep sequencing of mtDNA in brain tissue of a patient with severe encephalopathy did not identify genetic changes that explain the clinical phenotype. The low information yield on mtDNA variants was a deficit.

## 6 Zusammenfassung

Mitochondriale Erkrankungen sind mit ihrer phänotypischen Vielfalt und bislang eingeschränkten Behandlungsmöglichkeiten eine Herausforderung für die medizinische Versorgung. Die Prävalenz beträgt ungefähr 1 von 5000 Geburten. Whole Exome Sequencing (WES) ist eine effektive Form der genetischen Diagnostik für Patienten mit einer vermutlich vererbaren Erkrankung im Bereich mitochondrialer Störungen.

In dieser Studie wurde eine WES Trio Analyse durchgeführt mit Proben der Eltern und zweier betroffener Töchter, die eine unklare familiäre Enzephalopathie aufweisen. Das Krankheitsbild umfasst einen schubartigen Verlauf mit epileptischen Anfällen, Myoklonus, spastischer Lähmung der Extremitäten, Bewegungsstörungen wie zum Beispiel cerebelläre Ataxie, Schluck- und Sprechstörungen sowie okuläre Auffälligkeiten einschließlich Diplopie und Nystagmus. Außerdem wurden neuropsychiatrische Symptome, Polyneuropathie und Vigilanzstörungen bis hin zu komatösen Zuständen mit respiratorischer Insuffizienz beobachtet. Es wurde eine kombiniert heterozygote Missense- und Splicing-Mutation (p.G253S, c.665-1G>A) im *NAXE*-Gen gefunden. Es wurde gezeigt, dass durch die Splicing-Mutation ein alternatives Transkript entsteht, das in den Mutationsträgern signifikant überexprimiert wurde, wohingegen das reguläre Transkript in Splicing- und Missense-Mutationsträgern reduziert exprimiert wurde. Die mitochondriale Morphologie wurde durch eine Form-Faktor Analyse untersucht, die ergab dass das mitochondriale Netzwerk in den Fibroblasten der Patientin weniger ausgeprägt war als in der Kontrolle. Ein Western Blot zeigte eine verringerte Menge des NAXE-Proteins in der Probe der heterozygoten Splicing-Mutationsträgerin im Vergleich zu einer Kontrolle und dem Missense-Mutationsträger. In der Probe der kombiniert heterozygoten Mutationsträgerin war die Proteinmenge nicht darstellbar. Als Pathomechanismus wird ein Funktionsverlust des NAXE-Proteins durch die Mutationen vermutet. Durch die molekulare Diagnose erhielt die Patientin II.3 der Familie 1, vor dem Hintergrund der vermuteten Pathogenese in der Störung des NADH/NAD<sup>+</sup> Stoffwechsels, eine Therapie mit Coenzym Q<sub>10</sub>, Vitamin B<sub>3</sub> und zeitweise auch Vitamin B<sub>6</sub>. Hierunter verbesserte sich ihr gesundheitlicher Zustand über einen Zeitraum von mehr als 3 Jahren stetig auf niedrigem Niveau.

## Zusammenfassung

Desweiteren wurden in einer Replikationskohorte mit 4351 Patienten drei zusätzliche Patienten mit bislang unbekanntem homozygoten Missense-Mutationen (p.Lys245Gln, p.Asp218Asn, p.Ile214Val) im *NAXE*-Gen identifiziert, die einen ähnlichen Phänotyp aufweisen. Insgesamt mit den in der Literatur bereits publizierten Fällen ergeben sich bei 18 Patienten 14 unterschiedliche Mutationen, die sich in ihrer Symptomatik überlappen. Die häufigsten gemeinsamen Symptome sind: respiratorische Insuffizienz, Bewegungsstörungen, komatöse Zustände, Entwicklungsstörungen, muskuläre Hypotonie, auffällige Bildgebungsbefunde des zentralen Nervensystems, sowie schubartige Verläufe mit Fieber als Auslöser für Krankheitsschübe. Es fällt auf, dass die Patienten der Familie 1 einen späteren Zeitpunkt der Krankheitsmanifestation haben und einen generell milderen Verlauf zeigen. Insgesamt passt das klinische Bild in das Spektrum mitochondrialer Erkrankungen. Interessant ist der Vergleich mit den in der Literatur beschriebenen Patienten mit Mutationen im *NAXD*-Gen, die ebenso den NADH/NAD<sup>+</sup> Stoffwechsel betreffen und klinisch sehr ähnliche Charakteristika zeigen. Weitere Krankheitsursachen und Auslöser können nicht ausgeschlossen werden. Als möglicher Auslöser von Krankheitsschüben wird vor allem Fieber beziehungsweise Infektionen, aber auch der Konsum von Tetrahydrocannabinol und Alkohol in Betracht gezogen.

Außerdem beschäftigt sich diese Arbeit mit somatischen Mutationen in der mitochondrialen DNA (mtDNA), die mittels Deep Sequencing untersucht wurden. In einer Zelle können Mitochondrien mit unterschiedlicher mtDNA-Sequenz vorhanden sein, was als Heteroplasmie bezeichnet wird. Somatische Mutationen können ab einem Anteil von mindestens 15% Heteroplasmie Einfluss auf die Funktion der Zelle nehmen und somit pathogene Effekte haben. Die Prävalenz der zehn häufigsten pathogenen mtDNA Mutationen in der allgemeinen Bevölkerung liegt bei 1 zu 200. Trotz der hohen Prävalenz scheinen die Mutationen unter der Schwelle der Pathogenität zu bleiben. MtDNA Mutationen werden in Zusammenhang sowohl mit mitochondrialen als auch mit neurodegenerativen Erkrankungen gebracht, aber auch mit natürlichen Prozessen wie dem Altern selbst.

Im Vergleich von Proben jüngerer und älterer Probanden beobachteten wir für Mutationen <70% Heteroplasmie einen Trend der Zunahme von somatischen

## Zusammenfassung

Mutationen mit dem Alter. Mutationen der mtDNA wurden in unterschiedlichen Zelltypen untersucht. Blutzellen, Fibroblasten, induzierte pluripotente Stammzellen (iPSC), Neuron-Vorläufer-Zellen und Neurone eines einzigen Probanden wiesen in unseren Analysen unterschiedliche Mutationsprofile auf. Deshalb ist es entscheidend in der Diagnostik somatischer Mutationen sofern möglich das von der Erkrankung betroffene Gewebe zu untersuchen. Im Vergleich von unterschiedlichen iPSC-Klonen eines Probanden fiel auf, dass sich die Mutationen insbesondere bei einer Heteroplasmie <70% voneinander unterschieden und die Mutationen durch die Reprogrammierung von Fibroblasten zu iPSCs beeinflusst wurden. Während dem Differenzierungsprozess von iPSCs zu Neuronen zeigte sich das Mutationsprofil stabiler mit  $\geq 90\%$  Übereinstimmung für Mutationen mit einer Heteroplasmie >15%.

Zur Nutzung dieses Modells für die Untersuchung von somatischen Mutationen in Neuronen, sowie deren Auswirkungen auf die Zelle, empfiehlt es sich Fibroblasten einer frühen Passage zu wählen und mehrere iPSC Klone zu analysieren um die Aussagekraft zu erhöhen. Es ist unabdingbar, die Stärken und Schwächen eines Untersuchungsmodells zu kennen, um eine Interpretation der Ergebnisse vorzunehmen. Unterschiedliche Modelle sollten sich hier ergänzen, um die neurologische Forschung in diesem Bereich voranzutreiben.

Der letzte Teil der Dissertation untersucht die Ergebnisse des Deep Sequencing der mtDNA im Gehirngewebe der Patientin II.4 aus Familie 1, sowie von zwei Kontrollen. Von insgesamt 109 Mutationen waren Anmerkungen, die Auskunft über die Pathogenität geben, für zehn Mutationen verfügbar. Hierunter wurden sieben Mutationen als möglich pathogen oder pathogen eingestuft. Die Relevanz der Mutationen konnte nicht abschließend beurteilt werden. Es ergab sich kein Hinweis darauf, dass die identifizierten mtDNA Mutationen einen Einfluss auf das Krankheitsbild der Patientin II.4 aus Familie 1 haben. Der geringe Informationsgewinn über die mtDNA Mutationen ist ein Nachteil. Es wird eine Herausforderung für zukünftige Forschung sein mehr Aussagekraft für die Analyse der mtDNA Mutationen zu erreichen. Eine gute Zusammenarbeit von Datenbanken ist hierbei von großer Bedeutung.

## 7 References

1. Schon E, DiMauro S, Hirano M. Human mitochondrial DNA: roles of inherited and somatic mutations. *Nat Rev Genet.* 2012;13:878-890.
2. Ke R, Xu Q, Li C, Luo L, Huang D. Mechanisms of AMPK in the Maintenance of ATP Balance during Energy Metabolism. *Cell Biology International.* 2018;42:384-392.
3. Miller W. Steroid hormone synthesis in mitochondria. *Molecular and Cellular Endocrinology.* 2013;379:62-73.
4. Adams J. Ways of dying: multiple pathways to apoptosis. *Genes & Development.* 2003;17:2481-2495.
5. Williams G, Boyman L, Chikando A, Khairallah R, Lederer W. Mitochondrial calcium uptake. *PNAS.* 2013;110:10479-10486.
6. Zorov D, Juhaszova M, Sollott S. MITOCHONDRIAL REACTIVE OXYGEN SPECIES (ROS) AND ROS-INDUCED ROS RELEASE. *Physiol Rev.* 2014;94:909-950.
7. Slone J, Gui B, Huang T. The current landscape for the treatment of mitochondrial disorders. *Med Genet.* 2018;45(2):71-77. doi:10.1016/j.jgg.2017.11.008
8. McFarland R, Taylor R, Turnbull D. A neurological perspective on mitochondrial disease. *Lancet Neurol.* 2010;9:829-840.
9. Debray F-G, Lambert M, Mitchell GA. Disorders of mitochondrial function. *Curr Opin Pediatr.* 2008;20:471-482.
10. DiMauro S, Schon E, Carelli V, Hirano M. The clinical maze of mitochondrial neurology. *Nat Rev Neurol.* 2013;9:429-444.
11. Parikh S, Goldstein A, Koenig MK, et al. Diagnosis and management of mitochondrial disease: a consensus statement from the Mitochondrial Medicine Society. *Genet Med.* 2014;17:689.
12. Lee HK. Advances around technologies investigating mitochondrial function and insights gained by their applications. *J Diabetes Investig.* 2014;5:144-146.
13. Sagan L. On the origin of mitosing cells. *Journal of Theoretical Biology.* 1967;14:225-274.
14. Stewart JB, Chinnery PF. The dynamics of mitochondrial DNA heteroplasmy: implications for human health and disease. *Nat Rev Genet.* 2015;16:530-542.
15. Pinto M, Moraes CT. Mechanisms linking mtDNA damage and aging. *Free Radic Biol Med.* 2015;85:250–258.

## References

16. Wallace DC. Mitotic segregation of mitochondrial DNAs in human cell hybrids and expression of chloramphenicol resistance. *Somat Cell Mol Genet*. 1986;12(1):41-49. doi:10.1007/BF01560726
17. Rossignol R, Faustin B, Rocher C. Mitochondrial threshold effects. *Biochem J*. 2003;370:751-762.
18. Tuppen HAL, Blakely EL, Turnbull DM, Taylor RW. Mitochondrial DNA mutations and human disease. *Biochim Biophys Acta*. 2010;1797(2):113-128. doi:10.1016/j.bbabi.2009.09.005
19. Youle R, van der Bliek A. Mitochondrial Fission, Fusion, and Stress. *Science*. 2012;337:1062-1065.
20. Pinto M, Moraes CT. Mitochondrial genome changes and neurodegenerative diseases. *Biochim Biophys Acta*. 2014;1842:1198-1207.
21. Bender A, Krishnan KJ, Morris CM. High levels of mitochondrial DNA deletions in substantia nigra neurons in aging and Parkinson disease. *Nat Genet*. 2006;38:515-517.
22. Kang E, Wang X, Tippner-Hedges R. Age-Related Accumulation of Somatic Mitochondrial DNA Mutations in Adult-Derived Human iPSCs. *Cell Stem Cell*. 2016;18:625–636.
23. Haas R, Parikh S, Falk M, et al. The In-Depth Evaluation of Suspected Mitochondrial Disease: *Mol Genet Metab*. 2008;94:16-37.
24. Neupert W, Herrmann J. Translocation of Proteins into Mitochondria. *Annu Rev Biochem*. 2007;76:723-749.
25. Attwell D, Laughlin SB. An Energy Budget for Signaling in the Grey Matter of the Brain. *J Cereb Blood Flow Metab*. 2001;21(10):1133-1145. doi:10.1097/00004647-200110000-00001
26. Bratic A, Larsson N-G. The role of mitochondria in aging. *Journal of Clinical Investigation*. 2013;123:951-957.
27. Larsson N-G. Somatic Mitochondrial DNA Mutations in Mammalian Aging. *Annu Rev Biochem*. 2010;79:683-706.
28. Wallace DC. A Mitochondrial Paradigm of Metabolic and Degenerative Diseases, Aging, and Cancer: A Dawn for Evolutionary Medicine. *Annu Rev Genet*. 2005;39:359.
29. Gorman G, Schaefer A, Ng Y, et al. Prevalence of Nuclear and Mitochondrial DNA Mutations Related to Adult Mitochondrial Disease. *Ann Neurol*. 2015;77:753-759.
30. Skladal D, Halliday J, Thorburn D. Minimum birth prevalence of mitochondrial respiratory chain disorders in children. *Brain*. 2003;126:1905-1912.

## References

31. Elliott HR, Samuels DC, Eden JA, Relton CL, Chinnery PF. Pathogenic Mitochondrial DNA Mutations Are Common in the General Population. *Am J Hum Genet.* 2008;83(2):254-260. doi:10.1016/j.ajhg.2008.07.004
32. Munnich A, Rötig A, Chretien D, Saudubray J, Cormier V, Rustin P. Clinical presentations and laboratory investigations in respiratory chain deficiency. *Eur J Pediatr.* 1996;155:262-274.
33. Tranchant C, Anheim M. Movement disorders in mitochondrial diseases. *Revue neurologique.* 2016;172:524-529.
34. Rahman S. Mitochondrial disease and epilepsy. *Developmental Medicine & Child Neurology.* 2012;54:397-406.
35. Lax N, Gorman G, Turnbull D. Review: Central nervous system involvement in mitochondrial disease. *Neuropathology and Applied Neurobiology.* 2017;43:102-118.
36. Falk M. Neurodevelopmental Manifestations of Mitochondrial Disease. *J Dev Behav Pediatr.* 2010;31:610-621.
37. Ahuja A. Understanding mitochondrial myopathies: a review. *PeerJ.* 2018;6:e4790.
38. Barends M, Verschuren L, Morava E, Nesbitt V, Turnbull D, McFarland R. Causes of Death in Adults with Mitochondrial Disease. *JIMD Reports.* 2015;26:103-113.
39. Córdoba M, Rodríguez-Quiroga SA, Vega PA, et al. Whole exome sequencing in neurogenetic odysseys: An effective, cost- and time-saving diagnostic approach. *PLOS ONE.* 2018;13(2):e0191228. doi:10.1371/journal.pone.0191228
40. Trinh J, Lohmann K, Baumann H, et al. Utility and implications of exome sequencing in early-onset Parkinson's disease. *Mov Disord.* 2019;34(1):133-137. doi:10.1002/mds.27559
41. Walters WD, Garnica AD, Schaefer GB. McArdle Disease Presenting With Muscle Pain in a Teenage Girl: The Role of Whole-Exome Sequencing in Neurogenetic Disorders. *Case Stud Issue 5.* 2018;26:50-51. doi:10.1016/j.spen.2017.03.004
42. Meng L, Pammi M, Saronwala A, et al. Use of Exome Sequencing for Infants in Intensive Care Units: Ascertainment of Severe Single-Gene Disorders and Effect on Medical Management. *JAMA Pediatr.* 2017;171(12):e173438-e173438. doi:10.1001/jamapediatrics.2017.3438
43. Kuperberg M, Lev D, Blumkin L, et al. Utility of Whole Exome Sequencing for Genetic Diagnosis of Previously Undiagnosed Pediatric Neurology Patients. *J Child Neurol.* 2016;31(14):1534-1539. doi:10.1177/0883073816664836

## References

44. Monroe GR, Frederix GW, Savelberg SMC, et al. Effectiveness of whole-exome sequencing and costs of the traditional diagnostic trajectory in children with intellectual disability. *Genet Med*. 2016;18:949.
45. Howell KB, Eggers S, Dalziel K, et al. A population-based cost-effectiveness study of early genetic testing in severe epilepsies of infancy. *Epilepsia*. 2018;59(6):1177-1187. doi:10.1111/epi.14087
46. Best S, Wou K, Vora N, Van der Veyver IB, Wapner R, Chitty LS. Promises, pitfalls and practicalities of prenatal whole exome sequencing. *Prenat Diagn*. 2018;38(1):10-19. doi:10.1002/pd.5102
47. Warr A, Robert C, Hume D, Archibald A, Deeb N, Watson M. Exome Sequencing: Current and Future Perspectives. *G3 GenesGenomesGenetics*. 2015;5(8):1543. doi:10.1534/g3.115.018564
48. Wortmann SB, Koolen DA, Smeitink JA, van den Heuvel L, Rodenburg RJ. Whole exome sequencing of suspected mitochondrial patients in clinical practice. *J Inherit Metab Dis*. 2015;38(3):437-443. doi:10.1007/s10545-015-9823-y
49. Theunissen TEJ, Nguyen M, Kamps R, et al. Whole Exome Sequencing Is the Preferred Strategy to Identify the Genetic Defect in Patients With a Probable or Possible Mitochondrial Cause. *Front Genet*. 2018;9:400. doi:10.3389/fgene.2018.00400
50. Legati A, Reyes A, Nasca A, et al. New genes and pathomechanisms in mitochondrial disorders unraveled by NGS technologies. *EBEC 2016 19th Eur Bioenerg Conf*. 2016;1857(8):1326-1335. doi:10.1016/j.bbabbio.2016.02.022
51. Morava É, Heuvel L, Hol F, et al. Mitochondrial disease criteria - Diagnostic applications in children. *Neurology*. 2006;67:1823-1826. doi:10.1212/01.wnl.0000244435.27645.54
52. Pronicka E, Piekutowska-Abramczuk D, Ciara E. New perspective in diagnostics of mitochondrial disorders: two years' experience with whole-exome sequencing at a national paediatric centre. *J Transl Med*. 2016;14(1):174.
53. El-Hattab AW, Zarante AM, Almannai M, Scaglia F. Therapies for mitochondrial diseases and current clinical trials. *Mol Genet Metab*. 2017;122(3):1-9. doi:10.1016/j.ymgme.2017.09.009
54. Parikh S, Goldstein A, Karaa A, et al. Patient care standards for primary mitochondrial disease: a consensus statement from the Mitochondrial Medicine Society. *Genet Med*. 2017;19:1380.
55. Pfeffer G, Horvath R, Klopstock T, et al. New treatments for mitochondrial disease - No time to drop our standards. *Nat Rev Neurol*. 2013;9:474-481.
56. Rodriguez MC, MacDonald JR, Mahoney DJ, Parise G, Beal MF, Tarnopolsky MA. Beneficial effects of creatine, CoQ10, and lipoic acid in

## References

- mitochondrial disorders. *Muscle Nerve*. 2007;35(2):235-242. doi:10.1002/mus.20688
57. Schöndorf DC, Ivanyuk D, Baden P, et al. The NAD<sup>+</sup> Precursor Nicotinamide Riboside Rescues Mitochondrial Defects and Neuronal Loss in iPSC and Fly Models of Parkinson's Disease. *Cell Rep*. 2018;23(10):2976-2988. doi:10.1016/j.celrep.2018.05.009
  58. Houtkooper R, Auwerx J. Exploring the therapeutic space around NAD<sup>+</sup>. *J Cell Biol*. 2012;199:205–209.
  59. Tachibana M, Sparman M, Sritanaudomchai H, et al. Mitochondrial gene replacement in primate offspring and embryonic stem cells. *Nature*. 2009;461(7262):367-372. doi:10.1038/nature08368
  60. Srivastava S, Moraes CT. Manipulating mitochondrial DNA heteroplasmy by a mitochondrially targeted restriction endonuclease. *Hum Mol Genet*. 2001;10(26):3093-3099. doi:10.1093/hmg/10.26.3093
  61. Gammage PA, Rorbach J, Vincent AI, Rebar EJ, Minczuk M. Mitochondrially targeted ZFNs for selective degradation of pathogenic mitochondrial genomes bearing large-scale deletions or point mutations. *EMBO Mol Med*. 2014;6(4):458-466. doi:10.1002/emmm.201303672
  62. Zhang Y, Long C, Bassel-Duby R, Olson EN. Myoediting: Toward Prevention of Muscular Dystrophy by Therapeutic Genome Editing. *Physiol Rev*. 2018;98(3):1205-1240. doi:10.1152/physrev.00046.2017
  63. Pallotti F, Chen X, Bonilla E, Schon EA. Evidence that specific mtDNA point mutations may not accumulate in skeletal muscle during normal human aging. *Am J Hum Genet*. 1996;59:591-602.
  64. Dölle C, Flønes I, Nido GS, et al. Defective mitochondrial DNA homeostasis in the substantia nigra in Parkinson disease. *Nat Commun*. 2016;7:13548.
  65. Picard M, Zhang J, Hancock S, et al. Progressive increase in mtDNA 3243A>G heteroplasmy causes abrupt transcriptional reprogramming. *Proc Natl Acad Sci*. 2014;111(38):E4033. doi:10.1073/pnas.1414028111
  66. Rahman S, Poulton J, Marchington D, Suomalainen A. Decrease of 3243 A->G mtDNA mutation from blood in MELAS syndrome: a longitudinal study. *Am J Hum Genet*. 2001;68(1):238-240. doi:10.1086/316930
  67. Sue CM, Quigley A, Katsabanis S, et al. Detection of MELAS A3243G point mutation in muscle, blood and hair follicles. *J Neurol Sci*. 1998;161(1):36-39. doi:10.1016/S0022-510X(98)00179-8
  68. Petersen KF, Befroy D, Dufour S. Mitochondrial Dysfunction in the Elderly: Possible Role in Insulin Resistance. *Science*. 2003;300:1140-1142.
  69. Lorenz C, Lesimple P, Bukowiecki R, et al. Human iPSC-Derived Neural Progenitors Are an Effective Drug Discovery Model for Neurological mtDNA

## References

- Disorders. *Cell Stem Cell*. 2017;20(5):659-674.e9. doi:10.1016/j.stem.2016.12.013
70. Ma H, Folmes CDL, Wu J, et al. Metabolic rescue in pluripotent cells from patients with mtDNA disease. *Nature*. 2015;524:234.
71. Cherry ABC, Gagne KE, Mcloughlin EM, et al. Induced Pluripotent Stem Cells with a Mitochondrial DNA Deletion. *STEM CELLS*. 2013;31(7):1287-1297. doi:10.1002/stem.1354
72. Folmes CDL, Martinez-Fernandez A, Perales-Clemente E, et al. Disease-Causing Mitochondrial Heteroplasmy Segregated Within Induced Pluripotent Stem Cell Clones Derived from a Patient with MELAS. *STEM CELLS*. 2013;31(7):1298-1308. doi:10.1002/stem.1389
73. Hatakeyama H, Katayama A, Komaki H, Nishino I, Goto Y. Molecular pathomechanisms and cell-type-specific disease phenotypes of MELAS caused by mutant mitochondrial tRNA<sup>Trp</sup>. *Acta Neuropathol Commun*. 2015;3(1):52. doi:10.1186/s40478-015-0227-x
74. Soragni E, Miao W, Iudicello M, et al. Epigenetic therapy for Friedreich ataxia. *Ann Neurol*. 2014;76(4):489-508. doi:10.1002/ana.24260
75. Ng S-Y, Soh BS, Rodriguez-Muela N, et al. Genome-wide RNA-Seq of Human Motor Neurons Implicates Selective ER Stress Activation in Spinal Muscular Atrophy. *Cell Stem Cell*. 2015;17(5):569-584. doi:10.1016/j.stem.2015.08.003
76. Hossini AM, Megges M, Prigione A, et al. Induced pluripotent stem cell-derived neuronal cells from a sporadic Alzheimer's disease donor as a model for investigating AD-associated gene regulatory networks. *BMC Genomics*. 2015;16(1):84. doi:10.1186/s12864-015-1262-5
77. Israel MA, Yuan SH, Bardy C, et al. Probing sporadic and familial Alzheimer's disease using induced pluripotent stem cells. *Nature*. 2012;482:216.
78. Inak G, Lorenz C, Lisowski P, Zink A, Mlody B, Prigione A. Concise Review: Induced Pluripotent Stem Cell-Based Drug Discovery for Mitochondrial Disease. *STEM CELLS*. 2017;35(7):1655-1662. doi:10.1002/stem.2637
79. Li H, Durbin R. Fast and accurate short read alignment with Burrows–Wheeler transform. *Bioinformatics*. 2009;25:1754–1760.
80. Trujillano D, Bertoli-Avella A, Kandaswamy K. Clinical exome sequencing: results from 2819 samples reflecting 1000 families. *Eur J Hum Genet*. 2017;25(2):176–182.
81. Wang K, Li M, Hakonarson H. ANNOVAR: functional annotation of genetic variants from high-throughput sequencing data. *Nucleic Acids Res*. 2010;38(16):e164-e164. doi:10.1093/nar/gkq603

## References

82. Broad Institute. Exome Aggregation Consortium (ExAC). Accessed September 10, 2019. <http://exac.broadinstitute.org>
83. Broad Institute. Genome Aggregation Database (gnomAD). Accessed September 10, 2019. <https://gnomad.broadinstitute.org>
84. University of Washington, Hudson-Alpha Institute for Biotechnology and Berlin Institute of Health. CADD - Combined Annotation Dependent Depletion. Accessed September 10, 2019. <https://cadd.gs.washington.edu/score>
85. University of California. UCSC Genome Browser. Accessed September 14, 2019. <https://genome.ucsc.edu/>
86. U.S. National Library of Medicine. National Center for Biotechnology Information (NCBI). Accessed September 14, 2019. <https://www.ncbi.nlm.nih.gov/>
87. Stanford University Medical Center. Genomic Evolutionary Rate Profiling: GERP. Accessed September 14, 2019. <http://mendel.stanford.edu/SidowLab/downloads/gerp/index.html>
88. The UniProt Consortium. Universal Protein Resource (UniProt). Accessed September 14, 2019. <https://www.uniprot.org/>
89. Johns Hopkins University. Online Mendelian Inheritance in Man (OMIM). Accessed September 14, 2019. <https://www.omim.org/>
90. Ziegler A, Colin E, Goudenège D, Bonneau D. A snapshot of some pLI score pitfalls. *Hum Mutat.* 2019;40(7):839-841. doi:10.1002/humu.23763
91. Lek M, Karczewski KJ, Minikel EV, et al. Analysis of protein-coding genetic variation in 60,706 humans. *Nature.* 2016;536(7616):285-291. doi:10.1038/nature19057
92. European Bioinformatics Institute (EMBL-EBI). Ensembl. Accessed September 14, 2019. <https://www.ensembl.org/index.html>
93. Groza T, Köhler S, Moklenhauer D. The Human Phenotype Ontology: Semantic Unification of Common and Rare Disease. *Am J Hum Genet.* 2015;97:111-124.
94. Saiki R, Scharf S, Faloona F, et al. Enzymatic amplification of beta-globin genomic sequences and restriction site analysis for diagnosis of sickle cell anemia. *Science.* 1985;230(4732):1350-1354.
95. Sanger F, Nicklen S, Coulson A. DNA sequencing with chain-terminating inhibitors. *Proc Natl Acad Sci USA.* 1977;74(12):5463-5467.
96. Paul Stothard. Reverse Complement. Accessed September 14, 2019. [https://www.bioinformatics.org/sms/rev\\_comp.html](https://www.bioinformatics.org/sms/rev_comp.html)

## References

97. Whitehead Institute for Biomedical Research, Rozen S, Untergasser A, Remm M, Koressaar T, Skaletsky H. Primer3web version 4.1.0 - Pick primers from a DNA sequence. Accessed September 10, 2019. <https://genome.ucsc.edu>; <http://primer3.ut.ee>
98. Nikfarjam L, Farzaneh P. Prevention and detection of Mycoplasma contamination in cell culture. *Cell J*. 2012;13(4):203-212.
99. Uphoff C, Drexler H. Detection of Mycoplasma contamination in cell cultures. *Curr Protoc Mol Biol*. 2014;106(28):1-14.
100. Tajadini M, Panjehpour M, Javanmard S. Comparison of SYBR Green and TaqMan methods in quantitative real-time polymerase chain reaction analysis of four adenosine receptor subtypes. *Adv Biomed Res*. 2014;3:85.
101. Mortiboys H, Thomas KJ, Werner JHK, et al. Mitochondrial function and morphology are impaired in parkin mutant fibroblasts. *Ann Neurol*. 2008;64(5):555-565.
102. Grünewald A, Voges L, Rakovic A, et al. Mutant Parkin impairs mitochondrial function and morphology in human fibroblasts. *PLoS One*. 2010;5:e12962.
103. Richards S, Aziz N, Bale S. Standards and Guidelines for the Interpretation of Sequence Variants: A Joint Consensus Recommendation of the American College of Medical Genetics and Genomics and the Association for Molecular Pathology. *Genet Med*. 2015;17(5):405-424.
104. McElroy K, Thomas T, Luciani F. Deep sequencing of evolving pathogen populations: applications, errors, and bioinformatic solutions. *Microb Inform Exp*. 2014;4(1):1-1. doi:10.1186/2042-5783-4-1
105. Seibler P, Graziotto J, Jeong H, Simunovic F, Klein C, Krainc D. Mitochondrial Parkin recruitment is impaired in neurons derived from mutant PINK1 iPS cells. *J Neurosci*. 2011;31:5970-5976.
106. National Center for Biotechnology Information (NCBI), U.S. National Library of Medicine. ClinVar. Accessed September 14, 2019. <https://www.ncbi.nlm.nih.gov/clinvar/>
107. Elhassan Y, Philp A, Lavery G. Targeting NAD<sup>+</sup> in Metabolic Disease: New Insights Into an Old Molecule. *J Endocr Soc*. 2017;1:816–835.
108. Kremer L, Danhauser K, Herebian D. NAXE Mutations Disrupt the Cellular NAD(P)HX Repair System and Cause a Lethal neurometabolic disorder of Early Childhood. *Am J Hum Genet*. 2016;99:894–902.
109. Niehaus TD, Elbadawi-Sidhu M, Huang L, et al. Evidence that the metabolite repair enzyme NAD(P)HX epimerase has a moonlighting function. *Biosci Rep*. 2018;38(3):BSR20180223. doi:10.1042/BSR20180223
110. Bohannon RW, Smith MB. Interrater Reliability of a Modified Ashworth Scale of Muscle Spasticity. *Phys Ther*. 1987;67(2):206-207. doi:10.1093/ptj/67.2.206

## References

111. Spiegel R, Shaag A, Shalev S. Homozygous mutation in the APOA1BP is associated with a lethal infantile leukoencephalopathy. *Neurogenetics*. 2016;17:187–190.
112. Hoek JB, Cahill A, Pastorino JG. Alcohol and mitochondria: A dysfunctional relationship. *Gastroenterology*. 2002;122(7):2049-2063. doi:10.1053/gast.2002.33613
113. Fišar Z, Singh N, Hroudová J. Cannabinoid-induced changes in respiration of brain mitochondria. *Toxicol Lett*. 2014;231(1):62-71. doi:10.1016/j.toxlet.2014.09.002
114. International Parkinson and Movement Disorder Society. MDS Task Force Launches First Ever Genetic Mutation Database for Movement Disorders (MDSGene). Accessed September 14, 2019. <https://www.mdscongress.org/Congress-2016/News-Releases/Database-for-Movement-Disorders-MDSGene.htm>
115. Posey JE, Harel T, Liu P, et al. Resolution of Disease Phenotypes Resulting from Multilocus Genomic Variation. *N Engl J Med*. 2016;376(1):21-31. doi:10.1056/NEJMoa1516767
116. Trinh J, Kandaswamy KK, Werber M, et al. Novel pathogenic variants and multiple molecular diagnoses in neurodevelopmental disorders. *J Neurodev Disord*. 2019;11(1):11. doi:10.1186/s11689-019-9270-4
117. Van Bergen NJ, Guo Y, Rankin J, et al. NAD(P)HX dehydratase (NAXD) deficiency: a novel neurodegenerative disorder exacerbated by febrile illnesses. *Brain*. 2018;142(1):50-58. doi:10.1093/brain/awy310
118. Zhou J, Li J, Stenton SL, et al. NAD(P)HX dehydratase (NAXD) deficiency: a novel neurodegenerative disorder exacerbated by febrile illnesses. *Brain*. 2019;(awz375). doi:10.1093/brain/awz375
119. Piqué-Duran E, Pérez-Cejudo J, Cameselle D. Pellagra: A Clinical, Histopathological, and Epidemiological Study of 7 Cases. *Actas Dermosifiliogr*. 2012;103(1):51-58.
120. Salih M, Bender D, McCreanor G. Lethal Familial Pellagra-like Skin Lesion Associated With Neurologic and Developmental Impairment and the Development of Cataracts. *Pediatrics*. 1985;76(5):787-793.
121. Baron D, Dent C, Harris H. Hereditary pellagra-like skin rash with temporary cerebellar ataxia, constant renal aminoaciduria, and other bizarre biochemical features. *The Lancet*. 1956;271:421-428.
122. Gasperi V, Sibilano M, Savini I, Catani VM. Niacin in the Central Nervous System: An Update of Biological Aspects and Clinical Applications. *Int J Mol Sci*. 2019;20(4). doi:10.3390/ijms20040974
123. Nikiforov A, Kulikova V, Ziegler M. The human NAD metabolome: Functions, metabolism and compartmentalization. *Crit Rev Biochem Mol Biol*. 2015;50(4):284-297. doi:10.3109/10409238.2015.1028612

## References

124. Becker-Ketter J, Paczia N, Conrotte J-F, et al. NAD(P)HX repair deficiency causes central metabolic perturbations in yeast and human cells. *FEBS J.* 2018;285(18):3376-3401. doi:10.1111/febs.14631
125. Coxhead J, Kurzawa-Akanbi M, Hussain R, Pyle A, Chinnery P, Hudson G. Somatic mtDNA variation is an important component of Parkinson's disease. *Neurobiol Aging.* 2016;38:217.e1-217.e6. doi:10.1016/j.neurobiolaging.2015.10.036
126. Berenguer-Escuder C, Grossmann D, Massart F, et al. Variants in Miro1 Cause Alterations of ER-Mitochondria Contact Sites in Fibroblasts from Parkinson's Disease Patients. *J Clin Med.* 2019;8(12). doi:10.3390/jcm8122226
127. Kondoh H, Leonart M, Gil J, Beach D, Peters G. Glycolysis and cellular immortalization. *Drug Discov Today Dis Mech.* 2005;2:263-267. doi:10.1016/j.ddmec.2005.05.001
128. Wilkins HM, Carl SM, Swerdlow RH. Cytoplasmic hybrid (cybrid) cell lines as a practical model for mitochondriopathies. *Redox Biol.* 2014;2:619-631. doi:10.1016/j.redox.2014.03.006
129. Mertens J, Paquola ACM, Ku M, et al. Directly Reprogrammed Human Neurons Retain Aging-Associated Transcriptomic Signatures and Reveal Age-Related Nucleocytoplasmic Defects. *Cell Stem Cell.* 2015;17(6):705-718. doi:10.1016/j.stem.2015.09.001
130. Kelava I, Lancaster MA. Stem Cell Models of Human Brain Development. *Cell Stem Cell.* 2016;18(6):736-748. doi:10.1016/j.stem.2016.05.022
131. Lancaster MA, Renner M, Martin C-A, et al. Cerebral organoids model human brain development and microcephaly. *Nature.* 2013;501:373.
132. Charbord J, Poydenot P, Bonnefond C, et al. High throughput screening for inhibitors of REST in neural derivatives of human embryonic stem cells reveals a chemical compound that promotes expression of neuronal genes. *STEM CELLS.* 2013;31(9):1816-1828. doi:10.1002/stem.1430
133. The HD iPSC Consortium. Induced Pluripotent Stem Cells from Patients with Huntington's Disease Show CAG-Repeat-Expansion-Associated Phenotypes. *Cell Stem Cell.* 2012;11(2):264-278. doi:10.1016/j.stem.2012.04.027
134. Beckervordersandforth R, Ebert B, Schäffner I, et al. Role of Mitochondrial Metabolism in the Control of Early Lineage Progression and Aging Phenotypes in Adult Hippocampal Neurogenesis. *Neuron.* 2017;93(3):560-573.e6. doi:10.1016/j.neuron.2016.12.017
135. Nicholas CR, Chen J, Tang Y, et al. Functional Maturation of hPSC-Derived Forebrain Interneurons Requires an Extended Timeline and Mimics Human Neural Development. *Cell Stem Cell.* 2013;12(5):573-586. doi:10.1016/j.stem.2013.04.005

## References

136. Bénit P, Schiff M, Cwerman-Thibault H, Corral-Debrinski M, Rustin P. Drug development for mitochondrial disease: Recent progress, current challenges, and future prospects. *Expert Opinion on Orphan Drugs*. 2015;4.

## 8 Appendix

### 8.1 Chemicals

5x Sequencing Buffer	Thermo Fisher
10x Incubation Mix T. Pol with MgCl <sub>2</sub>	MP Biomedicals
10x Incubation Mix T. Pol without MgCl <sub>2</sub>	MP Biomedicals
100 bp DNA Ladder	New England Biolabs
Accutase	Life technologies
Agarose	Biozym Scientific
Fetal Bovine Serum (FBS)	Life technologies
Bovine Serum Albumin (BSA)	Sigma-Aldrich
Bromphenol Blue-Na-salt	Serva
DAPI Fluoromount-G	Southern Biotech
Deoxyribonucleotides (dNTPs)	MP Biomedicals
Dimethyl sulfoxide	Sigma-Aldrich
DNase I	Thermo Fisher
Dulbecco's Modified Eagle Medium (DMEM)	Life technologies Fetal
Dulbecco's Phosphate Buffered Saline (DPBS)	Life technologies
Ethanol	Merck
Exonuclease I	Thermo scientific
FastAP	Thermo scientific
Formaldehyde (37%)	Sigma-Aldrich
Glycerol	Sigma
HiDi-Formamide	Thermo Fisher
HPLC-water	Avantor Performance Materials
Midori Green	Nippon Genetics Europe
Oligonucleotides	Eurofins Genomics
Pen Strep	Life technologies

## Appendix

Proteinase K	Carl Roth
Sodium acetate buffer solution	Sigma-Aldrich
Sodium Acide (NaN <sub>3</sub> ) (5%)	Sigma-Aldrich
SYBR Green I Master	Roche
Taq-DNA-Polymerase	MP Biomedicals
Terminator v3.1	Thermo Fisher
Tris-Borate-EDTA buffer (TBE)	Lonza
Triton X-100	Sigma-Aldrich

### 8.2 Kits

Maxima First Strand cDNA Synthesis Kit	Thermo scientific
RNeasy Mini Kit	Qiagen

### 8.3 Antibodies

Goat-anti-rabbit, Alexa 488 (1:400)	Abcam
Rabbit anti-GRP75 (1mg/ml) (1:1000)	Life technologies

### 8.4 Solutions

Antibody dilution solution:	1x PBS with 3% BSA, 0.05% NaN <sub>3</sub>
Blocking solution:	4% Goat Serum, 0.1% BSA, 0.1% Triton X-100, 0.05% NaN <sub>3</sub> in 1x PBS
Fibroblast culture medium:	Dulbeccos Modified Eagle Medium (DMEM), 10% fetal bovine serum (FBS), 2mM L-glutamine, 1mM sodium pyruvate, 0.1mM nonessential amino acid solution (MEM-NEAA) and 1% penicillin/streptomycin (P/S).
Gel loading dye solution:	10X Glycerol, HPLC-water, EDTA, Bromphenol Blue-Na-Salt.

## 8.5 Equipment

3130XL Genetic Analyzer	Thermo Fisher
Agarose gel electrophoresis	Amersham Pharmacia Biotech
Axiovert 200M (microscope)	Zeiss
ChemiDoc MP Imager	BIO-RAD
Countess, automated cell counter	Invitrogen
Herasafe Biological Safety Cabinet	Thermo Scientific
LightCycler 480	Roche
ND-1000 Spectrophotometer	NanoDrop
Microfuge 16	Beckman Coulter
Multifuge 1S-R	Heraeus
Nalgene Cyro 1°C Freezing Container	Thermo Scientific
Observer Z.1 (confocale microscope)	Zeiss
Rotanta 460R	Hettich Zentrifugen
Thermocycler	BIO-RAD Eppendorf Analytik Jena
Thermo Heracell 150 CO2-Incubator	Thermo Scientific
TS1 Thermoshaker Biometra	Analytik Jena

## 8.6 Timeline of the clinical course for patients II.1, II.3 and II.4 of Family 1

**Table 29.** Clinical course for patient II.1.

Year	Clinical presentation
1985	<b>Clinical presentation:</b> unclear encephalopathy with vertigo, gait disturbance, visual impairment (diplopia) <b>Other clinical features with a fluctuating course:</b> aphasia, dysarthria, dysphagia, cognitive impairment, seizures, coma lasting for months
1985-1986	<b>Diagnostic updates:</b> no etiology of disease found (information on the diagnostic tools is not available)
1988	Death due to aspiration pneumonia, asphyxia

**Table 30** Clinical course for patient II.3.

Year	Clinical presentation
Disease history before first contact 2012 – Spring 2015	<p><b>Clinical presentation:</b> unclear familial encephalopathy including headache, sensory deficits, visual and speech problems</p> <p><b>Other clinical features with a fluctuating course:</b> cerebellar ataxia, dementia, aphasia</p> <p><u>Next deterioration:</u> reduced vigilance, spastic paresis of limbs; funicular myelosis suspected</p> <p><u>2014:</u> Spastic tetraparesis, generalized epileptic seizures, pneumonia, dysphagia</p> <p>Fluctuating course, general trend: progredient deterioration</p> <p><u>rehabilitation:</u> hyperthermia more than 39°C with poor response to medication, myoclonus of head and shoulders</p> <p><b>Therapeutic intervention:</b> 2014 tracheostomy and PEG</p> <p><b>Diagnostics:</b> slightly decreased blood levels for vitamin B12 and folic acid, unremarkable results for repetitive cranial MRI, CSF analysis, autoimmune diagnostics, viral serology, histopathologic investigation of an apocrine sweat gland (Lafora disease) and muscle biopsy (mitochondrial disease)</p>
Spring 2015	<p><b>Clinical presentation:</b> Somnolent, spastic tetraparesis, polytopic spontaneous myoclonus of head and shoulders, a deficit of adduction and ptosis of the right eye, communication due to tracheal cannula not possible, urinary tract infection, repetitive central fever over several weeks (up to 39,6°C)</p> <p><b>Diagnostic:</b> 72h video-EEG leading to the diagnosis of myoclonus epilepsy, unremarkable results for fundoscopy and dermatological consultation</p> <p><b>Initiation of genetic diagnostic tests:</b> neuronal ceroid lipofuscinosis, Unverricht-Lundborg disease (gene panel)</p> <p><b>Treatment:</b> lamotrigine 200mg/die, topiramate 200mg/die, levetiracetam 2000mg/die, clobazam 20mg/die, ibuprofen 1200mg/die, esomeprazole 20mg/die, dalteparin s.c. 5000 IU, scopolamine t.d., fentanyl t.d. 25µg/every 3<sup>rd</sup> day, introduction of piracetam 2400mg/die</p> <p>urinary tract infection: ceftriaxone 2g/die for 7 days, central fever: leg compresses</p>
Fall 2015	<p><b>Clinical presentation:</b> report of multiple infections in summer with an increased quantity of seizures, pain in extremities (spasms), patient</p>

Appendix

	<p>awake, orientated, communication possible, fluctuating deficit of abduction and ptosis left eye, spastic tetraparesis with atrophy of distal muscles</p> <p><b>Diagnostics:</b> 72h video-EEG shows slight myoclonus of left arm and orofacial, no characteristic epileptic potentials measured, ENT specialist consultation for tracheal cannula</p> <p><b>Treatment:</b> reduction of topiramate 150mg/die, Botulinum toxin A treatment (M. biceps brachii) with a positive effect</p>
Spring 2016	<p><b>Clinical presentation:</b> Family describes improved general condition with improved speech, awake, alternating compliance, no speech, hypomimia, divergent strabismus, improved cognitive function and mobility of the arms, fewer spasms</p> <p><b>Genetic diagnostic tests results:</b> Screening for neuronal ceroid lipofuscinosis (<i>CLN3</i>, <i>CLN5</i>, <i>CLN6</i>, <i>CLN8</i>, <i>CTSD</i>, <i>DNAJC5</i>, <i>MFSD8</i>, <i>PPT1</i>, <i>TPP1</i>) negative, mutations in <i>KCNC1</i> negative, variants or large deletion or duplication (qPCR) within <i>CLN3</i> negative, variants in <i>DNAJ5</i> negative (PCR and direct sequencing)</p>
Fall 2016	<p><b>Clinical presentation:</b> good compliance, relatively fluent speech, improved general status, improved vigilance, spasms of extremities, hypomimia, divergent strabismus</p> <p><b>Initiation of genetic diagnostic tests:</b> exome sequencing of parents and patient (NGS-trio)</p> <p><b>Treatment:</b> Botulinum toxin A treatment M. biceps femoris and M. tibialis posterior, reduction levetiracetam 1500mg/die, regularly physiotherapy at home, additionally training with MOTomed independently</p>
Spring 2017 1 <sup>st</sup> visit	<p><b>Clinical presentation:</b> report of visual hallucinations, reduced mood and compliance, patient awake, hypomimia, divergent strabismus, improved passive knee mobility (last visit: 110°, now: 140°)</p> <p><b>Therapeutic intervention:</b> tracheostomy removed one week before the visit</p> <p><b>Treatment:</b> elevation levetiracetam 2000mg/die in December, metamizole 500-1000mg/die to reduce pain in legs, end of Botulinum toxin A treatment (missing improvement), regularly physiotherapy and MOTomed training</p>
Spring 2017 2 <sup>nd</sup> visit	<p><b>Genetic diagnostic tests result:</b> Institute of Neurogenetics found <i>NAXE</i> variants in NGS-trio data</p> <p><b>Diagnostics:</b> skin biopsy for research issues</p> <p><b>Treatment:</b> ubiquinol (coenzyme Q<sub>10</sub>) 150mg/die, vitamin B<sub>3</sub> (niacin) 40mg</p>
Fall 2017	<p><b>Clinical presentation:</b> psychiatric symptoms (reports to be somebody</p>

Appendix

	<p>else, depersonalization), episodes of pain in extremities shorter (10 min), orientation to person (not to location and time), mood unsteady and frequently changing, improved oral intake, awake, hypomimia, divergent strabismus, fewer spasms, improved movement and posture</p> <p><b>Treatment:</b> MOTOmed training 2x/die, reduction of levetiracetam 1000mg/die, increase of lamotrigine 300mg/die, reduction of PEG feeding</p>
Winter 17/18	<p><b>Clinical presentation:</b> report of episodes of leg pain (5-10min), more jerky head movements, report of visual hallucinations, ability to read (30min), awake, orientated to person and location (not to time), divergent strabismus, gaze-evoked nystagmus, internuclear ophthalmoplegia left, improved mobility of the right arm</p> <p><b>Diagnostics:</b> consultation of an ophthalmologist: no evidence of ophthalmologic disease</p> <p><b>Treatment:</b> elevation niacin dose (80mg/die), new PEG MOTOmed training 2x/die, physiotherapy 4x/week, occupational therapy 2x/week, speech therapy 2x/week</p>
Summer 2018	<p><b>Clinical presentation:</b> report of improved memory of events in the past, increased oral intake, report of the lability of affect (angry, insulting) and episodes of pain, awake, orientated to person and location (vague to time), divergent strabismus, gaze-evoked nystagmus, internuclear ophthalmoplegia left, muscle tone softer, no pyramidal signs</p> <p><b>Treatment:</b> introduction of Levodopa/Benserazide (100/25mg) for episodes of pain (suspicion of restless legs syndrome), otherwise unchanged</p>
Fall 2018	<p><b>Clinical presentation:</b> visit of relatives in France had a positive effect on mood, less pain, ability to speak French, back in Germany more sadness, episodes of pain (no effect of Levodopa/Benserazide), improved trunk control and improved active arm elevation</p> <p><b>Treatment:</b> stop Levodopa/Benserazide, introduction of Vitamin B<sub>6</sub> (20mg/die), an anti-depressive therapy was recommended but not desired from the Family, otherwise unchanged</p>
Winter 2019	<p><b>Clinical presentation:</b> report of improved self-perception in the mirror, new ability to move her wheelchair slowly, fewer episodes of pain, increased perception of the desire to void, passive extension of her arms completely possible, otherwise unchanged</p> <p><b>Diagnostics:</b> elevated blood levels of vitamin B<sub>6</sub> under substitution (403 nmol/L, reference range: 16-78 nmol/L), vitamin B<sub>3</sub> slightly elevated (64</p>

Appendix

	<p>ng/ml, reference range: 8-52 ng/ml)</p> <p><b>Treatment:</b> reduction of fentanyl t.d. 25µg/every 3<sup>rd</sup> day to 12,5µg/every 3<sup>rd</sup> day, reduction of vitamin B<sub>6</sub> to every 2<sup>nd</sup> day</p>
Fall 2019	<p><b>Clinical presentation:</b> report of a respiratory tract infection treated outpatient with antibiotics, during that time reduced general health condition, no seizures, fentanyl therapy was stopped until the episodes of pain reemerged, medication was restarted with 12,5µg/every 3<sup>rd</sup> day, improved concentration, suspected polyneuropathy of the legs, otherwise unchanged</p> <p><b>Diagnostics:</b> normal levels of vitamin B<sub>6</sub> and B<sub>3</sub> under substitution</p> <p><b>Treatment:</b> introduction of pregabalin 125mg/die, reduction of topiramate, stop of fentanyl, reduction of vitamin B<sub>6</sub> to every 3<sup>rd</sup> day</p>
Spring 2020	<p><b>Clinical presentation:</b> report of more head tremor, improved oral intake, concentration for 30-45 minutes possible (e.g. card games), slight dysarthria and hypophonia, symmetrical hypesthesia and -algnesia of the lower extremities, otherwise unchanged</p> <p><b>Diagnostics:</b> normal levels of vitamin B<sub>6</sub> and B<sub>3</sub> under substitution, nerve conduction studies confirm severe polyneuropathy of the legs (N. tibialis, N. peroneus, N. suralis)</p> <p><b>Treatment:</b> elevation topiramate (75mg), otherwise unchanged</p>
Summer 2020	<p><b>Clinical presentation:</b> report of episodes of lability of affect, during the MOTOMed training ability to actively move her legs, pregabalin resulted in reduced leg pain, increased perception of the desire to void, improved control over finger and hand movements, improved trunk control in her wheelchair, otherwise unchanged</p> <p><b>Diagnostics:</b> normal levels of vitamin B<sub>6</sub> and B<sub>3</sub> under substitution</p> <p><b>Treatment:</b> elevation of pregabalin to 150mg/die, stop of vitamin B<sub>6</sub> substitution (control of blood level every 3 months recommended)</p>

Legend: PEG=percutaneous endoscopic gastrostomy; MRI=magnetic resonance imaging; incl.=inclusive; h=hour(s); mg=milligram; die=diem (latin)=day; EEG=electroencephalography; ENT=ears, nose and throat; NGS-trio=next-generation-sequencing-trio; WES=whole-exome-sequencing; min=minute(s).

**Table 31.** Clinical course for patient II.4.

Year	Clinical presentation
Fall 2014	<p><b>Clinical presentation:</b> Unclear familial encephalopathy, first symptoms: head and back pain, visual impairment (diplopia), vertigo further course: cerebellar ataxia, suspected progressive myoclonus</p>

Appendix

	<p>epilepsy, chorea-like movement disorder, alternating vertical and horizontal spontaneous nystagmus, dementia, psychosis</p> <p><b>Diagnostics:</b> EEG shows Frontal Intermittent Rhythmic Delta Activity (FIRDA) elevated NSE in CSF, unremarkable results for cranial MRI, MRS (lactate, NAA, lipids, choline, myoinositol), thoracic x-ray, x-ray of the spine, abdominal sonography, CSF analysis (except NSE elevation), autoimmune diagnostics, viral serology, muscle biopsy (mitochondrial disease)</p> <p><b>genetic diagnostic tests:</b> for Morbus Niemann-Pick type C (result: negative)</p>
Spring 2015	<p><b>Clinical presentation:</b> headache, vertigo, visual impairment, reduced mood, lack of concentration and attention, awake, orientated, no speech problems, ataxia, downbeat nystagmus, chorea-like movements of hands, hypomimia</p> <p><b>Diagnostics:</b> neuropsychological test: functional impairment, EEG (conspicuous delta-waves, but no typical epileptic potentials), unremarkable results for cCT, cMRI, CSF analysis, autoimmune diagnostics, EMG, ECG, histopathologic investigation of an apocrine sweat gland (Lafora disease)</p> <p><b>Treatment:</b> introduction of valproate ret. 600mg/die, acupuncture</p>
Summer 2015	<p><b>Clinical presentation:</b> awake, orientated, all symptoms during the period fall 2014 until spring 2015 disappeared, only slight impairment of the fine motor function (left) remains</p> <p><b>Treatment:</b> valproate reduction 450mg/die</p>
Spring 2016	<p><b>Clinical presentation:</b> reports episodes of vertigo lasting for days, episodes of weeks with gait disturbance and impaired balance, report of psychosis after a night out with friends: no drugs, no alcohol (lasting 2 days) and diplopia the following 4 days, concentration and memory impaired, speech impairment, awake, orientated, slight dysarthria, slight choreatic movements, fine motor function left reduced, no gait disturbance</p> <p><b>Treatment:</b> valproate elevation from latest dose 300mg/die to 600mg/die, alprazolam 0,5mg (if required)</p>
Summer 2016	<p><b>Clinical presentation:</b> patient awake, orientated, vertigo, fever (38,5°C), diplopia, speech impairment, psychomotor slowing, slight cerebellar ataxia, slight dysarthria, fine motor function reduced (left), in the hospital she develops psychosis with hallucinations, anxiety,</p>

	bizarre behavior, catatonia and stuporous states, coma, irregular and rhythmic myoclonus of head and arms, pneumonia <b>Diagnostics:</b> unremarkable results for cCT, cMRT, 31P-MRS, CSF analysis, autoimmune diagnostics, EEG, ECG, transthoracic echocardiography <b>Treatment:</b> stop of valproate treatment, introduction of levetiracetam 3000mg/die, lacosamide 400mg/die, lamotrigine 25mg/die, risperidone 1mg/die, lorazepam 0,5mg/die, dalteparin 2,500 IU, ubichinone 600mg/die
Summer 2016	Death due to pulmonary embolism

Legend: (c)MRI=(cerebral) magnetic resonance imaging; MRS=magnetic resonance spectroscopy; NAA=N-Acetylaspartat; EEG=electroencephalogram; incl.=inclusive; NSE=neuron specific enolase; ECG=electrocardiogram; EMG=electromyography; cCT=cerebral computerized tomography; ret.=retard; mg=milligram; die=diem (latin)=day; 31P-MRS=31- phosphorus- magnetic resonance spectroscopy; IU=international units.

## 8.7 Case descriptions for Family 2-4

### 8.7.1 Family 2 (homozygous c.733A>C: p.Lys245Gln)

The index case of this Family is a four-year-old boy born in Saudi Arabia to non-consanguineous parents. The patient had a progressive delay in motor development, muscular hypotonia and respiratory failure. He is intubated on a ventilator via an endotracheal tube (ETT). He had a chest infection and sepsis. His Family history is positive for a neurometabolic disorder (mitochondrial encephalopathy), though the information is not available on which Family members are affected.

### 8.7.2 Family 3 (homozygous c.652G>A: p.Asp218Asn)

This boy was born in Jordan to healthy and consanguineous parents. He developed bradycardia and desaturation with severe hypotonia on the second day of life due to respiratory failure. He was intubated and connected to the ventilator for two and a half months. He had also been diagnosed with decreased oral intake, left eye squint, mitral regurgitation, developmental regression, abnormal brainstem MRI signal intensity, cerebellar atrophy, abnormality of the periventricular white matter and intracranial hemorrhage. Laboratory findings included thrombocytosis. The patient was deceased at 6 months of age. In this

Family, there was a history of early deaths at the age of 4 to 6 months in relatives with similar phenotypes.

### 8.7.3 Family 4 (homozygous c.640A>G: p.Ile214Val)

This 7-year old boy is of Indian ancestry. His parents are healthy and consanguineous. The patient has one healthy sister and one deceased sister who had a similar clinical presentation. The patient presented with global developmental delay. Cranial MRI showed leukodystrophy, lissencephaly, cortical dysplasia, pachygyria, ventriculomegaly. Brain lactate levels were increased upon MRS. Furthermore, fundoscopy showed pigmentary retinopathy and elevated serum creatine phosphokinase.

## 8.8 Primer design

**Table 32** Primer design for the Sanger sequencing of the splice (c.665-1G>A) and the missense (c.757G>A, p.G253S) variant detected in Family 1.

Name	5'-3'-Sequence
<i>Missense_F</i>	GTTGGACGAGAGTTCCTCAG
<i>Missense_R</i>	GGAATCCACAGTTCTGGAAG
<i>Splicing_F</i>	GTGTCCTGAAGGGACTCAC
<i>Splicing_R</i>	TGCAGACGATAGACACACTC

Legend: F=forward primer; R=reverse primer.

**Table 33** Primer design for the three used *NAXE* gene transcripts (total, canonical and alternative transcript) for expression level analysis.

Name	5'-3'-Sequence
<i>Total Transcript_F</i>	ATTACCCCAAAGGCCTAAC
<i>Total Transcript_R</i>	ACAGTGAGTCCCTTCAGG
<i>Canonical Transcript_F</i>	AAGCCCCTCTTCACTGCATT
<i>Canonical Transcript_R</i>	GACGTCCCACATCCTGAGG
<i>Alternative Transcript_F</i>	CAAACCTTTGGCTACGAG
<i>Alternative Transcript_R</i>	TATTTTAGACCTGGTGTGGG

Legend: F=forward primer; R=reverse primer.

## 8.9 Association of mitochondrial DNA variant quantity and age

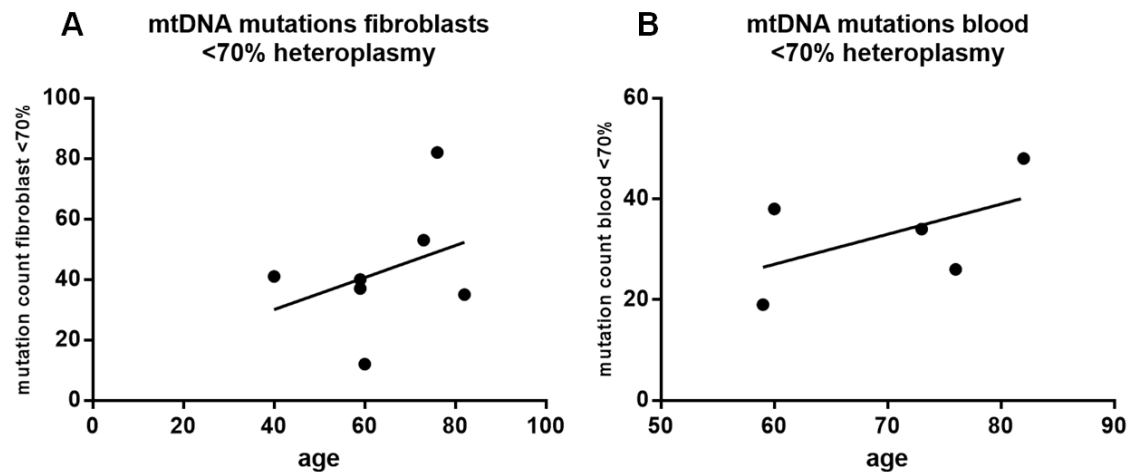


**Figure 16. mtDNA variant count in fibroblasts and blood of different aged individuals. A)** mtDNA variants in fibroblasts <70% heteroplasmy.  $p=0.4383$ ; non-significant. **B)** mtDNA variants in blood <70% heteroplasmy  $p=0.3440$ ; non-significant.

## 8.10 Votum der Ethikkommission

1) Aktenzeichen: 19-039

Sequenzierung der mitochondrialen DNA sowie Analyse des Transkriptoms aus RNA-Proben von Patienten mit Parkinson-Syndrom und gesunden Kontrollen.

2) Aktenzeichen: 07-130

Molekulargenetische Ursache der Ataxien.

3) Aktenzeichen: 16-068

RARE-Studie.

## 9 Acknowledgments

During the whole process of this dissertation, I felt very well supported and therefore I want to thank my 'Doktormutter' Priv.-Doz. Dr. Joanne Trinh (PhD), who always had an open ear for questions and taught me a lot about genetics and research in general. Thank you for your trust in me and this great experience.

I thank the Institute of Neurogenetics directed by Prof. Dr. Christine Klein (MD), who accompanied me with the writing process, gave me the opportunity to write my medical thesis about this fascinating project and provided the laboratory equipment.

Additionally, I thank the medical team of the Institute of Neurology, especially Prof. Dr. Norbert Brüggemann (MD) and Dr. Alexander Balck (MD), who performed the follow-ups and clinical examinations with the patients. Prof. Dr. Norbert Brüggemann (MD) offered me the chance to meet the patient in person and helped me to understand the clinical picture of this disease a lot better.

I thank Dr. Philip Seibler (PhD) for providing the different samples of the cell lines used for the mtDNA variant analysis across tissues and Dr. Marija Dulovic (MD, PhD), who performed the NAXE-protein expression analysis and accompanied me with new methods in the cell lab.

The publications of the projects I worked in were supported by all the co-authors, who are listed in section 10 and the laboratory team. Thank you a lot for the great work and the success.

I thank the whole team of the Institute of Neurogenetics, who lifted my morale and gave me a lot of good memories.

At this point, it is very important for me to mention all patients, who participate in research projects and donate samples. Without your help, research would not be possible.

Lastly, I thank my family and friends, who always supported me during my studies and the process of writing this medical thesis. Thank you for your motivating words and your patience.

## 10 Curriculum vitae



Name	Sophie Imhoff
Date of birth	15.04.1995
University education	2014 – 2021 Study of medicine, Universität zu Lübeck  First state exam 2016  Second state exam 2020  Approbation 2021
Student job	2017- 2019 study group: Sektion für Pädiatrische Pneumologie und Allergologie (led by Prof. Dr. Matthias Kopp, MD)
Dissertation	2017- 2021 Institute of Neurogenetics (led by Prof. Dr. Christine Klein, MD), study group: Integrative Omics in Parkinson's disease (group leader: Priv.-Doz. Dr. Joanne Trinh, PhD)
Publications	See section 10.1

## 10.1 Scientific publications

- 1) Trinh J, Hüning I, Yüksel Z, Baalman N, **Imhoff S**, Klein C, Rolfs A, Gillessen-Kaesbach G, Lohmann K. A KAT6A variant in a family with autosomal dominantly inherited microcephaly and developmental delay. *J Hum Genet* 2018: **63**: 997–1001.
- 2) Trinh J, Lohmann K, Baumann H, Balck A, Borsche M, Brüggemann N, Dure L, Dean M, Volkmann J, Tunc S, Prasuhn J, Pawlack H, **Imhoff S**, Lill CM, Kasten M, Bauer P, Rolfs A, International Parkinson's Disease Genomics Consortium (IPDGC), Klein C. Utility and implications of exome sequencing in early-onset Parkinson's disease. *Mov Disord* 2019: **34**: 133–137.
- 3) Germer EL\*, **Imhoff S\***, Vilariño-Güell C, Kasten M, Seibler P, Brüggemann N, International Parkinson's Disease Genomics Consortium, Klein C, Trinh J. The Role of Rare Coding Variants in Parkinson's Disease GWAS Loci. *Front Neurol* 2019: **10**: 1284.  
(\* = equal contribution)
- 4) Berenguer-Escuder C\*, Grossmann D\*, Massart F, Antony P, Burbulla LF, Glaab E, **Imhoff S**, Trinh J, Seibler P, Grünewald A, Krüger R. Variants in Miro1 Cause Alterations of ER-Mitochondria Contact Sites in Fibroblasts from Parkinson's Disease Patients. *J Clin Med* 2019: **8**: 2226.  
(\* = equal contribution)
- 5) Trinh J\*, **Imhoff S\***, Dulovic-Mahlow M\*, Kandaswamy KK, Tadic V, Schäfer J, Dobricic V, Nolte A, Werber M, Rolfs A, Münchau A, Klein C, Lohmann K, Brüggemann N. Novel NAXE variants as a cause for neurometabolic disorder: implications for treatment. *J Neurol* 2020: **267**: 770-782.  
(\* = equal contribution)

## 10.2 Oral presentations

- 1) Oral presentation, Neurowoche (DGN-Kongress), Berlin, November 2018  
'Novel NAXE mutations cause a neurometabolic disorder'  
**Sophie Imhoff\***, Joanne Trinh PhD\*, Krishna Kumar Kandaswamy, Martin Werber, Maximilian E.R. Weiss, Marija Dulovic MD, PhD, Arndt Rolfs, Christine Klein MD, Katja Lohmann PhD\*, Norbert Brüggemann MD\*  
(\*=equal contribution)

## 10.3 Grants

- 1) Travel grant for young scientists, 'Verein der Alumni, Freunde und Förderer der Universität zu Lübeck', Neurowoche (DGN-Kongress), Berlin, November 2018